

**Unclassified**

**NEA/CSNI/R(2000)6/VOL2**



Organisation de Coopération et de Développement Economiques  
Organisation for Economic Co-operation and Development

**OLIS : 06-Apr-2000**  
**Dist. : 07-Apr-2000**

PARIS

**English text only**

**NUCLEAR ENERGY AGENCY  
COMMITTEE ON THE SAFETY OF NUCLEAR INSTALLATIONS**

**NEA/CSNI/R(2000)6/VOL2**  
**Unclassified**

**INTERNATIONAL STANDARD PROBLEM (ISP) NO. 41**

**CONTAINMENT IODINE COMPUTER CODE EXERCISE BASED ON  
A RADIOIODINE TEST FACILITY (RTF) EXPERIMENT**

**89743**

Document complet disponible sur OLIS dans son format d'origine  
Complete document available on OLIS in its original format

**English text only**



<b>Coordinators:</b>	J. Clara Wren Jacques Royen	AECL (Canada) OECD/NEA
<b>Compiled by:</b>	Joanne Ball	AECL (Canada)
<b>Contributors:</b>	Joanne Ball	AECL (Canada)
	Glenn Glowa	AECL (Canada)
	J. Clara Wren	AECL (Canada)
	Adolf Rydl	NRIR (Czech Republic)
	Christian Poletiko	IPSN (France)
	Yann Billarand	IPSN (France)
	Falk Ewig	GRS, Köln (Germany)
	Friedhelm Funke	Siemens/KWU (Germany)
	Peter Zeh	Siemens/KWU (Germany)
	Akihide Hidaka	JAERI (Japan)
	Randall Gauntt	Sandia (USA)
	Mike Young	Sandia (USA)
	Robin Cripps	PSI (Switzerland)
	Berta Herrero	CIEMAT (Spain)

## **ORGANISATION FOR ECONOMIC CO-OPERATION AND DEVELOPMENT**

Pursuant to Article 1 of the Convention signed in Paris on 14th December 1960, and which came into force on 30th September 1961, the Organisation for Economic Co-operation and Development (OECD) shall promote policies designed:

- to achieve the highest sustainable economic growth and employment and a rising standard of living in Member countries, while maintaining financial stability, and thus to contribute to the development of the world economy;
- to contribute to sound economic expansion in Member as well as non-member countries in the process of economic development; and
- to contribute to the expansion of world trade on a multilateral, non-discriminatory basis in accordance with international obligations.

The original Member countries of the OECD are Austria, Belgium, Canada, Denmark, France, Germany, Greece, Iceland, Ireland, Italy, Luxembourg, the Netherlands, Norway, Portugal, Spain, Sweden, Switzerland, Turkey, the United Kingdom and the United States. The following countries became Members subsequently through accession at the dates indicated hereafter: Japan (28th April 1964), Finland (28th January 1969), Australia (7th June 1971), New Zealand (29th May 1973), Mexico (18th May 1994), the Czech Republic (21st December 1995), Hungary (7th May 1996), Poland (22nd November 1996) and the Republic of Korea (12th December 1996). The Commission of the European Communities takes part in the work of the OECD (Article 13 of the OECD Convention).

## **NUCLEAR ENERGY AGENCY**

The OECD Nuclear Energy Agency (NEA) was established on 1st February 1958 under the name of the OEEC European Nuclear Energy Agency. It received its present designation on 20th April 1972, when Japan became its first non-European full Member. NEA membership today consists of 27 OECD Member countries: Australia, Austria, Belgium, Canada, Czech Republic, Denmark, Finland, France, Germany, Greece, Hungary, Iceland, Ireland, Italy, Japan, Luxembourg, Mexico, the Netherlands, Norway, Portugal, Republic of Korea, Spain, Sweden, Switzerland, Turkey, the United Kingdom and the United States. The Commission of the European Communities also takes part in the work of the Agency.

The mission of the NEA is:

- to assist its Member countries in maintaining and further developing, through international co-operation, the scientific, technological and legal bases required for a safe, environmentally friendly and economical use of nuclear energy for peaceful purposes, as well as
- to provide authoritative assessments and to forge common understandings on key issues, as input to government decisions on nuclear energy policy and to broader OECD policy analyses in areas such as energy and sustainable development.

Specific areas of competence of the NEA include safety and regulation of nuclear activities, radioactive waste management, radiological protection, nuclear science, economic and technical analyses of the nuclear fuel cycle, nuclear law and liability, and public information. The NEA Data Bank provides nuclear data and computer program services for participating countries.

In these and related tasks, the NEA works in close collaboration with the International Atomic Energy Agency in Vienna, with which it has a Co-operation Agreement, as well as with other international organisations in the nuclear field.

## **CSNI**

The NEA Committee on the Safety of Nuclear Installations (CSNI) is an international committee made up of senior scientists and engineers, with broad responsibilities for safety technology and research programmes, and representatives from regulatory authorities. It was set up in 1973 to develop and co-ordinate the activities of the NEA concerning the technical aspects of the design, construction and operation of nuclear installations insofar as they affect the safety of such installations. The Committee's purpose is to foster international co-operation in nuclear safety amongst the OECD Member countries. CSNI's main tasks are to exchange technical information and to promote collaboration between research, development, engineering and regulation organisations; to review the state of knowledge on selected topics of nuclear safety technology and safety assessments, including operating experience; to initiate and conduct programmes to overcome discrepancies, develop improvements and reach consensus on technical issues; to promote co-ordination of work, including the establishment of joint undertakings.

## **PWG4**

CSNI's Principal Working Group on the Confinement of Accidental Radioactive Releases (PWG4) has been given two tasks: containment protection, and fission product retention. Its role is to exchange information on national and international activities in the areas of severe accident phenomena in the containment, fission product phenomena in the primary circuit and the containment, and containment aspects of severe accident management. PWG4 discusses technical issues/reports and their implications, and the results of International Standard Problem (ISP) exercises and specialist meetings, and submits conclusions to the CSNI. It prepares Technical Opinion Papers on major issues. It reviews the main orientations, future trends, emerging issues, co-ordination and interface with other groups in the field of confinement of accidental radioactive releases, identifies necessary activities, and proposes a programme of work to the CSNI.

## **FPC**

The Task Group on Fission Product Phenomena in the Primary Circuit and the Containment (FPC) is a specialised extension of PWG4. Its main tasks are to exchange information, discuss results and programmes, write state-of-the-art reports, organise specialist workshops, perform ISPs in the field of fission product phenomenology.



# **APPENDIX A**

## **CODE DESCRIPTIONS**

**(for first set of calculations)**



# **IMPAIR Calculations to ISP41**

by

Peter Zeh

Friedhelm Funke

Siemens/KWU  
Radiochemical Laboratory  
Erlangen, Germany  
June 1998



## 1. International Standard Problem (ISP-41)

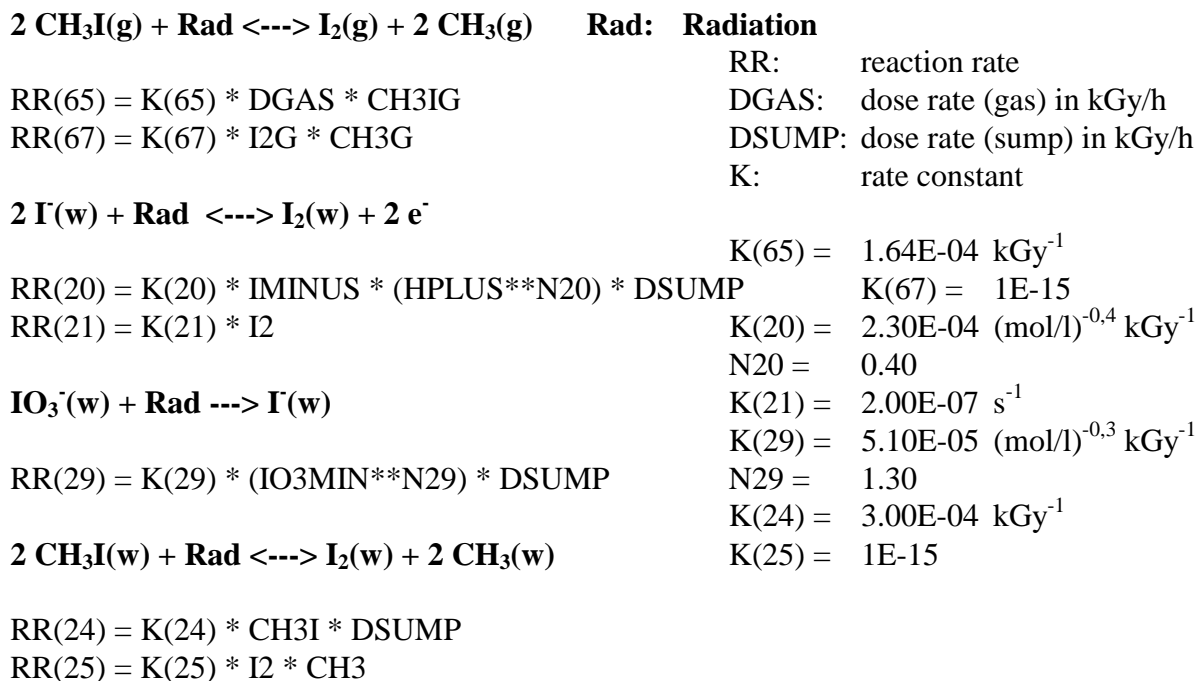
The calculation of iodine behaviour under the boundary conditions of an RTF experiment selected as ISP41 was performed with the PSI code IMPAIR [Güntay 1992].

The results are shown in the appended 8 figures for both stages 1 and 2. These two stages were considered as two identical experiments, but with different pH evolutions.

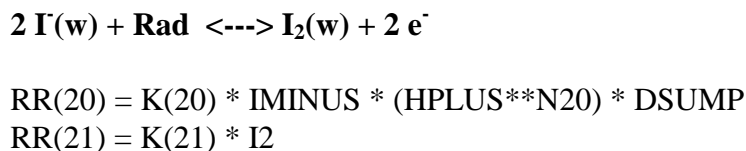
## 2. General description of the model used

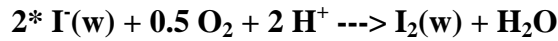
The iodine modelling in IMPAIR is described in [Güntay 1992]. However, modifications have been introduced which concern mass transfer and deposition/desorption behaviour at steel surfaces.

### 2.1 How is radiolysis modelled?



### 2.2 How is iodine transformed from non-volatile to volatile form?





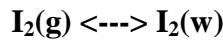
$$\text{RR}(16) = \text{K}(16) * \text{HPLUS} * \text{IMINUS}$$

$$\text{K}(16) (298\text{K}) = 1.00\text{E-}07$$

$$(\text{mol/l})^{-1} \text{s}^{-1}$$

$$E_A = 4.60\text{E+}04 \text{ J/mol}$$

### 2.3 How is mass transport/partitioning dealt with?



$$\text{RR}(35) = \text{K}(35) * (\text{PGF}/V_{\text{sump}}) * ([\text{I}_2]_{\text{w}} - [\text{I}_2]_{\text{g}} * P_{\text{I}_2})$$

$$\text{PGF} = \text{Surface area sump/gas interface (m}^2\text{)}$$

$\text{I}_2$  partition coefficient:

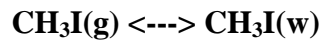
$$\log(P_{\text{I}_2}) = 9.132\text{E}5/T^2 - 4100/T + 5.404$$

$$T = T_{\text{sump}} (\text{K})$$

$$\text{K}(35) = 1/((1/\text{K}_w) + (P_{\text{I}_2}/\text{K}_g))$$

$$\text{K}_w = 1.00\text{E-}05 \text{ m/s}$$

$$\text{K}_g = 1.40\text{E-}03 \text{ m/s}$$



$$\text{RR}(36) = \text{K}(36) * (\text{PGF}/V_{\text{sump}}) * ([\text{CH}_3\text{I}]_{\text{w}} - [\text{CH}_3\text{I}]_{\text{g}} * P_{\text{CH}_3\text{I}})$$

$$\text{PGF} = \text{Surface area interface (m}^2\text{)}$$

$\text{CH}_3\text{I}$  partition coefficient:

$$\ln(P_{\text{CH}_3\text{I}}) = -6.97 + 2641/T$$

$$T = T_{\text{sump}} (\text{K})$$

$$\text{K}(36) = 1/((1/\text{K}_w) + (P_{\text{CH}_3\text{I}}/\text{K}_g))$$

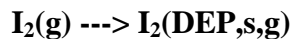
$$\text{K}_w = 1.00\text{E-}05 \text{ m/s}$$

$$\text{K}_g = 1.40\text{E-}03 \text{ m/s}$$

### 2.4 What is the general form of the surface adsorption models?

#### Deposition on steel in gas phase:

(no steam-condensing conditions)



The general IMPAIR modelling is:

$$\text{RR}(51) = \text{K}(51) * \text{I}_2\text{G}$$

$$\text{RR}(63) = \text{K}(63) * \text{DEPGS}$$

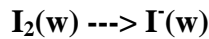
The rate constants used in the present calculations are based on Siemens experimental data [Funke 1996] and are different from the original IMPAIR values:

$$\text{K}(51) = 2.9\text{E-}11 \text{ m/s}, E_a = 150000 \text{ J/mol}$$

$$\text{K}(63) = 0.$$

## **Reaction with steel in water phase:**

Based on experimental data by Siemens [Funke 1996] the reaction between  $I_2$  and steel in the water phase is modelled as an  $I_2/\Gamma$  conversion. There is no remaining deposition of iodine on steel immersed in water. This model is different from the original IMPAIR model as cited in [Güntay 1992] and [Sims 1995].



$$RR(55) = K(55) * I_2 * S_w/V_w$$

$S_w$  = Surface area of immersed steel ( $m^2$ )

$V_w$  = Volume of water ( $m^3$ )

$K(55)=2.3E-9$  m/s,  $EA=80800$  J/mol

### **3 Description of the modelling process**

#### ***3.1 What parameters were provided as input and, if they were not provided in the data, how were they arrived at?***

The following iodine speciation at injection time was used in the calculations:

99.8 %  $\Gamma(w)$ , 0.11 %  $IO_3^-$ , 0.01 %  $CH_3I$

This corresponds to the measured speciation as given to the participants.

The general organic iodine modelling in IMPAIR contains starting concentrations for  $CH_3$  radicals in gas and water phase as an input parameter. No experimental values are available for the  $CH_3$  radical concentrations under ISP41 conditions. These were therefore set to  $[CH_3]_{water}=10^{-10}$  mol/L and  $[CH_3]_{gas}=10^{-9}$  mol/L. The appointment of these values influences the concentration of  $CH_3I$  in both phases. However, even by increasing the  $CH_3$  concentration by orders of magnitude,  $CH_3I$  does not become a dominant species.

The experimentators have stated that catalytic hydrogen recombiners used in the experiment should have also decomposed ozone. Therefore, the  $I_2$ /ozone reaction in IMPAIR was not considered. Its effect would have been an effective conversion of  $I_2$  into iodate within the gas phase.

A detailed description of all other parameters and their origin is given in [Güntay 1992] and in [Sims 1995].

#### ***3.2 What criteria were used to determine if the results were reasonable?***

No direct comparison with experimental data was made. The mass balance of the results was checked. The iodine speciation in gas and water phase was consistent with experience from reactor case applications.

### **4 Description and interpretation of the results**

#### ***4.1 What processes dominated the speciation and distribution of iodine?***

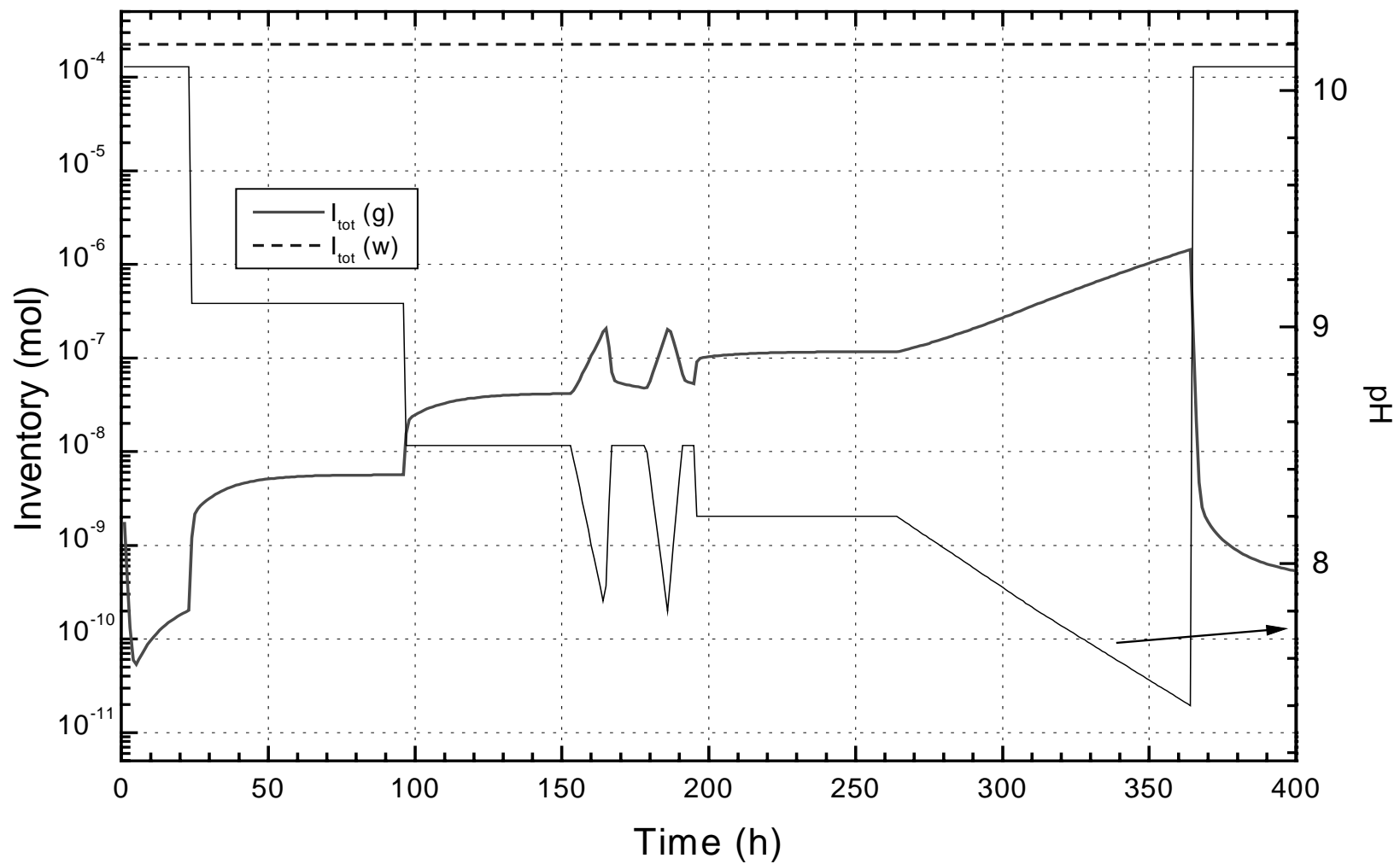
The phenomenological models in IMPAIR concerning hydrolysis (two reactions) and radiolysis in the water phase ( $\Gamma \rightarrow I_2$ ) dominate the iodine speciation in water and thus indirectly in the gas phase speciation.

#### **4.2** *What input parameters or variables was the behaviour of iodine most sensitive to?*

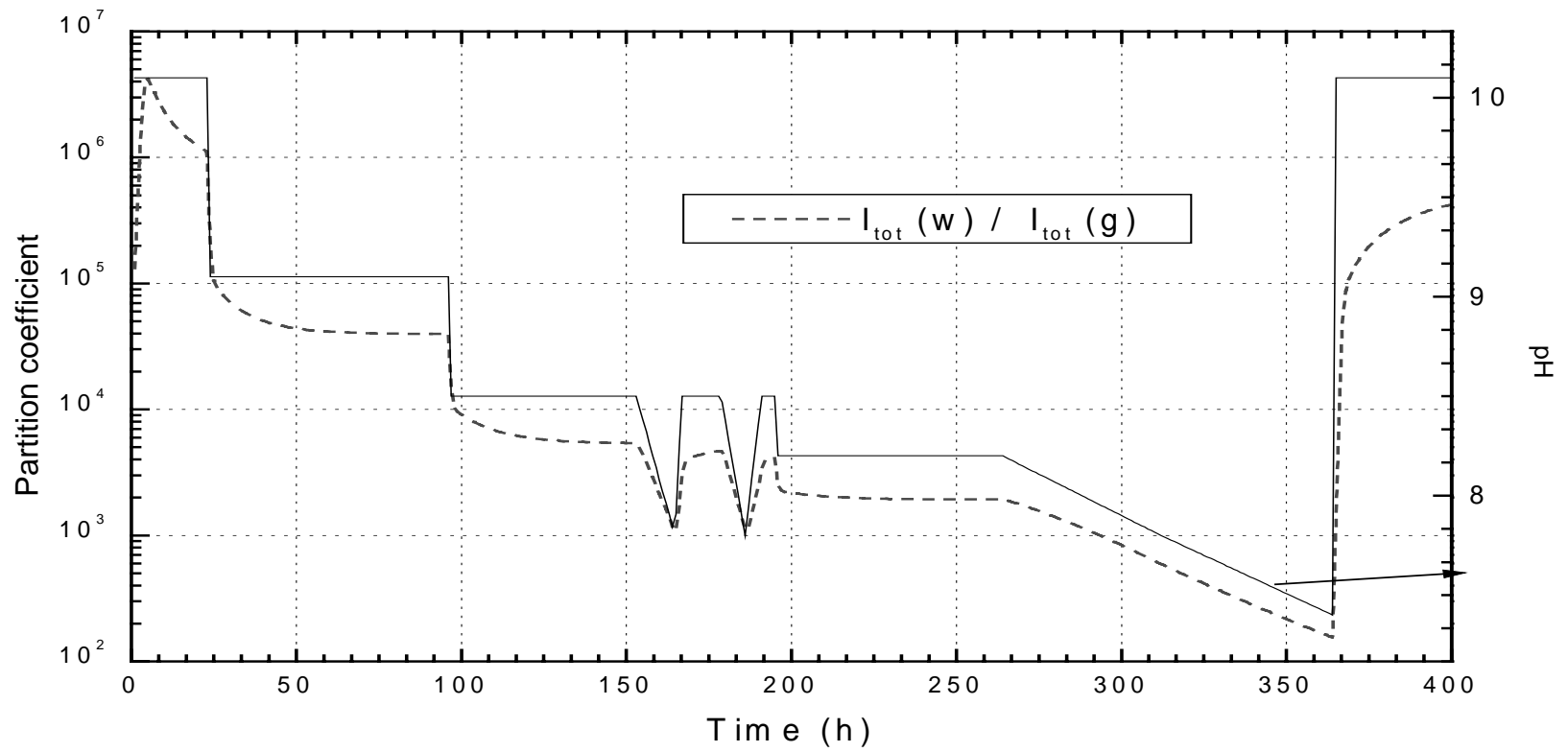
The most sensitive input parameter was the pH value.

### **5** **References**

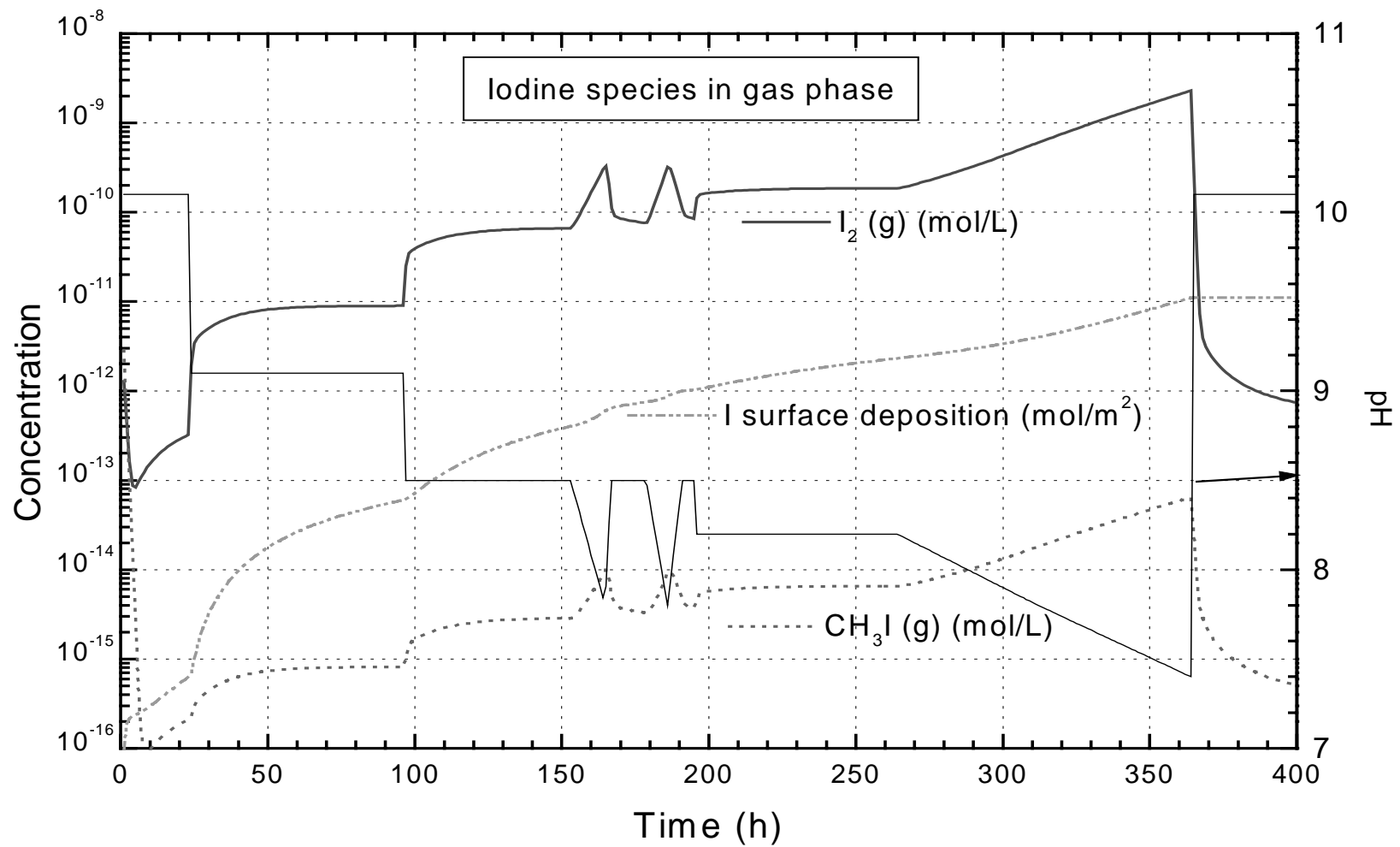
- [Funke 1996] F. Funke, G.-U. Greger, S. Hellmann, A. Bleier, W. Morell  
Iodine-steel reactions under severe accident conditions in light-water  
reactors  
Nucl. Eng. & Des. 166 (1996) 357
- [Güntay 1992] S. Güntay; R. Cripps  
IMPAIR/3: A computer program to analyze the iodine behaviour in multi-  
compartments of a LWR containment  
PSI-Bericht Nr. 128, 1992
- [Sims 1993] H. Sims; C. Hueber, J. Henshaw, F. Funke, G-U. Greger, S. Hellmann  
Iodine Code Comparison  
Report EUR 16507 EN, 1995



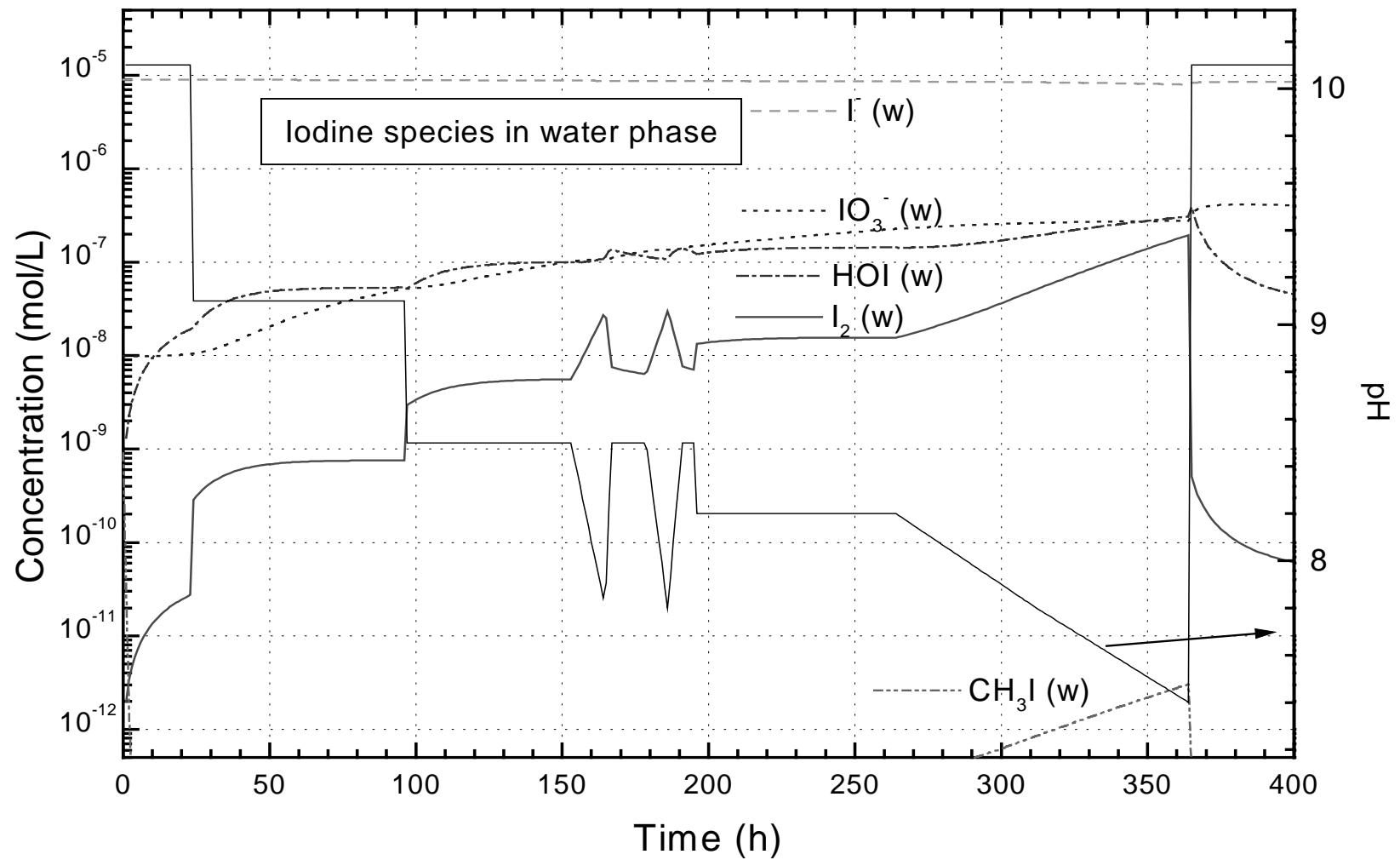
**Results to RTF-ISP-41, stage 1:** Inventory of iodine in gas (g) and water (w) phase and modelled pH evolution



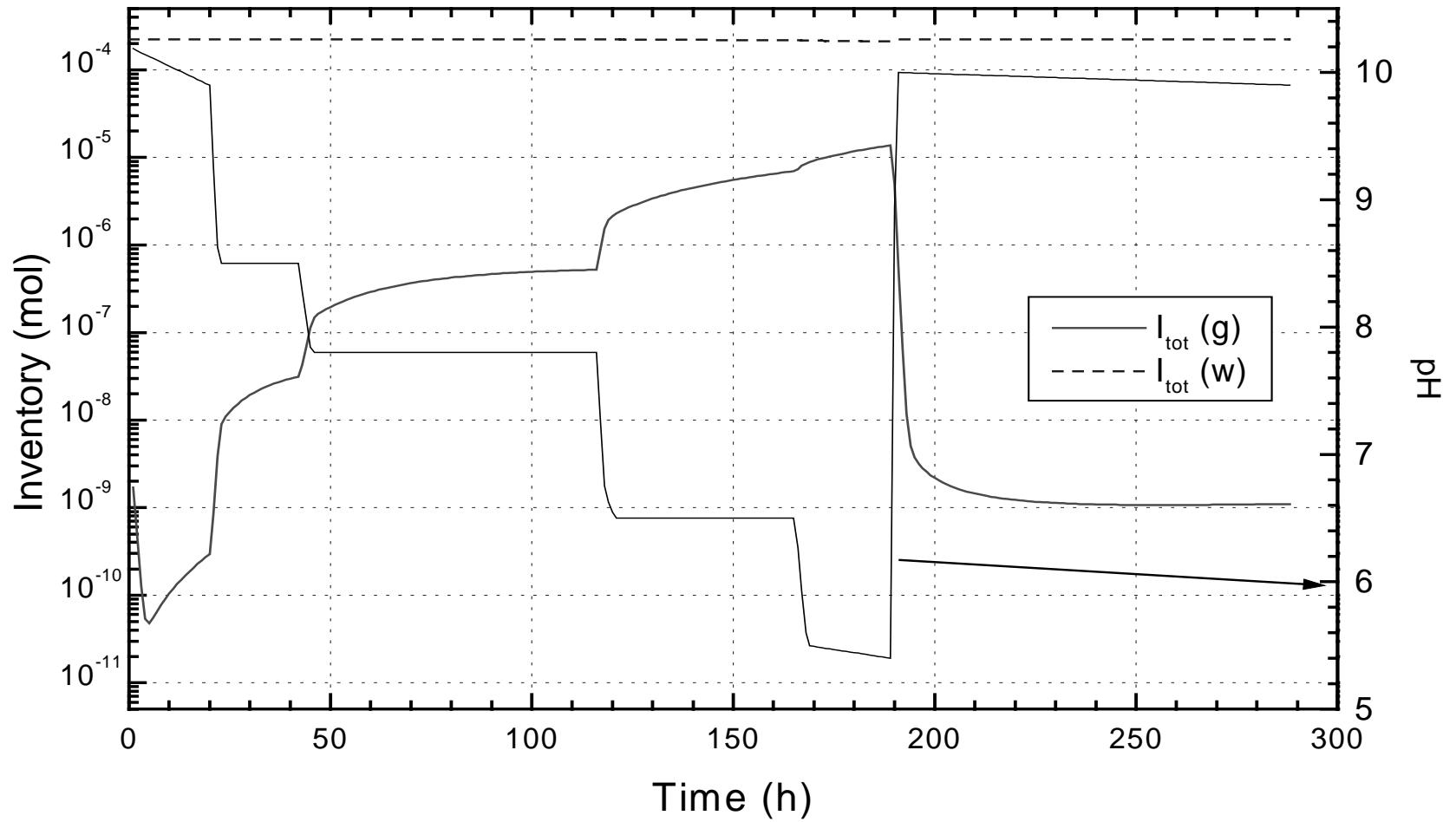
**Results to RTF-ISP-41, stage 1: Partition coefficient of total iodine and modelled pH evolution**



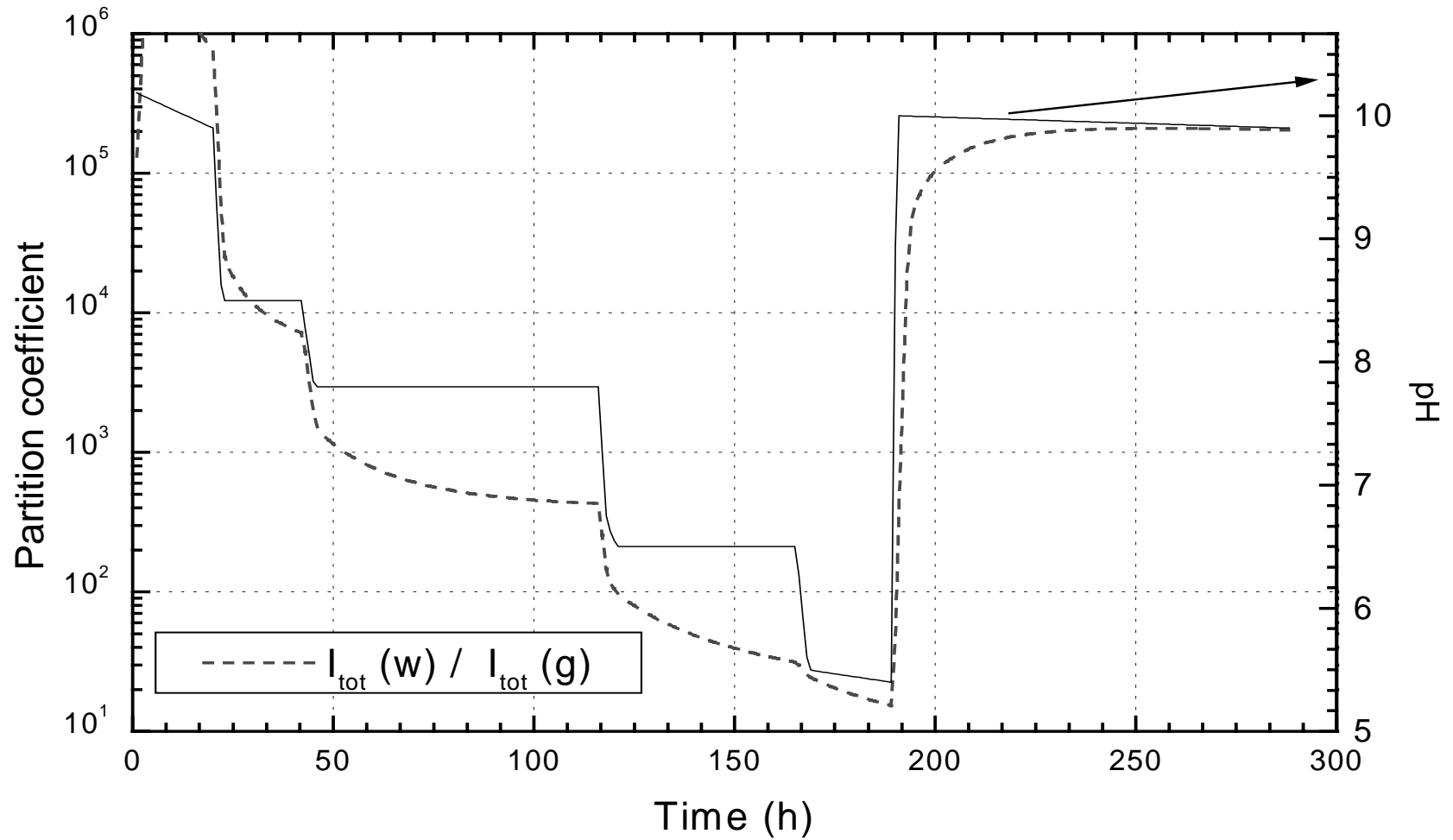
Results to RTF-ISP-41, stage 1: Iodine species in gas phase and modelled pH evolution



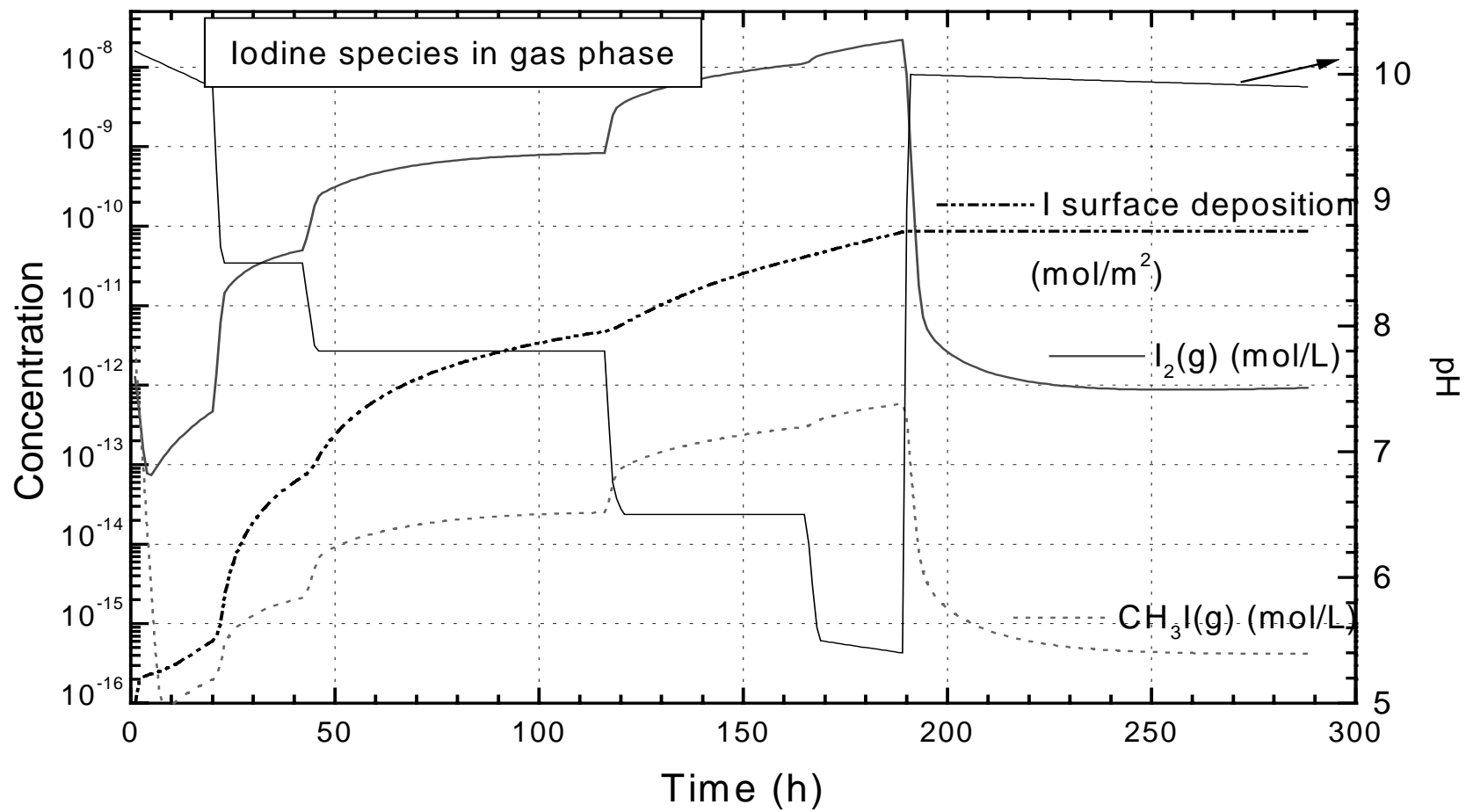
**Results to RTF-ISP-41, stage 1: Iodine species in water phase and modelled pH evolution**



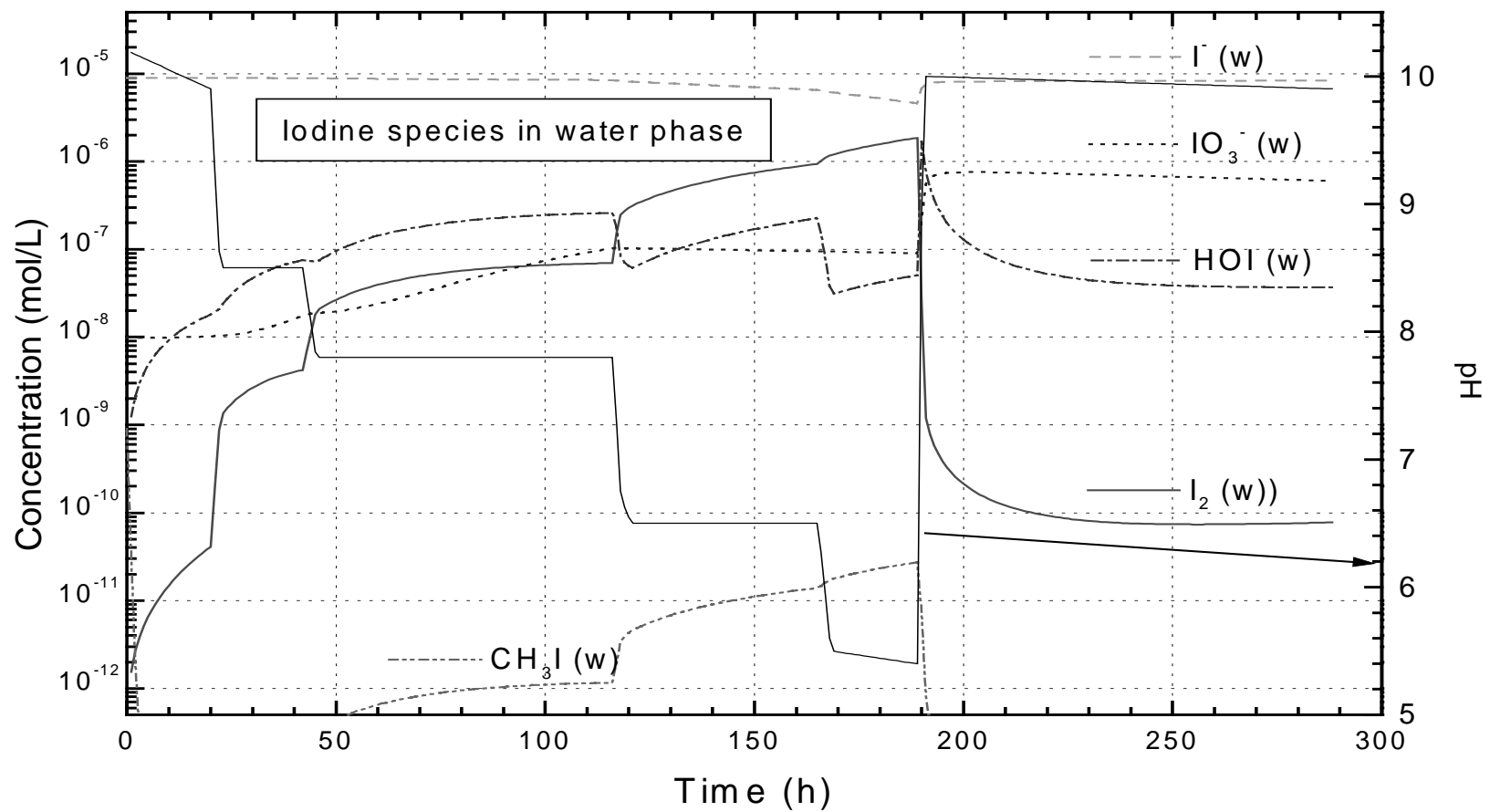
**Results to RTF-ISP-41, stage 2:** Inventory of iodine in gas (g) and water (w) phase and modelled pH evolution



**Results to RTF-ISP-41, stage 2: Partition coefficient of total iodine and modelled pH evolution**



Results to RTF-ISP-41, stage 2: Iodine species in gas phase and modelled pH evolution



Results to RTF-ISP-41, stage 2: Iodine species in water phase and modelled pH evolution

**SIMULATION OF ISP-41 EXPERIMENT  
WITH MODIFIED IODE CODE  
(IODINE BEHAVIOR IN CONTAINMENT UNDER SEVERE  
ACCIDENT CONDITIONS)**

Adolf Rydl  
Nuclear Research Institute Rez

Report UJV Rez, May 1998



## EXECUTIVE SUMMARY

### I. Introduction

The International Standard Problem (ISP) No.41 is the OECD CSNI (Committee on the Safety of Nuclear Installations) exercise on iodine behavior in containment under conditions relevant to reactor safety. The reason why the Czech Republic representatives decided to participate in this exercise was the need to examine the capabilities of the IODE code<sup>[1]</sup> for predicting the iodine behavior under severe accident conditions and to examine our abilities to use this code. This code is now our only tool which can be used for such purposes. As the contribution of radioiodine to risk -following the possible release of radioactivity to the environment at an accident in a commercial nuclear power plant- is the highest among all the fission products<sup>[2]</sup>, the necessity to try to understand the iodine behavior is obvious. The experience which may be gained from participating in ISP-41 exercise could help us to improve this understanding.

The primary objective of any ISP exercise is the evaluation of the capabilities and the performance of large thermal-hydraulic codes which are used to perform safety and licensing analyses of nuclear power plants<sup>[3]</sup>. This evaluation can be accomplished by comparing the code predictions with the results of the selected experiments. In our case, the capabilities of the codes used to predict the iodine behavior in containment under severe accident conditions are to be evaluated by comparing their predictions with the results of one of the RTF (Radioiodine Test Facility) tests which were carried out at AECL's Whiteshell Laboratories, Canada. The only similar exercise on iodine containment behavior under accident conditions was the Advanced Containment Experiments (ACE) Phase B program<sup>[15]</sup> to which several, but not all, OECD member countries participated<sup>[6]</sup>. In that time in Czech Republic we had no tool (no program) which could be used to simulate complex interactions of iodine in containment.

At the beginning of the work on this ISP we thought that this exercise would be a blind one, i.e. that the participants would have no access to the test results until the calculations are made and sent to the ISP organizer<sup>[3]</sup>. Only after having performed a lot of calculations trying to tune the program and the input data by the simulation of the ACE RTF 4 experiment results<sup>[4]</sup> (the only ACE iodine experiment carried out in the same stainless steel test vessel as the ISP experiment) we became aware that the results -not all the results, but the most important part of them- of the test which was offered as an ISP were published in the open literature<sup>[5]</sup>. Afterwards it was much easier for us to do some calculations. However, it is not sure now whether the results of our calculations and particularly our rationale would be the same (or even similar) as without this knowledge.

## II. Background

The study of the radioiodine behaviour in the event of a severe accident in LWR suggests that iodine would be released from RCS to containment primarily in the form of CsI carried on aerosols (airborne). CsI is non-volatile species under containment conditions. In the case when the aerosols are successfully removed from the containment atmosphere to the sump water by the engineered safety systems (sprays) or by natural processes, the formation of gaseous iodine species becomes a risk-significant issue. Non-volatile iodide anion I<sup>-</sup> initially formed by the dissolution of CsI in the sump water can be oxidised by radiolytic or thermal reactions to volatile molecular iodine I<sub>2</sub>. Reactions with organics can lead to formation of volatile organic iodides. All these volatile iodine species are relatively quickly transferred to the containment atmosphere and, as they cannot be easily removed from the atmosphere, they can represent long term threat to safety (e.g. leakage of gaseous iodine to the environment). Such defined iodine volatility (i.e. something like a total amount of gaseous iodine species in containment atmosphere) is then an issue which is now one of the most important parts of the research concerning iodine behaviour under accident conditions. In determining the formation of volatile iodine in the aqueous phase under radiation conditions the most important parameter is the sump pH<sup>[18]</sup> (the lower the pH is the higher is the iodine volatility). The maintenance of a high pH (approximately pH>8) is recognised to be an important accident management tool.

The ISP experiment is one of approximately 20 AECL's RTF tests, which were designed to study iodine volatility in a simulated containment environment<sup>[6]</sup>. All the RTF tests were intermediate-scale, "all-effects" experiments. A detailed description of the RTF and of the procedures used in the experiments is given in [4]. In the ISP experiment the containment building was simulated by a 340dm<sup>3</sup> stainless steel cylindrical vessel with the aqueous phase volume of 25dm<sup>3</sup>. Inside the vessel there was placed a Co-60 radiation source providing an average dose rate of 1.36kGy/hr. The main objective of the test was to investigate the effect of pH on iodine volatility at 25°C in the presence of radiation<sup>[5]</sup>. The pH of the water phase was being changed in a step-wise manner during the test. The test had 2 stages, the first one lasted 360 hours and the second 285 hours. Between the 2 stages the vessel was thoroughly washed and air dried. Both stages were initiated with the addition of <sup>131</sup>I-labeled solution of CsI into the vessel to get there 25 liters of 9x10<sup>-6</sup>M CsI. The input pH profile for both stages is given in figures V.01 and V.02. During the test the aqueous pH, dissolved oxygen concentration, total aqueous and gas phases iodine concentrations, iodine speciation, and some other parameters were measured<sup>[6]</sup>. A detailed description of what was measured at the RTF tests and how is given in [4]. The ISP exercise participants were asked to calculate the total concentrations of iodine in both phases, speciation of iodine in both phases, and the mass of adsorbed iodine on surfaces exposed to the gas and aqueous phases. The participants should explain their rationale on what processes dominate the speciation and distribution of iodine and they also should identify the input parameters or variables which the iodine behaviour is most sensitive to in their calculations.

In this report, when speaking about the current understanding of iodine behaviour in containment under accident conditions, we will almost exclusively use reports and relevant papers written in Canada. One reason is that the RTF tests are Canadian tests and we must suppose that Canadians know best about their own experiments. The other reason is connected with the fact that the whole integrated Canadian iodine chemistry program <sup>[6]</sup> is the most comprehensive experimental program we know about.

As we had known the results of the ISP experiment beforehand we did not try in our simulations to obtain the best estimate, instead we wanted to be sure that the IODE code is capable to calculate conservative estimate. We thought that for an empirical model like IODE it would be much more useful to ensure ourselves that we are able to get (even highly) conservative results. It means that for various simulations we would always like to get conservative estimates with IODE, even though the differences in results between the calculation and the experiment would be very high for some cases. In fact, for the ISP simulation it turned up to be difficult (it was not easy to obtain with IODE a conservative estimate for the ISP test). We also tried to obtain the results using only the most important (most important in our opinion) reactions or correlations from all those available in IODE, neglecting as much of those less important processes as we could (e.g. aqueous reactions involving organics or gas phase reactions). This was aimed at the verification of IODE capabilities to model just the important processes without necessity to use all the available reaction schemes at the same time.

### **III. Tools for predictions of iodine volatility**

Iodine volatility (as was spoken of above) is determined mainly by the aqueous phase radiochemistry, mass transfer of volatile species between water and the atmosphere, and the sorption on surfaces in the aqueous and gas phases. Under the conditions, which one can expect in a severe accident, on a time scale of the accident, thermodynamic equilibria among aqueous iodine species will not be achieved <sup>[10]</sup>. Therefore, to determine the iodine speciation and distribution we must be able to model all the dominating time-dependent processes, which are usually very complex. This task simply requires having a computer program, which can model all the important kinetic phenomena at once.

Various kinetics codes for predicting iodine behaviour have been developed <sup>[7]</sup>. They can be divided -according to the approaches used- to 2 groups: mechanistic and empirical. Mechanistic codes, such as LIRIC (Canada) and INSPECT (UK), consist of a large set of reactions which should represent actual chemical processes in a way that is as mechanistic as it is possible. On the other hand, in the empirical codes their developers are trying to model only the most important phenomena and a small number of chemical reactions. Some of the reactions do not represent real chemical processes but they just

model the overall effects of various parameters on the formation of volatile iodine species. Such modelling requires empirical fitting of correlation constants against the experimental data. Representatives of this approach are French code IODE and PSI Switzerland code IMPAIR. These 2 codes are very much alike <sup>[7]</sup>. In Nuclear Research Institute (NRI) Rez, which is the only institution in the Czech Republic where the codes capable of modeling severe accident phenomena are used, we are working with the French code IODE. We had obtained this code on the basis of the co-operation with IPSN/CEA Cadarache, France <sup>[8,9]</sup>. The newest version of the code we have is IODE Release 4.0 <sup>[11]</sup> which is a multi-compartment version of IODE. However, for the ISP simulation we decided to use older, single-compartment version of the code and we made some modifications to this version. The model and all the modifications to it will be described in detail in the next chapter. General information of what and how the IODE code calculates can be found in its manual <sup>[1,11]</sup> and in the European Commission report Iodine Code Comparison <sup>[7]</sup>

#### **IV. Iodine volatility in containment and its modelling with modified IODE**

The most important processes, which determine the iodine volatility, are the aqueous iodine chemistry, mass transfer of the volatile iodine species from the water phase to the containment atmosphere and sorption of iodine species on various surfaces both in gas phase and in water phase. Iodine chemistry in gas phase is not so much important <sup>[10]</sup>.

Most of all our sensitivity calculations was performed for the stage 1 of the ISP experiment. We hoped that if we are able to simulate the first stage of the test somehow we could obtain reasonable results with the same input parameters also for the second stage and it really has happened.

##### ***IV.1 Aqueous phase***

In the presence of radiation, the most important reactions with regard to iodine volatility are the reactions of iodine species with water radiolysis products, hydrolysis of molecular iodine followed by disproportionation of HOI and reactions with organics <sup>[12]</sup>. In the IODE code all the aqueous iodine chemistry is modelled by 13 reactions (as mentioned earlier these do not necessarily represent actual chemical processes). Any of those 13 reactions can be switched off in the input, which means that the process represented by such a reaction will not be modelled.

##### ***IV.1.1 Inorganic thermal reactions***

In fact, the most important thermal reaction from the point of view of iodine volatility is the reaction of iodine species with hydrogen peroxide <sup>[12]</sup>. However, this reaction itself is not modelled in IODE. As H<sub>2</sub>O<sub>2</sub> would be formed as a primary water-radiolysis product

(i.e. only in the presence of radiation), its effect on iodine volatility is in IODE modelled together with the effect of radiation induced reactions in a global parametric reaction scheme (there are 2 such reactions in IODE: oxidation of iodide by radiation and decomposition of iodate by radiation). Therefore, we will not speak about the reaction with H<sub>2</sub>O<sub>2</sub> in this paragraph but in the next one. Also the thermal reactions with organics will be dealt with in a separate paragraph. In this paragraph we will first speak about the other thermal reactions as they are modelled in IODE and then we will comment on how this part of IODE modelling corresponds -in our opinion- to actual iodine sump water chemistry under accident conditions.

For the first three aqueous reactions in IODE which will be described below we always used in our simulations default values of kinetic constants. Most of the values of kinetic constants (for 25°C) in IODE can be changed in user input. Our only try to change the defaults for first 3 reactions was the comparison of using the so called Bell-Thomas model of HOI disproportionation with Toth model (cf. below). The models, the original references, and the recommended values for various user input parameters are described in [11].

The first modelled aqueous reaction in the code is the hydrolysis of molecular iodine



This reaction is relatively fast, with the reaction rate being modeled as

$$d[\text{I}_2] / dt = -d[\text{HOI}] / dt = -k[\text{I}_2] + k'[\text{I}_2] [\text{HOI}] [\text{H}^+],$$

where the default value of kinetic constant  $k$  for 25°C is  $3.0\text{s}^{-1}$ ,  $k' = k / K$ , and  $\log_{10}K = -5.634 \times 10^{-5} / T^2 + 575.7 / T - 7.893$  ( $T$  -water temperature in K). Subsequent HOI dissociation



is considered in the code to be very fast, reaching thus the equilibrium immediately. Reaction equilibrium constant used in the program is

$$K = [\text{OI}^-] [\text{H}^+] / [\text{HOI}], \quad \text{where } \log_{10}K = -80670 / T + 2800.48 + 0.7335 T - 1115.1 \log_{10}T$$

The third reaction is the slow disproportionation of HOI



For this reaction there can be used 2 different schemes in the code (input option): either so-called Bell-Thomas formalism (default in IODE) or Toth formalism (which is in exactly the same form used as the only choice in the IMPAIR code). According to the Bell-Thomas formalism the reaction rate is expressed as

$$d[\text{HOI}] / dt = -3 d[\text{IO}_3^-] / dt = -k [\text{HOI}]^2 + 3 k' [\text{IO}_3^-] [\text{I}]^2 [\text{H}^+]^2 - k'' K [\text{HOI}]^2 / [\text{H}^+]$$

with the default values of kinetic constants at 25°C  $k=100.0\text{M}^{-1}\text{s}^{-1}$ ,  $k''=0.0\text{M}^{-1}\text{s}^{-1}$ ,  $k'=6.7\times 10^8\text{M}^{-4}\text{s}^{-1}$ , and  $K$  is the dissociation constant of HOI (using the recommended value for  $k''$  means that the third term in the reaction rate definition disappears). The Toth formalism gives the reaction rate

$$d[\text{HOI}] / dt = -3 d[\text{IO}_3^-] / dt = -k [\text{HOI}]^2 - 3 k' [\text{IO}_3^-] [\text{I}] [\text{H}^+]^2 \quad (\text{IV.1.04})$$

where  $k'=1.1\times 10^5\text{M}^{-3}\text{s}^{-1}$  at 25°C and  $k$  is tabulated in the program as a function of pH<sup>1</sup>. The main difference between the two approaches is the modeling of the reverse reaction (Dushman reaction) which is the second order in  $[\text{I}]$  in the Bell-Thomas model and the first order in  $[\text{I}]$  in the Toth model. Anyway, according to [7] the two models are very similar. For the stage 1 of the ISP experiment we have tried to compare 2 IODE calculations using these 2 models and the results are in figures IV.01 and IV.02 (all other input parameters and various IODE options used in these calculations were similar to those described later in this chapter and in chapter V., i.e. similar to those used for the calculation which reproduces best the ISP iodine behavior)<sup>2</sup>. It can be seen that the difference is really not very big.

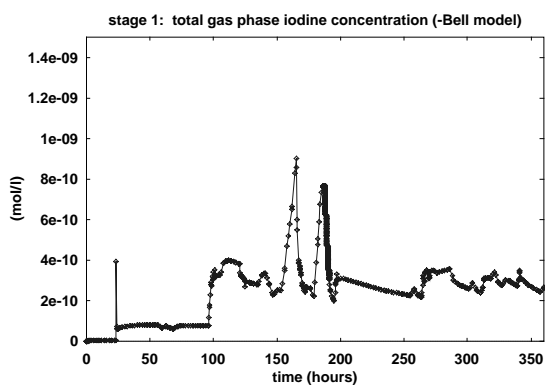


Figure IV.01

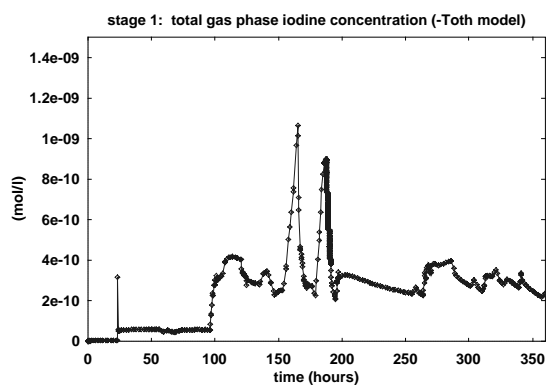


Figure IV.02

1. The algorithm which is used in our version of IODE to calculate  $k$  is given in Appendix.
2. Particularly, the sorption model described in paragraph IV.4 was used with the values of sorption coefficients  $k_{\text{ads}}=6\times 10^{-3}\text{dm/s}$  and  $k_{\text{des}}=7.5\times 10^{-7}\text{s}^{-1}$ .

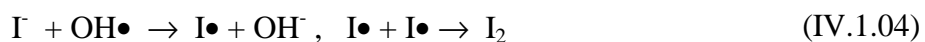
The last inorganic thermal reaction modelled in IODE is a slow oxidation of I<sup>-</sup> by the oxygen dissolved in the sump water. As this reaction is unlikely to have great impact under radiolysis conditions (even in the code manual <sup>[11]</sup> it is written that “this reaction is generally considered to have little impact on iodine chemistry in reactor conditions”) it was not used in our simulations.

Even though the chemistry represented in IODE by the reactions discussed above is likely to be much more complex in reality <sup>[13]</sup> we may say that this part of IODE model is good enough. We did not play with the default values of kinetic constants for the reaction IV.1.03 when simulating the ISP. We have found that for the ACE RTF 4 experiment these defaults gave reasonable results but it need not mean anything as the ACE RTF 4 test was carried out at 60°C and the temperature dependence, though it is modeled in IODE, can change a lot of things. With all the defaults we were able to get slightly conservative results for ISP (compare figures IV.01, IV.02 with figures 3 and 4 in [5]). As the hydrolysis of iodine is one of the two principal reactions that are pH dependent <sup>[13]</sup> we were awaiting an adequate response of the amount of gas phase iodine on pH changes and we are satisfied with that. Anyway, we think that iodine volatility is more sensitive to changes in parameters for reactions with water-radiolysis products than for the thermal reactions discussed above. Because the reaction IV.1.03 is the main source of IO<sub>3</sub><sup>-</sup> we were also awaiting a reasonable ratio of I<sup>-</sup> to IO<sub>3</sub><sup>-</sup> concentrations in the ISP simulation -in our opinion it should be something similar as in the ACE RTF 4 test <sup>[4]</sup>- and we are also satisfied with that (cf. figure V.13).

#### IV.1.2 Iodine reactions with water radiolysis products

In this paragraph, we first summarise some Canadian views concerning the aqueous iodine chemistry in the presence of radiation in order to know roughly what we are to model and then we describe the IODE approach and show the results of the various calculations which were carried out to find the best reproduction of the iodine behaviour in the ISP test.

According to [5] there are 2 iodine reactions particularly important in determining iodine volatility under accident conditions. The first reaction is the oxidation of I<sup>-</sup> by OH• radical (primary water-radiolysis product) to I• radical followed by combining I• radicals to form I<sub>2</sub>



The second reaction is the reduction of I<sub>2</sub> by a range of water-radiolysis products, particularly the reduction of free iodine (I<sub>2</sub> / HOI / OI<sup>-</sup>) by hydrogen peroxide and the reduction of molecular iodine by superoxide O<sub>2</sub><sup>-</sup> which is formed in aerated water solutions by the reaction of dissolved oxygen with radiolytically produced electron

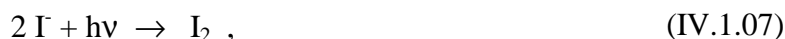


and



According to [5] the first reaction IV.1.04 is mainly responsible for the significant increase in iodine volatility in the presence of radiation, whereas the second reaction IV.1.05, IV.1.06 can explain the observed pH dependence of this volatility. Reactions IV.1.05 and IV.1.06 exhibit a strong inverse dependence on [H<sup>+</sup>] which means that the rate of iodine reduction will be drastically reduced with decreasing pH allowing thus the build-up of volatile molecular iodine<sup>[12]</sup>. In [5] there is also mentioned the role of metal impurities which can, even at trace concentrations, influence the iodine volatility by the reactions with H<sub>2</sub>O<sub>2</sub> and O<sub>2</sub><sup>-</sup>. The role of organic impurities will be discussed in the next paragraph.

All the complex chemistry described above is modeled in IODE by 2 reaction schemes<sup>[11]</sup>: The first reaction is the oxidation of iodide by radiation



reaction rate being modelled as

$$\frac{1}{2} \frac{d[I^-]}{dt} = -\frac{d[I_2]}{dt} = -k_7[I^-] [H^+]^n D + k_7'[I_2] \quad (IV.1.08)$$

with these defaults: n=0.5 (n represents character of pH dependence), k<sub>7</sub>=1.7x10<sup>-3</sup>M<sup>-0.5</sup>Gy<sup>-1</sup>, k<sub>7</sub>'=2.0x10<sup>-5</sup>s<sup>-1</sup>. D is (radiation) dose rate in Gy/s. This model is similar to that used in the IMPAIR code<sup>[7]</sup>; different is the effect of the reverse reaction which is negligible in IMPAIR (k<sub>7</sub>'=0). The second reaction is the decomposition of iodate by radiation



with the reaction rate

$$\frac{1}{2} \frac{d[IO_3^-]}{dt} = -\frac{d[I_2]}{dt} = -k[IO_3^-] [H^+]^n D + k'[I_2] \quad (IV.1.10)$$

The IODE model links the reaction rates of reactions IV.1.07 and IV.1.09 through the default values of kinetic constants and through the value of the exponent n: the default values of kinetic constants k and k' in IV.1.10 are equal to the default values of kinetic constants k<sub>7</sub> and k'<sub>7</sub> (k=k<sub>7</sub>, k'=k'<sub>7</sub>) and there can be given only one value of the exponent n in the IODE input deck for the definition of both reaction rates IV.1.08 and IV.1.10.

In our simulations we had found that in IODE the key aqueous phase reaction (to which the iodine volatility is the most sensitive) is the reaction IV.1.07. This was, of course, anticipated and it corresponds to general understanding of the relevant chemistry under radiation conditions (cf. above). Our understanding is that the other reaction, reaction IV.1.09, simply serves as a sink for IO<sub>3</sub><sup>-</sup> produced by the reaction IV.1.03 (in the code there is no other way of getting rid of IO<sub>3</sub><sup>-</sup>). This corresponds to the modeling approach in the IMPAIR code where the two reactions are not linked together as they are in IODE and where the second reaction is modeled in a different way<sup>[7]</sup>



with the reaction rate

$$d[\text{IO}_3^-] / dt = -k_{\text{IMP}}[\text{IO}_3^-]^{1.3} D \quad (\text{IV.1.12})$$

The reaction rate definition (IV.1.12) means that, as opposed to IODE, the reverse reaction is not modeled. According to our results -particularly with regard to calculated ratios of IO<sub>3</sub><sup>-</sup> to I<sup>-</sup> water phase concentrations- the reaction model IV.1.11 and the reaction rate definition IV.1.12 are more suitable than those used in IODE<sup>3</sup> (for calculations we used both the original version and the modified version of IODE which was prepared to enable us modeling similar to that in IMPAIR). Therefore, for our simulations we were using later on the reaction model IV.1.11 with the corresponding reaction rate IV.1.12 in a modified version of the IODE code. Values of the relevant kinetic constants for both IV.1.11 and IV.1.07 were not taken from IMPAIR; instead, they were estimated from the comparison with the experimental results.

With all the defaults for the inorganic thermal reactions (cf. paragraph IV.1.1) the reactions IV.1.07 and IV.1.09 are crucial for iodine volatility modeling in IODE. This means that given we have the reversible physical sorption model (as it is proposed in [5], cf. paragraph IV.3) for I<sub>2</sub> sorption on surfaces in gas phase (and no sorption on water phase surfaces) and a fast mass transfer between the sump and the atmosphere, the only adjustable parameters in IODE which can affect the results considerably are the values of n in IV.1.08 and of the kinetic constants in IV.1.08 and IV.1.12. With the given sorption model and with the values of the sorption coefficients taken from [5] it was difficult to obtain conservative estimation of the gas phase iodine concentration for almost any

---

3. Even the French researchers who are responsible for the development of the code [14] have already questioned the mechanism of the reaction IV.1.09 as it is coded in this version of IODE. They then proposed the mechanism which is more like IMPAIR model (IO<sub>3</sub><sup>-</sup> → I<sup>-</sup>) but which still keeps the link between this reaction and the reaction IV.1.07.

reasonable combination of  $n$  and corresponding kinetic constants (for us reasonable meant something between  $n=0.1$  and  $n=0.5$  -cf.[11]). The results of the IODE calculation with the input values which are, according to [7], similar to those used in IMPAIR ( $n=0.1$ ,  $k_7=2 \times 10^{-5}$ ,  $k_{IMP}=1.4 \times 10^{-5}$  and dose rate  $D$  in Gy/s; always used  $k_7'=0$ ; IMPAIR  $k_7$  is lower than  $2 \times 10^{-5}$ ) are given in figures IV.03 and IV.04<sup>4</sup>.

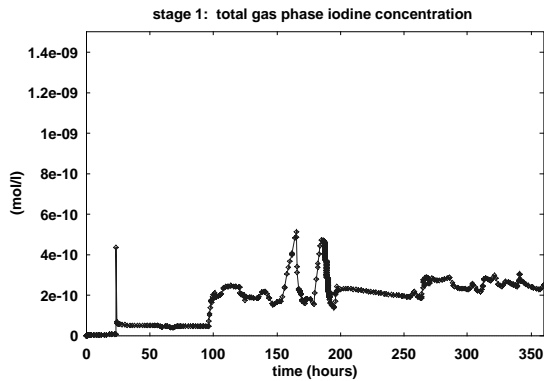


Figure IV.03

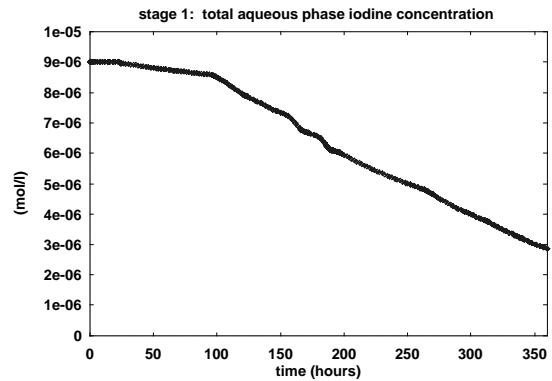


Figure IV.04

To get such a result which is close enough to the experiment but not conservative (cf. figures 2 and 3 in [5]) the value of  $k_7$  had to be higher than that given in [7]; with the number given in [7] which is something like  $k_7=1.1 \times 10^{-6}$  the results would be much worse (highly non-conservative). Also the ratio of  $[IO_3^-]$  to  $[I^-]$  was in this calculation higher than we thought it should be. With further increasing the value of  $k_7$  the effect was different from what we were expecting. Thus, as it was not possible to obtain conservative results for the pH dependence  $n=0.1$  even with higher  $k_7$  we decided to use the dependence  $n=0.5$  which is much “stronger”: the value of  $[H^+]^{0.5}$  increases with the pH decrease much sharply than  $[H^+]^{0.1}$ . The result for  $n=0.5$ ,  $k_7=0.1$ , and  $k_{IMP}=0.01$  is given in figure IV.02. In our simulations with IODE this character of pH dependence (i.e.  $n=0.5$ ) complied best with our requirement to be able to get conservative estimates of the experimental results. However, for a different temperature than  $25^\circ\text{C}$  this approach would need more profound insight into, as was indicated by our simulations of ACE RTF 4 test (temperature  $60^\circ\text{C}$ ).

Comparing the very simple modeling scheme in IODE (IV.1.08 and IV.1.12) with very complex processes it should represent (IV.1.05, IV.1.09) one can anticipate difficulties which will arise when this empirical scheme is to model something at different conditions than at those which were used at deriving the scheme. With the original model in IODE [11] we were not able to get conservative estimate of the ISP test (it was also difficult for ACE RTF 4 test). Even with the modified IODE we have some problems to obtain conservative estimate for known experimental results of the ISP. Our feeling is that the

4. As in the calculations presented in paragraph IV.1.1, figures IV.01 and IV.02, the sorption model described in paragraph IV.4 was used with the values of sorption coefficients  $k_{ads}=6 \times 10^{-3} \text{ dm/s}$  and  $k_{des}=7.5 \times 10^{-7} \text{ s}^{-1}$ .

IODE model of the pH dependence for the iodine reactions with the water radiolysis products is overly simplified. Because we do not have any relevant experimental data we cannot say anything about the IODE modelling of the dose rate dependence. As there is no radiolysis model in IODE such things like the amount of dissolved oxygen (which would influence the formation of O<sub>2</sub><sup>-</sup>) and the amount of metal impurities which can be important in real accident situations have no effect on the results obtained with IODE.

#### IV.1.3 Reactions with organics

During an accident various types of organic impurities may be found in the sump water. They can be released to the water from various paints, oils, cable insulation, and other organic materials. Organic compounds can react thermally and radiolytically with iodine to form organic iodides<sup>[5]</sup>. Some of these iodides are likely to be volatile (like, for instance, CH<sub>3</sub>I) and these can be readily transferred to the atmosphere increasing thus the amount of volatile iodine species in gas phase. On the other hand, formation of relatively involatile iodides of various ketones, alcohols and phenols can reduce iodine volatility by reducing the amount of I<sub>2</sub> in water<sup>[17]</sup>. Under radiation conditions organic species can readily decompose to carboxylic acids which may significantly decrease the pH of the water<sup>[5]</sup>. According to [10] this action of organics may be their strongest influence on iodine volatility. However, this is not important for the ISP exercise where the pH profiles are the input parameters and where there was only very small amount of organics present anyway.

For the ISP experiment, which was carried out in a stainless steel vessel with no deliberate addition of organic compounds, the aqueous organic iodide concentration was observed to be about the same as that of I<sub>2</sub> and the organic iodide concentration in the gas phase remained during the test constant and small compared to the I<sub>2</sub> concentration<sup>[5]</sup>.

Because very little is known about the organic iodides, which are actually formed in containment, the IODE code uses generic name (and formula) methyl iodide, CH<sub>3</sub>I, to represent all the organic iodides<sup>[11]</sup>. There are five aqueous reactions involving organics. Two of them are irrelevant to the ISP simulation: the hydrolysis of methyl iodide with OH<sup>-</sup> ions which is said in the code manual to be negligible in the ISP relevant pH range (and we had found that it really is negligible) and the formation of CH<sub>3</sub>I by surface processes. The other three reactions are these:  
correlation called formation of methyl iodide



where R represent some organic radical,  
methyl iodide radiolytic decomposition



and hydrolysis of methyl iodide



In our modified version of IODE we changed the definition of the reaction IV.1.13 to have there, instead of  $\text{CH}_3\text{R}$  species, the same  $\text{CH}_3\bullet$  species as in reaction IV.1.14. Taking into account all the reaction rate definitions and the recommended values of kinetic constants (cf. [11]) this modified way of modelling, in fact, will represent the case with the constant amount of organics available all the time to react with  $\text{I}_2$  (and thus to form the organic iodide). Anyway, this is not very important, especially not for the ISP simulation.

When simulating the ISP we were assuming that the organic iodide formation and behaviour in both phases is determined by homogeneous aqueous phase reactions<sup>[17]</sup>. It means that we did not model any reaction of  $\text{I}_2$  with organics in the atmosphere and that we suppose that all methyl iodide in the atmosphere was formed in the sump and then transferred to the gas phase (cf. paragraph IV.3).

By the comparison of IODE calculations with the experimental data from the ACE RTF-4 and ISP tests we have found that the IODE aqueous phase reactions involving organics do not represent the observed iodine behaviour in a proper way. For instance, when the model predicts similar amounts of  $\text{CH}_3\text{I}$  and  $\text{I}_2$  in the atmosphere then in water it has the  $\text{I}_2$  concentration by more than an order of a magnitude higher than the  $\text{CH}_3\text{I}$  concentration<sup>5</sup>. This contradicts the experimental findings in both the ACE RTF 4<sup>[4]</sup> and ISP tests. One likely explanation can be the fact that in IODE all organic iodides are represented by  $\text{CH}_3\text{I}$  and thus transferred to the atmosphere as  $\text{CH}_3\text{I}$ , i.e. much faster than  $\text{I}_2$  taking into account equilibrium partition coefficients for  $\text{CH}_3\text{I}$  and  $\text{I}_2$ . This approach does not take into account the presence of relatively involatile organic iodides which were identified in water phase and which reduce the total organic iodide volatility. As we know that the actual organics involving chemistry in the sump is much more complex than the IODE model and even that this chemistry still needs further research, we are not surprised by the limited capabilities of the code. On the other hand, our results also indicate that the IODE aqueous reactions with organics do not influence considerably the other chemical processes (which are here much more important for determining the iodine volatility). It means that the concentrations of the important species and their ratios will remain similar no matter if the reactions IV.1.13, IV.1.14, and IV.1.15 are used or not. For the ISP simulation this enables us to omit not only the gas phase organic reactions with  $\text{I}_2$  but all such reactions (i.e. also reactions IV.1.13, IV.1.14 and IV.1.15). It can be done also because the amount of the volatile organic iodides in the atmosphere was measured to be very small compared to  $\text{I}_2$ <sup>[5]</sup>. Thus, in our results there are no organic iodides present, neither in water nor in the atmosphere. For the ACE RTF-4 simulation, the situation was

---

5. Again, this result was obtained with the given sorption model (cf. paragraph IV.4) for  $\text{I}_2$  sorption on gas phase surfaces (and no sorption on water phase surfaces) and a fast mass transfer between the water and the atmosphere. No reaction of  $\text{I}_2$  with organics in gas phase was used.

different (cf. [4]) and we had to use the reactions IV.1.13, IV.1.14 and IV.1.15 and to try to get as good results as it was possible with the given model. Our results then were nothing too much. The omission of all the organics involving reactions for the ISP simulation complies also with our wish to have the model as simple as it is possible.

## IV.2 Mass transfer

The understanding of the transfer of molecular iodine and volatile organic iodides between water and the atmosphere is an important step in determining the iodine volatility. The transfer of a single volatile species across an interface is usually modeled by assuming a two-film model<sup>[16]</sup>. This model assumes that steady-state concentration profiles have been established in the boundary regions of both phases and that interfacial kinetics are not limiting<sup>[22]</sup>. Such a model is used also in IODE:

$$\text{flux of a species across the interface} = K (C_w + P C_g), \quad (\text{IV.2.01})$$

where K (in m/s) is the so called overall mass transfer coefficient, and  $C_w$  and  $C_g$  are bulk concentrations of a species in water and gas phases, respectively. P is the equilibrium partition coefficient of a species, i.e. the ratio of the volume concentration of a species in the aqueous phase to that in the gas phase at equilibrium ( $C_w^*$  and  $C_g^*$  are equilibrium concentrations)

$$P = (C_w^* / C_g^*)$$

The IODE code considers the water-atmosphere material transfer of 2 species: molecular iodine and methyl iodide ( $\text{CH}_3\text{I}$  should represent all organic iodides). Partition coefficients of these 2 species are defined in the code as follows

$$P(\text{I}_2) = 231.285 \exp(1.65017 \times 10^{-4} (T - 571.243) (T - 273.15)) \quad (\text{IV.2.02})$$

and

$$P(\text{CH}_3\text{I}) = \exp(-6.97 + 2641./T), \quad (\text{IV.2.03})$$

where T is water temperature in K. These definitions are very similar to those given in [16]. With the given value of P, the overall mass transfer coefficient K whose value reflects the thermal hydraulic conditions (flow characteristics near the interface and the properties of the fluid medium) is the key variable to be determined. In IODE, K can be either input by the user or it can be calculated by the code from the analogy between mass and heat transfer for natural convection conditions (cf. [11]). In our calculations we had to input some value of K because when there is no temperature gradient between water and the atmosphere the model in IODE does not calculate any transfer. Our modified version of IODE enables us to calculate diffusion of  $\text{I}_2$  and  $\text{CH}_3\text{I}$  across the interface<sup>[9]</sup> even under conditions of zero temperature gradient, but this model is not very useful for

accident conditions where one can expect that induced flows will drive the transfer (for example circulating flows induced by venting or temperature gradients with respect to wall surfaces in the gas phase or recirculation of water). Under such conditions we can expect relatively fast mass transfer compared to the rate of the water phase chemical reactions. This is also the case of the ISP test where good mixing of both gas and aqueous phases was ensured by forced recirculation (30 liters/minute circulation in the gas phase and 10 liters /minute in the aqueous phase). Thus, in our simulations, we assumed that the mass transfer in the experiment was so fast that it did not influence the iodine volatility. Therefore we had chosen such a value of K so that any faster transfer (any higher value of K) did not affect the results. As we did not model organic iodide formation (cf. paragraph IV.1.3) the only transferred species was I<sub>2</sub>. The chosen value of K for I<sub>2</sub> was 5x10<sup>-5</sup> m/s. This number then represents the mass transfer of I<sub>2</sub> between water and the atmosphere which is fast enough to not interfere with other processes which determine the iodine volatility.

As can be seen in figures V.03, V.04, V.05, and V.06 and in figures 2, 3, 5, and 6 in [5], our results obtained with the fast mass transfer model look reasonable. One interesting thing is the iodine behaviour in the stage 2 of the ISP test. According to IODE, after rapid increase in pH value from 5.5 to 10 at 192hr, there was sudden decrease in water phase concentration of I<sub>2</sub>. This was probably caused by immediate transfer of all I<sub>2</sub> which was at that time in water when new aqueous I<sub>2</sub> was being formed at such a high pH only very slowly. According to IODE, since this time the concentration of I<sub>2</sub> in water is lower than the concentration of I<sub>2</sub> in gas phase, only slowly returning to equilibrium (cf. fig. V.12). During all this time the mass transfer of I<sub>2</sub> goes from the gas phase to the water phase. In our version of IODE this mass transfer uses the same value of K as the mass transfer from water to the atmosphere. In new versions of IODE there is a possibility to input different values of K for different directions of the transfer. In fact, we were not sure what value of K should be input for the reverse direction of the transfer, so we did not change our version of the code and we let it calculate the transfer in both directions with the same value of K.

### ***IV.3 Gas phase***

Probably the only interesting gas phase chemical process from the point of view of iodine volatility is the potential production of organic iodides in the atmosphere. In IODE there is an empirical scheme which could model this somehow. However, as we do not model in our simulations any organic involving reactions (cf. paragraph IV.1.3) we also have not used this reaction. Anyway, some new experimental results suggest <sup>[10]</sup> that neither thermal nor radiolytic production of organic iodides in the atmosphere is important compared to their production in water.

#### IV.4 Sorption on surfaces

Our sorption modelling was based on what was written about it in [5]. As already has been observed in ACE RTF-4 [4], sorption on stainless steel can affect the iodine volatility considerably (sorption on painted surfaces can be even more important but this was not studied in the ISP experiment). In fact, most of the iodine which has been lost from the water in both the ACE RTF-4 and the ISP tests was likely to be deposited on surfaces (this lost iodine represented about 80% or even more of the initial iodine inventory -cf. figure 2 in [5] and figure 6 in [12]). It is assumed that the chemical form of iodine which will adsorb on surfaces is molecular iodine  $I_2$ . According to [21] the most important process is the sorption on surfaces in the gas phase. This means that after radiolytic formation of aqueous  $I_2$  and subsequent volatilisation, deposition of this  $I_2$  on gas phase surfaces occurs [12]. Though the iodine balance in the ACE RTF-4 test suggests that considerable amount of iodine can also be deposited on water phase surfaces [4], we decided in accordance with [5] to model only the sorption on gas phase surfaces. With this approach we got not bad results for the ACE RTF-4 test and very good results for ISP. As explained in [21] the experimental data suggest that a considerable portion of the iodine on surfaces was adsorbed reversibly. In modelling this corresponds to employing a reversible physical adsorption model [5]. Such a model is available in IODE for both gas phase and water phase surfaces. For surfaces exposed to the gas phase this IODE model can be written as follows (for water phase surfaces it is exactly the same):

$$(1/A_s) d[I_2]_g / dt = -(1/V_g) k_{ads} [I_2]_g + (1/V_g) k_{des} [I_2]_s, \quad (IV.4.01)$$

where  $[I_2]_g$  is  $I_2$  concentration in gas phase in  $\text{mol}/\text{dm}^3$ ,  $[I_2]_s$  concentration on surface in  $\text{mol}/\text{dm}^2$ ,  $V_g$  and  $A_s$  are gas phase volume and surface area, respectively, and  $k_{ads}$  ( $\text{dm}/\text{s}$ ) and  $k_{des}$  ( $\text{s}^{-1}$ ) are adsorption and desorption rate coefficients, respectively. As this modelling seemed to us to be too simple (particularly for the purpose of the ACE RTF-4 test simulation) we decided to add into our modified version of IODE the sorption model proposed in ORNL report [16]. This model which is based on fitting the experimental data enables to simulate both reversible and irreversible sorption with temperature dependent rate coefficients. To include this model into IODE was a lot of work and eventually we have found that for ISP it predicts (with all its defaults) much less adsorbed iodine than it should whereas the original simple model with the values of the sorption rate coefficients taken from [5] is quite sufficient. The reason why the ORNL model (with all its defaults) was in a way good enough for the ACE RTF-4 simulation but not for the ISP could be in the character of the temperature dependence which is very sharp in this model (sorption increases sharply with temperature). The comparison of our results for ACE RTF-4 and ISP would suggest rather no temperature dependence of the sorption but it is too difficult to say as there are too many factors, which could influence the sorption.

According to [16] it has been verified qualitatively in many experimental efforts that the surface reaction rate does not depend on the concentration of deposited iodine or on the number of surface sites available. The IODE modelling is in agreement with that. In our modelling we neglected the sorption on the surfaces of the sampling, recirculation and ventilation loops. With all the given input values (sorption coefficients according to [5] and the surface area something between 220 and 280dm<sup>3</sup>) this neglect had some, though small, effect on results but we were not able to tell which value of the surface area should be used preferably so we have used the value denoted in the ISP input data memo as “Gas Surface Area”, i.e. 220dm<sup>2</sup>. In our first sensitivity calculations with respect to sorption modeling we had taken the values of the sorption coefficients from [5]. With these values ( $k_{\text{ads}}=9 \times 10^{-3} \text{ dm/s}$ ,  $k_{\text{des}}=9 \times 10^{-7} \text{ s}^{-1}$ ) we got for stage 1 the decrease of the total aqueous iodine concentration which seemed to us to be too high (compare fig. IV.06 with fig. 2 in [5]). Thus we tried to decrease the sorption coefficient  $k_{\text{ads}}$  step by step to get -in accordance with experimental results- total aqueous iodine concentration at 350h higher than  $1 \times 10^{-6} \text{ M}$  (cf. fig. 2 in [5]). Lower value of  $k_{\text{ads}}$  should represent slower sorption process and thus the amount of adsorbed iodine should be less and, consequently, the total decrease in aqueous iodine concentration should be less. With the value of  $k_{\text{ads}}=4 \times 10^{-3} \text{ dm/s}$  (and  $k_{\text{des}}=9 \times 10^{-7} \text{ s}^{-1}$ ) we got at 350h the total aqueous iodine concentration which was just above the  $1 \times 10^{-6} \text{ M}$  (fig. V.05). So the numbers  $k_{\text{ads}}=4 \times 10^{-3} \text{ dm/s}$  and  $k_{\text{des}}=9 \times 10^{-7} \text{ s}^{-1}$  were chosen for our simulation. The difference in the gas phase iodine concentrations for the 2 calculations can be seen in figures IV.05 and V.03.

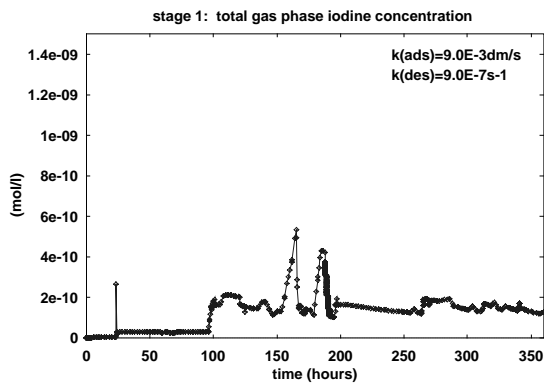


Figure IV.05

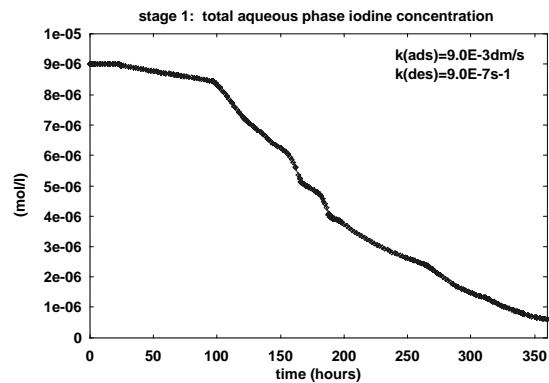


Figure IV.06

One interesting thing concerning the sorption modelling is iodine behaviour in the stage 2 of the ISP test. As was already mentioned in paragraph IV.2, at about 192hr after rapid increase in pH value, IODE predicts a change in the sign of the I<sub>2</sub> concentration gradient between water and the atmosphere (volume concentration of I<sub>2</sub> in the gas phase is then higher than that in the aqueous phase -cf. fig. V.12). Consequently, the I<sub>2</sub> goes back from the atmosphere to water and, as the ratio between the I<sub>2</sub> concentration in the atmosphere and on surfaces is being shifted, we can observe the desorption of I<sub>2</sub> from surfaces (cf. fig. V.08).

## V. Results of the calculations

In this chapter the results of the two calculations which best simulate (or better: which give reasonably conservative estimate of) the iodine behaviour in 2 stages of the ISP test are presented. These calculations were carried out with the modified version of the IODE code (cf. previous chapter). The rationale for selecting used input parameters and various IODE options -which were basically the same for calculations of both test stages- was given in the previous chapter. Listings of the input files for both calculations are given in Appendix.

Only five IODE “reactions” (reaction schemes) were used in the calculation. Three inorganic thermal reactions were used: reactions IV.1.01, IV.1.02 and IV.1.03 (Toth model) with all the defaults, which are described in paragraph IV.1.1. Two reactions representing the reactions of iodine with water radiolysis products were used: reaction IV.1.07 with reaction rate IV.1.08 ( $n=0.5$ ,  $k_7=0.1$ ,  $k_7'=0.0$  and  $D=0.3778\text{Gy/s}$ ) and reaction IV.1.11 with reaction rate IV.1.12 ( $k_{\text{IMP}}=0.01$ ,  $D=0.3778\text{Gy/s}$ ). The mass transfer of  $\text{I}_2$  from water to the atmosphere was calculated using the model IV.2.01 with the partition coefficient  $P$  calculated from IV.2.02 and with the constant overall mass transfer coefficient  $K=5\times 10^{-5}\text{m/s}$ . The value of  $K$  just means that we wanted to have the mass transfer fast enough (cf. paragraph IV.2). The sorption model IV.4.01 was used for sorption of  $\text{I}_2$  on gas phase surfaces with sorption rate coefficients  $k_{\text{ads}}=4\times 10^{-3}\text{dm/s}$  and  $k_{\text{des}}=9\times 10^{-7}\text{s}^{-1}$  ( $A_s=220\text{dm}^2$ ,  $V_g=315\text{dm}^3$ ). The input pH profiles are given in figures V.01 and V.02.

In trying to get proper results we started with given sorption model and the values of sorption coefficients taken from [5] (cf. paragraph IV.4) and with a fast mass transfer of  $\text{I}_2$  between water and the atmosphere (cf. paragraph IV.2). Then we tried to play with iodine reactions in water phase, especially iodine reactions with water radiolysis products. When we thought that the aqueous reactions and their rate constants are set up properly, we returned to the sorption modeling and tried to figure out the best values of the sorption constants which would not be, however, too different from those given in [5]. All the sensitivity calculations were carried out only for the stage 1 of the experiment. The stage 2 simulation was then performed with exactly the same parameters which were identified to be the best for the stage 1.

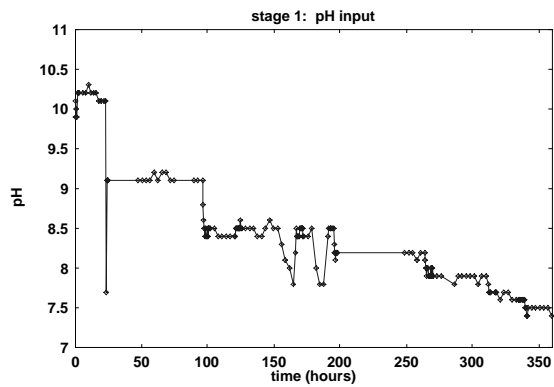


Figure V.01

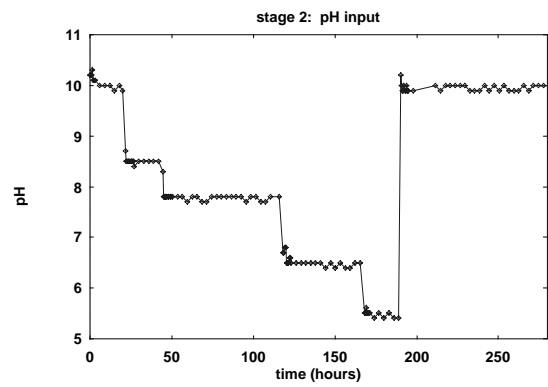


Figure V.02

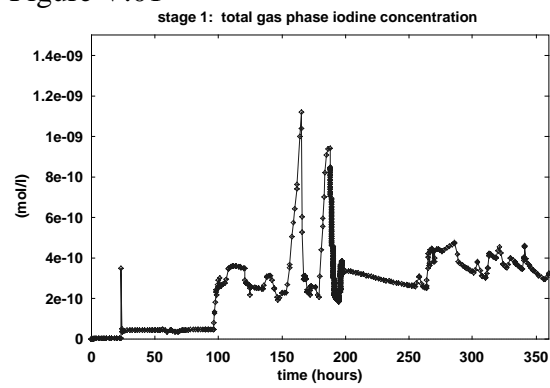


Figure V.03

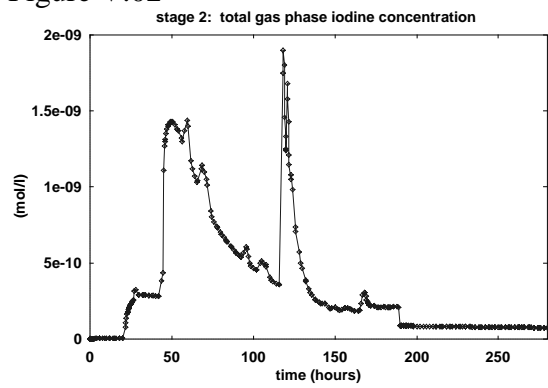


Figure V.04

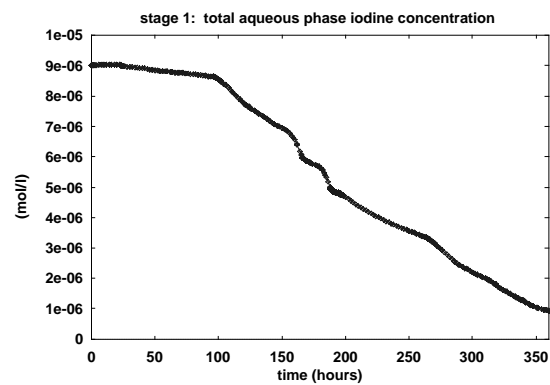


Figure V.05

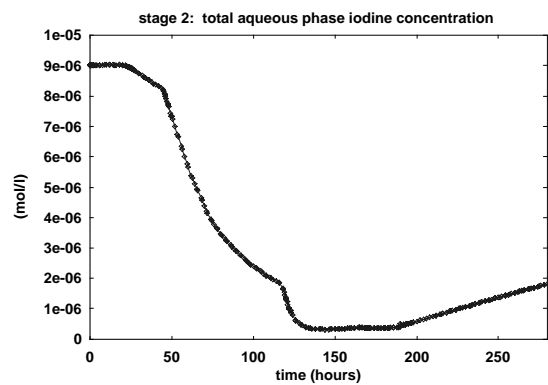


Figure V.06

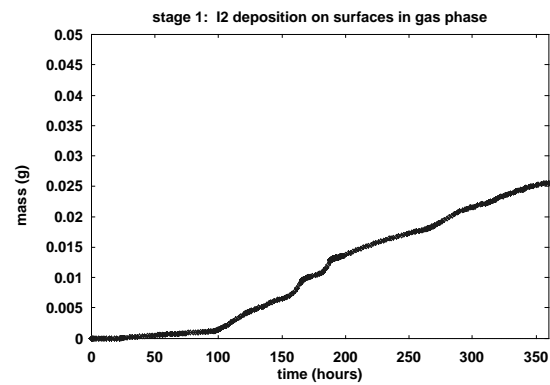


Figure V.07

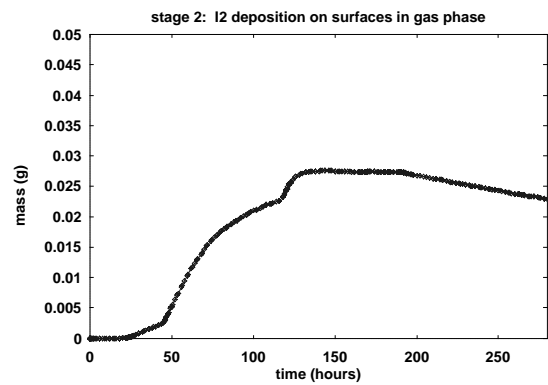


Figure V.08

As was previously mentioned (cf. paragraph IV.2) at about 192hr in the stage 2 of the experiment, according to IODE a change occurred in the direction of the  $I_2$  transfer which, afterwards on, went from the atmosphere to the water phase (volume concentration of  $I_2$  in the gas phase was higher than that in water -cf. fig. V.12). As we did not know how to present the flow rate dependence in the graph, we have used for the stage 2 the integral of flow (fig. V.10) instead of flow rate (fig. V.09).

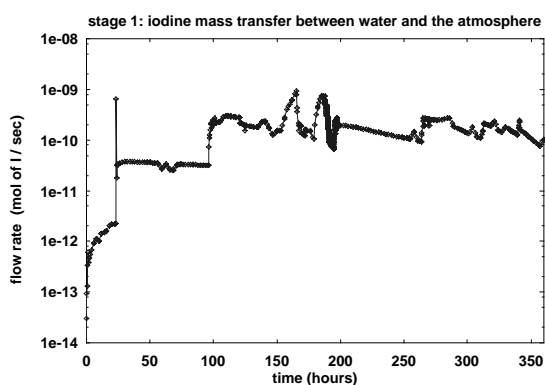


Figure V.09

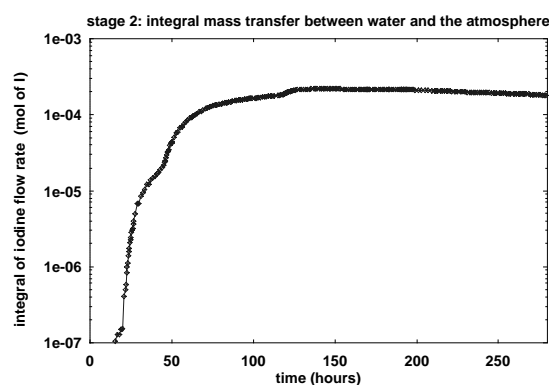


Figure V.10

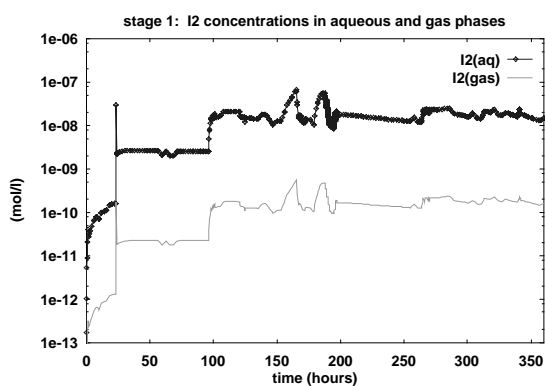


Figure V.11

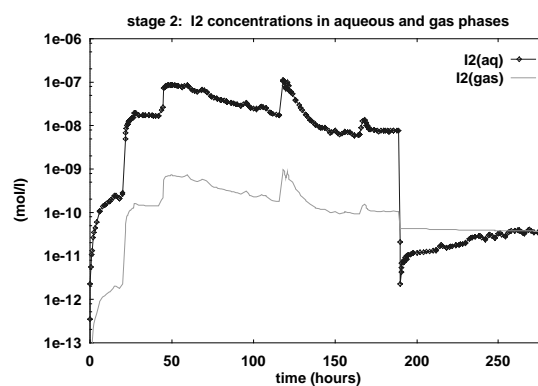


Figure V.12

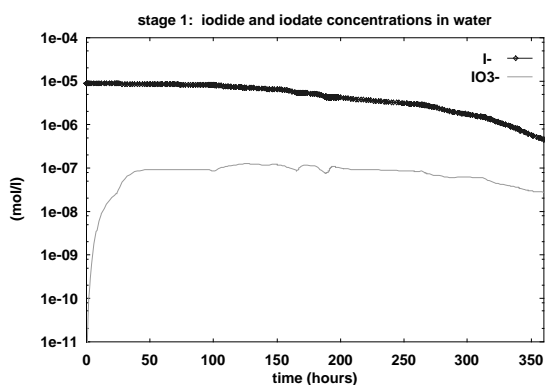


Figure V.13

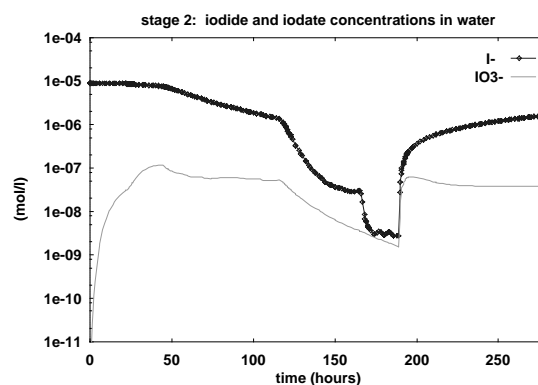


Figure V.14

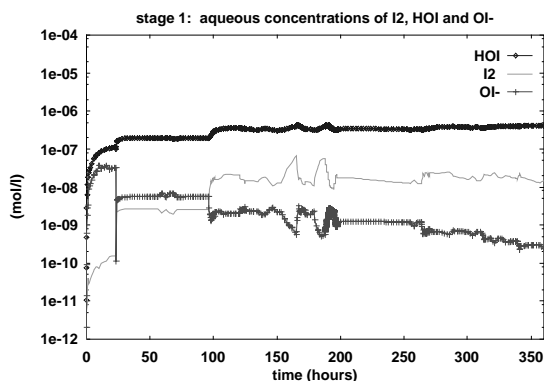


Figure V.15

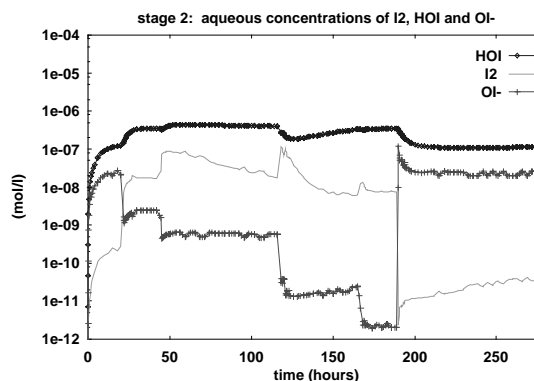


Figure V.16

## VI. Conclusions

With modified single compartment version of the IODE code we modelled the iodine behaviour in the ISP-41 test (one AECL RTF experiment) some results of which were published in the open literature <sup>[5]</sup>. This test was designed to study the effect of pH on iodine volatility under conditions relevant to reactor safety (severe accidents). We wanted to know if we are able -with reasonable values of the input parameters- to obtain conservative estimate of the amount of iodine in the atmosphere. We have found that with the input which was as simple as it could be (we used only 5 IODE reactions) it is not a big problem with IODE to obtain results which are of the same order of magnitude as the experimental data. However, if we had not known the experimental results beforehand, our estimate probably would not be conservative. It means that with the default IODE model of the iodine reactions with water radiolysis products it was difficult to get conservative estimate. The processes, which the iodine volatility is the most sensitive to, are the reactions of iodine with water radiolysis products and the sorption of  $I_2$  on surfaces. If we assume -in agreement with [5]- that the major part of the adsorbed iodine is deposited on surfaces exposed to gas phase, then the mass transfer of  $I_2$  between water and the atmosphere is also very important. Taking into account the thermal-hydraulic conditions in the test, we assumed that the mass transfer should be so fast that it would not influence the results. It means that we modelled so rapid mass transfer that all the volatile iodine (in our modelling it was only  $I_2$ ) formed in water was almost immediately transferred to the atmosphere. With the assumption of a fast mass transfer we have obtained results which reproduce the iodine behaviour quite well. One uncertainty remains, i.e. if there is a considerable sorption on water phase surfaces, then our sorption modelling need not be necessarily correct. However, the results with reversible sorption model for sorption only on gas phase surfaces are so nice (maybe even too nice) that we do not suppose big sorption on water phase surfaces.

If we do not take into account the inorganic thermal reactions in water (paragraph IV.1.1) the dependence of iodine volatility on pH is determined by the reactions of iodine with water radiolysis products (effect of these reactions on volatility is much stronger than of those inorganic thermal reactions). In IODE these complex processes are represented by only 2 reactions (IV.1.07, IV.1.09). With the default approach in IODE, represented by these 2 reactions, and with the recommended default values of the corresponding kinetic constants we could not get a conservative estimate for the total iodine concentration in the atmosphere. In our modified version of IODE we had changed the approach and simplified it. Now this model resembles the model used in the IMPAIR code. With this approach we were able to get conservative results for the ISP test. Something similar can be said about the ACE RTF-4 (experiment at 60°C) simulation. There, however, the situation was complicated by the necessity to use reactions involving organics. The approach in the original IODE which links the 2 reactions (IV.1.07 and IV.1.09) together seems to us to be something redundant. On the other hand, to get reasonable results with the modified IODE our values of kinetic constants in reactions IV.1.011 and IV.1.12 (which in our model substitute for reactions IV.1.07 and IV.1.09) had to be much higher than defaults used in IMPAIR<sup>[7]</sup>. We did not try to explain this discrepancy.

The same empirical model in the modified IODE which -in our opinion- best simulated the character of the iodine volatility pH dependence in the stage 1 of ISP was used also for the stage 2. The input pH profile in the stage 2 was different from stage 1 (cf. figures V.01, V.02) and its lowest pH value (pH=5.5) was much less than that in the stage 1 (pH=7.5). The results of the calculation for the stage 2 were also quite reasonable. This suggests that our model can be applied at this temperature (25°C) to as low pHs as 5.5. On the other hand, in modified IODE we have thus only 2 input parameters ( $k_7$  in IV.1.08 and  $k_{IMP}$  in IV.1.12) which can influence the way in which the code models all the iodine reactions with water radiolysis products. The similar situation is with the original IODE. We assume that it could be worth to think about having in the code some simplified radiolysis model. As there is nothing like that in the code now, some parameters (e.g. the amount of dissolved oxygen and metal impurities) which were identified experimentally to affect the iodine volatility cannot influence the IODE results. However, in our opinion the main reason why to think about including some simple radiolysis model is the overly simplified approach now used in IODE which -based on only 2 reactions- does not yield to the user enough room for manoeuvre at all likely pH ranges under radiation conditions at the accident. As for the dose rate influence on iodine volatility we did not try to make any sensitivity calculations because we did not have any relevant experimental data. Thus we cannot say anything about the IODE capability to model it.

In our simulations we did not use any gas phase reactions. We believe -in agreement with [10]- that the iodine volatility for both  $I_2$  and organic iodides is mainly determined by the water phase chemistry, mass transfer of the volatiles and the sorption, and that the gas phase reactions will play a minor role.

In our ISP simulations we did not use any iodine reactions with organics. We think that for the ISP experiment simulation it probably does not matter (cf. paragraph IV.1.3). We made a lot of sensitivity calculations using IODE organic involving reactions in water for the ACE RTF-4 test where organics played more important role. Our feeling is that the IODE model of organic involving reactions is too simple but, on the other hand, we think that too little is known about this to enable the developers to prepare any model which would be much better.

We have found that the iodine volatility in our simulations is the most sensitive to the stainless steel sorption modelling (cf. paragraph IV.4). As we knew the Canadian results, our situation was not very complicated. As was proposed in [5], we used a simple reversible sorption model which is available in IODE with the values of the sorption constants similar to those given in [5] and our results were quite acceptable. This model and these values of the sorption constants look reasonable. One important thing is that we neglected the sorption on water phase surfaces. For given sorption model our results suggest that this neglect does not represent any problem.

We think, that for the ISP test, the simple way we modelled the sorption is acceptable. On the other hand, we feel that we do not know much about the sorption mechanisms even for the unpainted stainless steel where it should be easiest to know something. We do not know much about the temperature dependence (if any), about the influence of humidity, not speaking about such queer things like, for instance, dose rate dependence. Thus we are not sure if the simple model which was used to simulate the ISP iodine behaviour could be used without further profound study for predictions of the iodine behaviour under various accident conditions of interest.

## REFERENCES

1. J.Gauvain, M.Filippi : ESCADRE System - IODE code release 2.1, Reference document, Rapport technique SEAC/91-04
2. Technical Bases for Estimating Fission Product Behavior During LWR Accidents, NUREG-0772, June 1981
3. Contribution from 22 Years of CSNI International Standard Problems, NEA/CSNI/R(97)29, March 1998
4. W.C.H.Kupferschmidt at al. : Final Report on the ACE-RTF Experiments, ACE-TR-B3, July 1992
5. J.C.Wren, G.A.Glowa, J.M.Ball : Modelling Iodine Behaviour Using LIRIC 3.0, Proceedings of the Fourth CSNI Workshop on the Chemistry of Iodine in Reactor Safety, Wurenlingen, Switzerland, 1996
6. W.C.H.Kupferschmidt : Preliminary Proposal for an ISP Based on One RTF Experiment, OECD CSNI, March 1997
7. Iodine Code Comparison, European Commission, EUR 16507 EN, 1995
8. J.Dienstbier, A.Rydl : Improved Version of the IODE Code, Final report for CEA/IPSN France (Contract No. 3140061), Report NRI Rez, UJV Z-9-T, February 1994
9. A.Rydl : Development of the IODE Code, Final report for CEA/IPSN France (Contract No. 404524), Report NRI Rez, UJV Z-44-T, February 1995
10. K.R.Weaver, W.C.H.Kupferschmidt, J.C.Wren, J.M.Ball : The Present Status of Iodine Chemistry Research in Canada and its Application to reactor Safety Analysis, Proceedings of the Fourth CSNI Workshop on the Chemistry of Iodine in Reactor Safety, Wurenlingen, Switzerland, 1996
11. J.Gauvain, M.Filippi, D.Jacquemain, D.Tarabelli : ESCADRE System - IODE code release 4.0, Reference report, Note technique SEMAR 95/80, January 1996
12. W.C.H.Kupferschmidt at al. : The Advanced Containment Experiments (ACE) Radioiodine Test Facility Experimental Program, Proceedings of the Third CSNI Workshop on the Chemistry of Iodine in Reactor Safety, Tokai-mura, Japan, 1992
13. J.C.Wren, N.H.Sagert, H.E.Sims: Modelling of Iodine Chemistry: The LIRIC Database, Proceedings of the Third CSNI Workshop on the Chemistry of Iodine in Reactor Safety, Tokai-mura, Japan, 1992
14. C.Poletico, C.Hueber, B.Fabre : Parametric Studies of Radiolytic Oxidation of Iodide Solutions with and without Paint : Comparison with Code Calculations, Proceedings of the Fourth CSNI Workshop on the Chemistry of Iodine in Reactor Safety, Wurenlingen, Switzerland, 1996
15. R.Ritzman : Containment Iodine Behavior Experiments, Research Project 2802, TR-103212, EPRI, November 1993
16. C.F.Weber, E.C.Beahm, T.S.Kress : Models of Iodine Behavior in Reactor Containments, ORNL-TM-12202, 1992

17. J.C.Wren, J.M.Ball, G.A.Glowa, R.Portman, G.G.Sanipelli : The Interaction of Iodine with Organic Material in Containment, Proceedings of the Fourth CSNI Workshop on the Chemistry of Iodine in Reactor Safety, Wurenlingen, Switzerland, 1996
18. The Chemistry of Iodine in Reactor Safety, Summary and Conclusions from OECD Workshop, Wurenlingen, Switzerland, NEA/CSNI/R(96)7, OECD/GD(96)192, 1996
19. D.A.Powers et al. : Technical Bases for the Management of Severe Reactor Accident Source Terms, Technical Note, Draft Revision 1, OECD CSNI, March 1998
20. J.T.Bell, M.H.Lietzke, D.A.Palmer : Predicted Rates of Formation of Iodine Hydrolysis Species at pH Levels, Concentrations, and Temperatures Anticipated in LWR Accidents, NUREG/CR-2900, ORNL-5876, 1982
21. J.M.Ball, W.C.H.Kupferschmidt, J.C.Wren : Results from Phase 2 of the RTF Experimental Program, Proceedings of the Fourth CSNI Workshop on the Chemistry of Iodine in Reactor Safety, Wurenlingen, Switzerland, 1996
22. R.C.Hewison, R.S.Rodliffe : Transfer of Volatile Species from a Pool of Water into Air, CEGB-TPRD/B/0889/R87, Berkeley Nuclear Laboratory, 1987

**IPSN, FRANCE**



# *ISP 41*

## **General description of IODE code 4.1**

*By C. Poletiko*

The behaviour of iodine, which is one of the major fission products emitted, requires a special approach. The iodine is assumed to be mainly emitted in the containment in the form of non-volatile aerosols, which, in consistency with aerosol physics, should ultimately be found in the stagnant sump water on the containment floor. However, experiments have shown that the gamma ionising radiation (emitted by the fission products) transforms part of the  $I^-$  iodine into  $I_2$  molecular iodine, this process is referred to as iodide radiolysis. This iodine participates strongly in disproportionation reactions, but also, to a lesser extent, in transfer to the atmosphere, owing to partitioning between the iodine in solution in the water and that present in the atmosphere above it. In addition, the  $I_2$  iodine in the atmosphere is liable to be deposited on painted or unpainted steel or concrete walls. Finally, there are a certain number of other chemical reactions (trapping by the silver (Ag) originating from degradation of the Ag-In-Cd control rods, formation of organic iodine, etc.) which can alter equilibrium patterns, thereby modifying potential iodine release through a containment leak.

This note provides a presentation of the physico-chemical phenomena (chemical reactions, mass transfer processes) modelled in the code IODE version 4.1 which is part of the ESCADRE code system, version mod1.1. The objective of the code IODE 4.1 is to compute the concentrations of iodine species in the gas phase, in the sump and the amount of iodine irreversibly trapped on various surfaces (containment surfaces, silver in the sump originating from the control rods degradation) in each compartment of a reactor containment in the event of a severe accident.

IODE is a semi-mechanistic code which employs well-known mechanistic chemical reactions and use a phenomenological approach for the modelling of complex reactions where the mechanistic approach is not reliable (radiolysis reactions, organic iodides formation). The code IODE models the thermal and radiolysis reactions of mineral species ( $I^-$ ,  $I_2$ , HOI,  $IO_3^-$ , AgI) in the water solution, the formation and decomposition reactions of organic species ( $CH_3I$  is the only species considered) and the mass transfer of the volatile  $I_2$  (sump-atmosphere interfacial mass transfer, adsorption on and desorption from surfaces, dissolution in condensed steam and washing-down to the sump) and  $CH_3I$  species (sump-atmosphere interfacial mass transfer, dissolution in condensed steam and washing-down to the sump).

A large number of experimental programmes devoted to the study of the iodine behaviour in containment under accidental conditions were performed in the last years (both small scale, intermediate scale (RTF at AECL/Canada and CAÏMAN at IPSN/France) and large scale experiments (PHEBUS-PF)). The code IODE benefited strongly from the analysis of those experiments both for the development and validation of the models used in the code. The validation status and the planned development for the IODE code over the next years was recently described in reference 1. A large number of experimental programs are still in progress or are being designed to study the iodine behaviour in containment and one can forecast that in the next years the modelling will be greatly improved.

### ***Exchanges of volatile iodine species between the sump water and the containment atmosphere***

The mass flux of a chemical species through a surface  $A_e$  can be written :

$$\Phi = \oint_{A_e} \mathbf{J} \, d\mathbf{S}$$

where  $\mathbf{J}$  is the mass flux vector per unit surface and  $d\mathbf{S}$  is a unit surface vector. Since transport through  $A_e$  is by molecular diffusion, Fick's law is applicable and the material current vector is given by :

$$\mathbf{J} = -D \, \text{grad } C$$

where  $D$  is the diffusion coefficient and  $C$  the mass concentration of the chemical species.

Interfacial mass transfer is a complex phenomenon and therefore a model is needed to simulate the basic features of the process. Commonly, interfacial mass transfer is modelled by a system consisting of four components :

bulk gas  $\Leftrightarrow$  interfacial gas film  $\Leftrightarrow$  interfacial liquid film  $\Leftrightarrow$  bulk liquid

Assuming that bulk gas and bulk liquid are well mixed and that there is a uniform concentration gradient through the surface  $A_e$ ,

The interfacial concentrations  $C_g^*$  and  $C_l^*$  are unknown, but equilibrium is assumed to be reached very rapidly so that the exchanging gas obeys Henry's law :

$$1/H = H^* = C_l^*/C_g^*$$

### Implementation in the code IODE

The code considers the water-atmosphere material transfers of iodine I<sub>2</sub> and methyl iodide CH<sub>3</sub>I such that the total flux through the interface is given by :

$$\Phi_1^T = 2 \Phi_1^{I_2} + \Phi_1^{CH_3I}$$

The experimental values for the partition coefficient  $H^*$  as a function of the temperature of the liquid phase  $T_l$  are derived using the empirical formulae established elsewhere :

The diffusion coefficients  $D_{I_2}$  and  $D_{CH_3I}$  are computed in the code using the theory of ordinary diffusion in gases at low density . With the knowledge of  $H^*$  and  $D$ , the code computes the mass transfer coefficients for I<sub>2</sub> and CH<sub>3</sub>I.

The global mass transfer coefficients of iodine I<sub>2</sub> and methyl iodide CH<sub>3</sub>I are either calculated by the code or entered by the user.

When entered by the user, two values for the global mass transfer coefficient should be entered, one for the transfer of the volatile species from the sump to the atmosphere  $K_{l1}$  and one for the transfer of the volatile species from the atmosphere to the sump  $K_{l2}$ . The gas will flow from the water to the atmosphere with the flow  $\Phi_1 = K_{l1} A_e (C_l - C_g H^*)$  positive when  $C_l / C_g > H^*$ . The gas will flow from the atmosphere to the sump with the flow  $\Phi_1 = K_{l2} A_e (C_l - C_g H^*)$  negative when  $C_l / C_g < H^*$ .

When calculated by the code, the global mass transfer coefficient is derived using a heat transfer-material transfer analogy which is expressed by  $\lambda / h = D / H^* K_l$ , where  $\lambda$  is the thermal conductivity in the atmosphere and  $h$  is the heat transfer coefficient .

Here also, two sub-cases are considered:

- If the gas concentration is higher in the atmosphere ( $C_g > C_g^*$ ), the flow  $\Phi_1$  is computed using the Uchida approach . In this approach, the effective heat transfer coefficient  $h$  is given by  $h = h_T P_{QC} / P_{QT}$  where  $h_T$  is an overall heat transfer coefficient;  $P_{QC}$ ,  $P_{QT}$  are the convection and total heating powers on the water-atmosphere surface. Uchida's formula gives :

$$h_T = 11.351 + 283.77 X$$

with  $X = m_v / m_i$ ;  $m_v$  is the mass of steam and  $m_i$  the mass of non condensable gases. In this case, the gas flow  $\Phi_1$  and the global mass transfer  $K_l$  are given by :

$$\Phi_1 = D/\lambda \ h_T \ P_{QC}/P_{QT} \ A_e (C_l - C_g H^*) / H^*$$

$$K_l = D/\lambda \ h_T \ P_{QC}/P_{QT} \ 1/ H^*$$

- If the gas concentration is higher in the water phase ( $C_g^* > C_g$ ), the flow  $\Phi_1$  is computed with a heat transfer correlation in use in the case of natural convection conditions. This correlation is expressed in terms of the Nusselt number  $N_u$ , the Grashof number  $G_r$  and the Prandtl number  $P_r$  :

$$N_u = a (G_r P_r)^m$$

where :

$$N_u = h / \lambda$$

$l$  is the length of heat exchange area or the sump diameter given by  $l = (4 A_e / \pi)^{1/2}$

$$G_r = g l^3 / \nu^2 \ |T_g - T_l| / T_l$$

with  $g$  the acceleration due to gravity,  $\nu$  the atmosphere kinematics viscosity,  $T_l$  and  $T_g$  the water and atmosphere temperatures

$$P_r = C_p \mu / \lambda$$

with  $C_p$  the atmosphere specific heat and  $\mu$  the dynamic viscosity.

The  $a$  and  $m$  coefficients take specific values :

$$\begin{aligned} \text{when } 10^4 < G_r < 2 \cdot 10^7 & \quad \text{and } T_g > T_l \\ & \quad \text{and } T_g \leq T_l \end{aligned}$$

$$\begin{aligned} \text{when } 2 \cdot 10^7 \leq G_r < 10^{20} & \quad \text{and } T_g > T_l \\ & \quad \text{and } T_g \leq T_l \end{aligned}$$

Note that in the code the limit for  $G_r$  values have been extended. Further, the  $a$  and  $m$  coefficients are determined with respect to  $G_r$  ( they are determined with respect to the product  $G_r P_r$ ).

The flux  $\Phi_1$  and the global mass transfer coefficient are then computed by :

$$\Phi_1 = D / l a (G_r P_r)^m (C_l - C_g H^*) / H^* A_e$$

$$K_l = D / l a (G_r P_r)^m 1/H^*$$

Steam condensation on the containment walls and on the water surface

Under condensing steam conditions, a strong mass flux towards surfaces is expected to enhance the removal of iodine vapours, including molecular iodine and organic iodides, into the surface liquid. In the formalism of this phenomenon, the gases are assumed to be ideal, as such they obey to the state equation :

$$\text{for gas A, } P_A V_g = n_A R T_g$$

where  $P_A$  is the gas A partial pressure,  $V_g$  the total gas phase volume,  $n_A$  the number of moles of gas A

( $n_A = m_A / M_A$ ),  $R$  the constant of ideal gases and  $T_g$  the temperature of the gas phase.

If one assumes ideal transport, *i.e.* that the ratio of steam mass and gas A mass ( $m_v/m_A$ ) is constant, then one can write :

$$dm_v / m_v = dm_A / m_A$$

Introducing the molecular concentration of gas A and using the law of ideal gases for steam as follows :

$$dm_A / m_A = dC_A / C_A$$

$$1 / m_v = R T_g / (M_v P_v V_g)$$

one can deduce :

$$dm_v / dt R T_g / (M_v P_v V_g) = dC_A / dt 1 / C_A$$

$\eta_s = - dm_v / dt$  is the condensed steam mass on the containment walls and on the water surface per unit of time, with the convention  $dm_v / dt < 0$ .

$\Phi_2^A$  the flux of gas A dissolved in the condensed steam is :

$$\Phi_2^A = V_g dC_A / dt = k_s C_A$$

with  $k_s = - \eta_s R T_g / (M_v P_v)$

## Implementation in the code IODE

The code considers that steam condensation entrains gases including molecular iodine  $I_2$ , hypoiodous acid HOI, organic iodides  $CH_3I$ , alkyl radicals R and alkanes  $RCH_3$  as well as aerosols containing iodine species  $I^-$ ,  $IO_3^-$  and AgI. It is assumed that the condensate formed on the containment walls is entirely recovered in the sump water. The atmosphere is considered to be well mixed so that the condensation constant  $k_s$  is the same for all the condensed species.  $\eta_s$ , the condensed steam mass per unit of time is entered by the user.

The total flux of iodine dissolved in the sump water is the sum of the individual flux of the species listed above :

$$\Phi_2^T = 2 \Phi_2^{I_2} + \Phi_2^{CH_3I} + \Phi_2^{HOI} + \dots$$

Molecular iodine  $I_2$  adsorption/desorption onto/from surfaces in the containment

The flux of molecular iodine adsorbed onto a surface  $A_i$  can be expressed by :

$$\Phi_{a_i} = K_{a_i} A_i C_{I_2}$$

where  $C_{I_2}$  is the concentration of  $I_2$  in the phase (gas or liquid) in which the surface  $A_i$  sits and  $K_{a_i}$  is the global adsorption coefficient of surface  $A_i$ .

## Surface adsorption

The adsorption phenomenon is a two-steps process. Firstly, the  $I_2$  molecules have to diffuse through the atmosphere to the surface  $A_i$ ; secondly, they are adsorbed onto the surface. If the diffusion of  $I_2$  in the atmosphere is the rate-limiting step then  $K_{a_i}$  is the mass transfer coefficient of  $I_2$  in the atmosphere. If the adsorption onto the surface is the rate-limiting step then  $K_{a_i}$  is the adsorption speed of  $I_2$  onto surface  $A_i$ . In the latter case,  $K_{a_i}$  depends on the type of the surface  $A_i$  (concrete surface, steel surface or painted surface); the adsorption may be of a physical or a chemical nature, reversible or irreversible.

If the adsorption is reversible, I<sub>2</sub> desorbs from surface A<sub>i</sub>. The flux of molecular iodine which desorbs from A<sub>i</sub> can be expressed as follows :

$$\Phi_{d_i} = -K_{d_i} m_{I_2 d_i} / M_{I_2} = -K_{d_i} n_{I_2 d_i}$$

where  $n_{I_2 d_i}$  and  $m_{I_2 d_i}$  are respectively the number of moles and the mass of I<sub>2</sub> adsorbed on surface A<sub>i</sub> and  $K_{d_i}$  is the rate of desorption.  $K_{d_i}$  depends on the nature of the surface A<sub>i</sub> and on the character of the adsorption of I<sub>2</sub> onto A<sub>i</sub>.

The total adsorption/desorption flux of I<sub>2</sub> onto/from a surface A<sub>i</sub> is then :

$$\Phi_i = \Phi_{a_i} + \Phi_{d_i} = K_{a_i} A_i C_{I_2} - K_{d_i} n_{I_2 d_i}$$

### Implementation in the code IODE

The code allows for three types of surfaces which could be, for instance : a concrete surface, a steel surface and a painted surface. The user enters for each type of surface the adsorption coefficient  $K_{a_i}$  and the desorption rate  $K_{d_i}$ .

The code computes the adsorption/desorption flux of I<sub>2</sub> onto/from all surfaces A<sub>i</sub> :

- in the gas phase :

$$\Phi_6^T = \sum \{ K_{a_{ig}} A_{ig} C_{I_2g} - K_{d_{ig}} n_{I_2 d_{ig}} \}$$

where the sum is over the various types (maximally three) of surface A<sub>ig</sub> in contact with the gas phase.

- in the liquid phase :

$$\Phi_7^T = \sum \{ K_{a_{il}} A_{il} C_{I_2l} - K_{d_{il}} n_{I_2 d_{il}} \}$$

where the sum is over the various types of surfaces A<sub>il</sub> in contact with the liquid phase. Note that the surface loading of other species than I<sub>2</sub>, (*i.e.*, CH<sub>3</sub>I and HI) is not modelled in the code.

### Painted surfaces (epoxy paints)

In the gas phase, paints can be efficient traps for molecular iodine since, on this type of surface, irreversible adsorption most probably of a chemical nature can occur. The adsorption/desorption processes may however depend strongly on parameters which are not necessarily known with accuracy such as local thermalhydraulic conditions at the gas-paint interface which will create very different adsorption conditions (different gas flows along the surface, different condensation regimes on the surface : dry surface or droplets condensation or liquid film formation). Adsorption velocity as high as  $10^{-2}$  m/s were measured in small scale experiments in which there was no limitation due to molecular iodine mass transfer in the gas, in an air/steam environment but in the absence of condensation on the paint. Under dry conditions, similar experiments yielded adsorption velocity of the order of  $10^{-3}$  m/s or lower for temperatures expected in the reactor case. However, limitations to the transfer of molecular iodine to the painted surfaces may be significant, especially if the surface is covered by a film of condensed steam (in that case, the chemistry in the film of water may play a significant role in reducing the iodine adsorption). Also, the paint ability to absorb irreversibly iodine under condensing steam conditions, at temperatures, as high as  $150^{\circ}\text{C}$  and in the presence of representative dose rates needs to be measured.

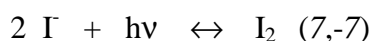
### Steel surfaces

As opposed to adsorption on paints, adsorption on steel is reversible. The adsorption on gas phase steel is only effective when there is no steam condensation on the surface and measured adsorption velocity are usually lower than  $10^{-4}$  m/s. Recent studies showed that under steam condensing conditions, at temperatures representative of the reactor case, the adsorption of  $\text{I}_2$  on steel can be neglected mostly due to the fact that  $\text{I}_2$  is converted into  $\text{I}^-$  in the condensates via formation of metal iodides by reaction with the surface. The same process occurs on steel surfaces in contact with the sump.

### **Radiolysis**

Two reactions enable the modelling of radiolysis in the code

#### ***Reaction (7) : Oxidation of iodide by radiation***



where  $h\nu$  represents the photon energy coming from  $\gamma$  radiation. The rate of oxidation from iodide to elemental iodine is not only dependent on radiation dose rate and liquid phase pH but also on catalytic effects due to suspended particles (Ag, In, Cd, etc.) and dissolved metal ions. Information concerning these catalytic effects is hardly available. The reaction velocity can be modelled by an empirical formula:

$$V_c (7) = - k_7 [\text{I}^-]_l [\text{H}^+]^{0.25} D_o + k_{-7} [\text{I}_2]_l$$

where  $D_0$  is the radiation dose rate, the term  $[H^+]^{0.25}$  is used to obtain the experimentally derived pH-dependence.

Analysis of analytical experiments performed at CEA showed that this model underestimates the effect of reaction (7) and of the forward reaction (-7) on the chemistry of the system. To model correctly these experiments, the pH-dependency of  $V_c$  (7) was increased from  $[H^+]^{0.25}$  to  $[H^+]^{0.5}$ .

### Remarks

A different analysis performed with the code IMPAIR using the ACE-RTF test data yielded to the conclusion that the pH-dependency of  $V_c$  (7) need to be decreased from  $[H^+]^{0.25}$  to  $[H^+]^{0.1}$ . Some additional experimental work is required to establish with more accuracy the temperature, pH and dose rate dependency of the kinetics of the radiolytical oxidation of iodide. In the code IODE, the user is left with the possibility to modify the pH-dependency of  $V_c$  (7) which is given by :

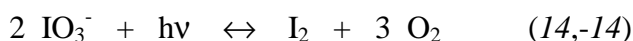
$$V_c (7) = - k_7 [I^-]_l [H^+]^n D_0 + k_{-7} [I_2]_l$$

where  $D_0$  is the radiation dose rate and  $n$  is the power of the radiolysis law, both can be given in input by the user. Note that a change in the pH-dependency of the radiolysis law also implies a change in the value of the correlated kinetic constant  $k_7$  and  $k_{-7}$ .

The dose rate dependency of the radiolysis law needs to be checked as well as the temperature dependency. Experimental, interpretation and validation work concerning these aspects is underway .

### ***Reaction (14) : Decomposition of iodate by radiation***

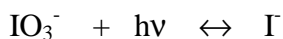
This reaction makes a significant contribution to sump iodine chemistry. It can be written:



where  $hv$  represents the photon energy coming from  $\gamma$  radiation. As for reaction (7), the reaction velocity is given in the code IODE by the empirical formula :

$$V_c (14) = - k_{14} [IO_3^-]_l [H^+]^n D_0 + k_{-14} [I_2]_l$$

where  $D_0$  is the radiation dose rate and  $n$  is the power of the radiolysis law, both are given in input by the user. This modelling is based solely on the observation that the rate of formation of  $I_2$  by radiolytic decomposition of  $IO_3^-$  is the same than that of the radiolytic decomposition of  $I^-$ . Thus in the code it is assumed that  $k_{14} = k_7$  and  $k_{-14} = k_{-7}$ . In the code IMPAIR 2.2, this reaction was modelled in an alternative way, considering the global reduction reaction :



## Kinetic data base of the IODE code

For the calculation, the code allows the user to activate only a certain number of chemical reactions. It is important to note that if the system is not irradiated then the user should deactivate all the radiolysis reactions. Activating simultaneously reaction (8) and (15) is redundant. The code gives the user the possibility to change in an easy way the kinetic constants and the activation energies of all chemical reactions.

Additional notes :

- the kinetic constants at temperature T are calculated using Arrhenius law :

$$k(T) = k^0 \exp ( E_a (T-T_0) / RT_0T )$$

where  $k^0$  is the kinetic constant at  $T_0 = 298.15$  K,  $E_a$  is the activation energy and R is the ideal gas constant,

- most of the reactions follow Van't Hoff's law.

## **Data input**

The geometry data include constant data (the total volume of the containment and the exchange area with the sump water) and time dependent data (the water volume and the immersed surface area).

The thermodynamic data only include time dependent data (the composition of the atmosphere, the water and atmosphere temperatures and the total and partial steam pressure in the atmosphere).

The physical data include constant data (the deposition surface areas, the deposition rates and desorption rates on the various types of surfaces both in the gas phase and in the liquid phase, and, if they are required, the mass transfer coefficients for  $I_2$  and  $CH_3I$  both for liquid-gas and gas-liquid mass transfer) and time dependent data (the rate of containment out leakage, the ratio of calorific convection power to total calorific power, the condensation rates on the sump water and on the containment walls, the iodine  $I_2$  and aerosol I sources and the radiation dose rate in the water).

The chemical data include constant data (the silver specific area, the molar mass of the radical R, the initial concentrations of the chemical species in the gas phase and in the water phase and the value of the exponent n of the term  $[H+]^n$  for the radiolysis laws) and time dependent data : the pH of the sump solution when entered by the user. When the sump pH is calculated by the code, constant data must be entered by the user : the initial boric acid, the base (KOH,  $NH_4OH$ , LiOH,  $H_2O$ ) and the strong acid concentrations if any.

The chemical data also include a certain number of option cards. For the calculation, the user has the possibility to activate only the desired chemical reactions. In particular, if the system is not irradiated then all the radiolysis reactions should not be activated. The user has the option to modify the kinetic constants and the activation energies of the chemical reactions.

The input data include a timetable defining the imposed output times.

## Calculation

The code derives from the chemical composition of the atmosphere the coefficients for gas diffusion, viscosity, density and thermal conductivity together with the specific heat of the atmosphere which are required to calculate the water-atmosphere iodine transfer flux.

As the initial state is given, a system of differential equations can be solved at each instant required. To do this, a digital integrator of the predictor corrector type is used, already implemented in various ESCADRE codes.

## Results

The code results are grouped under four main headings. At each requested output time, we obtain :

- the material transfer flows :

the transfer flow of iodine I at the boundary phase area ( $\Phi_1^T$ ), the condensation flow of iodine I ( $\Phi_2^T$ ), the leak flow of iodine I ( $\Phi_3^T$ ), the source flow of iodine  $I_2$  in the gas phase ( $\Phi_4$ ), the source flow of iodine I<sup>-</sup> in the liquid phase ( $\Phi_5$ ), the deposition flow of iodine  $I_2$  in the gas phase ( $\Phi_6^T$ ) and the deposition flow of iodine  $I_2$  in the liquid phase ( $\Phi_7^T$ )

- the chemical constituent concentrations in the gas phase and in the water phase, obtained directly by digital integration
- the iodine masses in the gas phase, in the liquid phase and on deposition surfaces derived from the concentration values
- the  $I_2$  and  $CH_3I$  interfacial mass transfer coefficients

- the sump pH

- the overall iodine partition coefficient P :

$$P = \frac{\text{atomic iodine concentration in the liquid phase}}{\text{atomic iodine concentration in the gas phase}}$$

Finally, results are safeguarded in a file held for subsequent graphic processing. These files can be treated with the graphic post-processors TIC and DRAKKAR .

**ISP-41: RESULTS OF THE CALCULATIONS PERFORMED**  
**WITH THE CODE IODE 4.0**

B. Herrero  
Departamento de Fisión Nuclear

**Ciemat** Centro de Investigaciones Energéticas,  
Medioambientales y Tecnológicas  
Miner

CENTRO DE INVESTIGACIONES ENERGETICAS, MEDIOAMBIENTALES Y TECNOLOGICAS

**DEPARTAMENTO DE FISION NUCLEAR**  
**Avda. Complutense, 22**  
**28040 MADRID**



## ISP 41

### **1. GENERAL DESCRIPTION OF IODE CODE 4.0**

The behaviour of iodine, which is one of the major fission products emitted, requires a special approach. Iodine is assumed to be mainly emitted in the containment in the form of non-volatile aerosols, which, in consistency with aerosol physics, should ultimately be found in the stagnant sump water on the containment floor. However, experiments have shown that the gamma ionising radiation (emitted by the fission products) transforms part of the I- iodine into I<sub>2</sub>, molecular iodine, this process being referred to as iodide radiolysis. Molecular iodine participates strongly in disproportionation reactions, but also, to a lesser extent, in transfer to the atmosphere, owing to partitioning between the iodine in solution in the water and that present in the atmosphere above it. In addition, the I<sub>2</sub> iodine in the atmosphere is liable to be deposited on painted or unpainted steel or concrete walls. Finally, there is a certain number of other chemical reactions (trapping by the silver (Ag) originating from degradation of the Ag-In-Cd control rods, formation of organic iodine, etc.) which can alter equilibrium patterns, thereby modifying potential iodine release through a containment leak.

This note provides a presentation of the physico-chemical phenomena (chemical reactions, mass transfer processes) modelled in the code IODE version 4.0 which is part of the ESCADRE code system, version mod1.1. The objective of the code IODE 4.0 is to compute the concentrations of iodine species in the gas phase, in the sump and the amount of iodine irreversibly trapped on various surfaces (containment surfaces, silver in the sump originating from the control rods degradation) in each compartment of a reactor containment in the event of a severe accident.

IODE is a semi-mechanistic code which employs well-known mechanistic chemical reactions and uses a phenomenological approach for the modelling of complex reactions where the mechanistic approach is not reliable (radiolysis reactions, organic iodides formation). The code IODE models the thermal and radiolysis reactions of mineral species (I<sup>-</sup>, I<sub>2</sub>, HOI, IO<sub>3</sub><sup>-</sup>, AgI) in the water solution, the formation and decomposition reactions of organic species (CH<sub>3</sub>I is the only species considered) and the mass transfer of the volatile I<sub>2</sub> (sump-atmosphere interfacial mass transfer, adsorption on and desorption from surfaces, dissolution in condensed steam and washing-down to the sump) and CH<sub>3</sub>I species (sump-atmosphere interfacial mass transfer, dissolution in condensed steam and washing-down to the sump).

A large number of experimental programmes devoted to the study of the iodine behaviour in containment under accidental conditions has been performed in the last years (both small scale, intermediate scale (RTF at AECL/Canada and CAÏMAN at IPSN/France) and large scale experiments (PHEBUS-PF)). The code IODE has benefited strongly from the analysis of those experiments both for the development and validation of the models used in the code. A large number of experimental programs is still in progress or are being designed to study the iodine behaviour in containment and one can forecast that in the next years the modelling will be greatly improved.

In this report a brief summary of the interactions relevant to the ISP-41 exercise is presented.

### **1.1. Exchanges of volatile iodine species between the sump water and the containment atmosphere.**

The mass flux of a chemical species through a surface  $A_e$  can be written :

$$\Phi = \oint_{A_e} \mathbf{J} \, d\mathbf{S}$$

where  $\mathbf{J}$  is the mass flux vector per unit surface and  $d\mathbf{S}$  is a unit surface vector. Since transport through  $A_e$  is by molecular diffusion, Fick's law is applicable and the material current vector is given by :

$$\mathbf{J} = -D \, \text{grad } C$$

where  $D$  is the diffusion coefficient and  $C$  the mass concentration of the chemical species.

Interfacial mass transfer is a complex phenomenon and therefore a model is needed to simulate the basic features of the process. Commonly, interfacial mass transfer is modelled by a system consisting of four components:

bulk gas  $\Leftrightarrow$  interfacial gas film  $\Leftrightarrow$  interfacial liquid film  $\Leftrightarrow$  bulk liquid

Assuming that bulk gas and bulk liquid are well mixed and that there is a uniform concentration gradient through the surface  $A_e$ ,

The interfacial concentrations  $C_g^*$  and  $C_l^*$  are unknown, but equilibrium is assumed to be reached very rapidly so that the exchanging gas obeys Henry's law :

$$1/H = H^* = C_l^*/C_g^*$$

## Implementation in the code IODE

The code considers the water-atmosphere material transfer of iodine  $I_2$  and methyl iodide  $CH_3I$  such that the total flux through the interface is given by :

$$\Phi_{1T} = 2 \Phi_{1I_2} + \Phi_{1CH_3I}$$

The experimental values for the partition coefficients  $H^*$  as a function of the temperature of the liquid phase  $T_l$  are derived using empirical formulas established elsewhere.

The diffusion coefficients  $D_{I_2}$  and  $D_{CH_3I}$  are computed in the code using the theory of ordinary diffusion in gases at low density . With the knowledge of  $H^*$  and  $D$ , the code computes the mass transfer coefficients for  $I_2$  and  $CH_3I$ .

The global mass transfer coefficients of iodine  $I_2$  and methyl iodide  $CH_3I$  are either calculated by the code or entered by the user.

When entered by the user, two values for the global mass transfer coefficient should be entered, one for the transfer of the volatile species from the sump to the atmosphere  $K_{l1}$  and one for the transfer of the volatile species from the atmosphere to the sump  $K_{l2}$ . The gas will flow from the water to the atmosphere with the flow  $\Phi_1 = K_{l1} A_e (C_l - C_g H^*)$  positive when  $C_l / C_g > H^*$ . The gas will flow from the atmosphere to the sump with the flow  $\Phi_1 = K_{l2} A_e (C_l - C_g H^*)$  negative when  $C_l / C_g < H^*$ .

When calculated by the code, the global mass transfer coefficient is derived using a heat transfer-material transfer analogy which is expressed by  $\lambda / h = D / H^* K_l$ , where  $\lambda$  is the thermal conductivity in the atmosphere and  $h$  is the heat transfer coefficient .

Here also, two sub-cases are considered :

- If the gas concentration is higher in the atmosphere ( $C_g > C_g^*$ ), the flow  $\Phi_1$  is computed using the Uchida approach. In this approach, the effective heat transfer coefficient  $h$  is given by  $h = h_T P_{QC}/P_{QT}$  where  $h_T$  is an overall heat transfer coefficient;  $P_{QC}$ ,  $P_{QT}$  are the convection and total heating power on the water-atmosphere surface. Uchida's formula gives :

$$h_T = 11.351 + 283.77 X$$

with  $X = m_v / m_i$ ;  $m_v$  is the mass of steam and  $m_i$  the mass of non condensable gases. In this case, the gas flow  $\Phi_1$  and the global mass transfer  $K_l$  are given by :

$$\Phi_1 = D/\lambda \ h_T \ P_{QC}/P_{QT} \ A_e \ (C_l - C_g H^*) / H^*$$

$$K_l = D/\lambda \ h_T \ P_{QC}/P_{QT} \ 1 / H^*$$

- If the gas concentration is higher in the water phase ( $C_g^* > C_g$ ), the flow  $\Phi_1$  is computed with a heat transfer correlation in use in the case of natural convection conditions. This correlation is expressed in terms of the Nusselt number  $N_u$ , the Grashof number  $G_r$  and the Prandtl number  $P_r$  :

$$N_u = a \ (G_r \ P_r)^m$$

where :

$$N_u = h \ l / \lambda$$

$l$  is the length of heat exchange area or the sump diameter given by  $l = (4 A_e / \pi)^{1/2}$

$$G_r = g \ l^3 / \nu^2 \ |T_g - T_l| / T_l$$

with  $g$  the acceleration due to gravity,  $\nu$  the atmosphere kinematic viscosity,  $T_l$  and  $T_g$  the water and atmosphere temperatures

$$P_r = C_p \ \mu / \lambda$$

with  $C_p$  the atmosphere specific heat and  $\mu$  the dynamic viscosity.

The  $a$  and  $m$  coefficients take specific values :

$$\begin{aligned} \text{when } 10^4 < G_r < 2 \cdot 10^7 & \quad \text{and } T_g > T_l \\ & \quad \text{and } T_g \leq T_l \end{aligned}$$

$$\begin{aligned} \text{when } 2 \cdot 10^7 \leq G_r < 10^{20} & \quad \text{and } T_g > T_l \\ & \quad \text{and } T_g \leq T_l \end{aligned}$$

Note that in the code the limit for  $G_r$  values has been extended. Further, the  $a$  and  $m$  coefficients are determined with respect to  $G_r$  ( they are determined with respect to the product  $G_r P_r$ ).

The flux  $\Phi_1$  and the global mass transfer coefficient are then computed by :

$$\Phi_1 = D / l a ( G_r P_r )^m ( C_l - C_g H^* ) / H^* A_e$$

$$K_l = D / l a ( G_r P_r )^m 1 / H^*$$

## **1.2. Steam condensation on the containment walls and on the water surface**

Under condensing steam conditions, a strong mass flux towards surfaces is expected to enhance the removal of iodine vapours, including molecular iodine and organic iodides, into the surface liquid. In the formalism of this phenomenon, the gases are assumed to be ideal, as such they obey to the state equation :

$$\text{for gas A,} \quad P_A V_g = n_A R T_g$$

where  $P_A$  is the gas A partial pressure,  $V_g$  the total gas phase volume,  $n_A$  the number of moles of gas A

( $n_A = m_A / M_A$ ),  $R$  the constant of ideal gases and  $T_g$  the temperature of the gas phase.

If one assumes ideal transport, *i.e.* that the ratio of steam mass and gas A mass ( $m_v/m_A$ ) is constant, then one can write :

$$dm_v / m_v = dm_A / m_A$$

Introducing the molecular concentration of gas A and using the law of ideal gases for steam as follows :

$$\begin{aligned} dm_A / m_A &= dC_A / C_A \\ 1 / m_v &= R T_g / (M_v P_v V_g) \end{aligned}$$

one can deduce :

$$dm_v / dt \ R T_g / (M_v P_v V_g) = dC_A / dt \ 1 / C_A$$

$\eta_s = - dm_v / dt$  is the condensed steam mass on the containment walls and on the water surface per unit of time, with the convention  $dm_v / dt < 0$ .

$\Phi_{2^A}$  the flux of gas A dissolved in the condensed steam is :

$$\Phi_{2^A} = V_g \ dC_A / dt = k_s \ C_A$$

with  $k_s = - \eta_s \ R T_g / (M_v P_v)$

### Implementation in the code IODE

The code considers that steam condensation entrains gases including molecular iodine  $I_2$ , hypoiodous acid HOI, organic iodides  $CH_3I$ , alkyl radicals R and alkanes  $RCH_3$  as well as aerosols containing iodine species  $I^-$ ,  $IO_3^-$  and AgI. It is assumed that the condensate formed on the containment walls is entirely recovered in the sump water. The atmosphere is considered to be well-mixed so that the condensation constant  $k_s$  is the same for all the condensed species.  $\eta_s$ , the condensed steam mass per unit of time is entered by the user.

The total flux of iodine dissolved in the sump water is the sum of the individual flux of the species listed above:

$$\Phi_{2^T} = 2 \Phi_{2^I_2} + \Phi_{2^CH_3I} + \Phi_{2^HOI} + \dots$$

Molecular iodine  $I_2$  adsorption/desorption onto/from surfaces in the containment

The flux of molecular iodine adsorbed onto a surface  $A_j$  can be expressed by :

$$\Phi_{a_j} = K_{a_j} \ A_j \ C_{I_2}$$

where  $C_{I_2}$  is the concentration of  $I_2$  in the phase (gas or liquid) in which the surface  $A_j$  sits and  $K_{a_j}$  is the global adsorption coefficient of surface  $A_j$ .

### 1.3. Surface adsorption

The adsorption phenomenon is a two-steps process. Firstly, the  $I_2$  molecules have to diffuse through the atmosphere to the surface  $A_j$  ; secondly, they are adsorbed onto the surface. If the diffusion of  $I_2$  in the atmosphere is the rate-limiting step then  $K_{a_j}$  is the mass transfer coefficient of  $I_2$  in the atmosphere. If the adsorption onto the surface is the rate-limiting step then  $K_{a_j}$  is the adsorption speed of  $I_2$  onto surface  $A_j$  . In the latter case,  $K_{a_j}$  depends on the type of the surface  $A_j$  (concrete surface, steel surface or painted surface); the adsorption may be of a physical or a chemical nature, reversible or irreversible.

If the adsorption is reversible,  $I_2$  desorbs from surface  $A_j$  . The flux of molecular iodine which desorbs from  $A_j$  can be expressed as follows:

$$\Phi_{d_j} = -K_{d_j} m_{I_2 d_j} / M_{I_2} = -K_{d_j} n_{I_2 d_j}$$

where  $n_{I_2 d_j}$  and  $m_{I_2 d_j}$  are respectively the number of moles and the mass of  $I_2$  adsorbed on surface  $A_j$  and  $K_{d_j}$  is the rate of desorption.  $K_{d_j}$  depends on the nature of the surface  $A_j$  and on the character of the adsorption of  $I_2$  onto  $A_j$  .

The total adsorption/desorption flux of  $I_2$  onto/from a surface  $A_j$  is then :

$$\Phi_j = \Phi_{a_j} + \Phi_{d_j} = K_{a_j} A_j C_{I_2} - K_{d_j} n_{I_2 d_j}$$

### Implementation in the code IODE

The code allows for three types of surfaces, which could be, for instance: a concrete surface, a steel surface and a painted surface. The user enters for each type of surface the adsorption coefficient  $K_{a_j}$  and the desorption rate  $K_{d_j}$ .

The code computes the adsorption/desorption flux of I<sub>2</sub> onto/from all surfaces A<sub>i</sub> :

- in the gas phase :

$$\Phi_6^T = \sum \{ K_{aig} A_{ig} C_{I_2g} - K_{dig} n_{I_2dig} \}$$

where the sum is over the various types (maximally three) of surface A<sub>ig</sub> in contact with the gas phase.

- in the liquid phase :

$$\Phi_7^T = \sum \{ K_{ail} A_{il} C_{I_2l} - K_{dil} n_{I_2dil} \}$$

where the sum is over the various types of surfaces A<sub>il</sub> in contact with the liquid phase.

Note that the surface loading of other species than I<sub>2</sub>, (*i.e.*, CH<sub>3</sub>I and HI) is not modelled in the code.

### **Painted surfaces (epoxy paints)**

In the gas phase, paints can be efficient traps for molecular iodine since, on this type of surface, irreversible adsorption most probably of a chemical nature can occur. The adsorption/desorption processes may however depend strongly on parameters which are not necessarily known with accuracy such as local thermal-hydraulic conditions at the gas-paint interface which will create very different adsorption conditions (different gas flows along the surface, different condensation regimes on the surface : dry surface or droplets condensation or liquid film formation). Adsorption velocity as high as 10<sup>-2</sup> m/s were measured in small scale experiments in which there was no limitation due to molecular iodine mass transfer in the gas, in an air/steam environment but in the absence of condensation on the paint. Under dry conditions, similar experiments yielded an adsorption velocity of the order of 10<sup>-3</sup> m/s or lower for temperatures expected in the reactor case. However, limitations to the transfer of molecular iodine to the painted surfaces may be significant, especially if the surface is covered by a film of condensed steam (in that case, the chemistry in the film of water may play a significant role in reducing the iodine adsorption). Also, the paint ability to absorb irreversibly iodine under condensing steam conditions, at temperatures as high as 150°C and in the presence of representative dose rates needs to be measured.

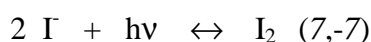
## Steel surfaces

As opposed to adsorption on paints, adsorption on steel is reversible. The adsorption on gas phase steel is only effective when there is no steam condensation on the surface and measured adsorption velocity are usually lower than  $10^{-4}$  m/s. Recent studies showed that under steam condensing conditions, at temperatures representative of the reactor case, the adsorption of  $I_2$  on steel can be neglected mostly due to the fact that  $I_2$  is converted into  $I^-$  in the condensates via formation of metal iodides by reaction with the surface. The same process occurs on steel surfaces in contact with the sump.

### **1.4 Radiolysis**

Two reactions enable the modelling of radiolysis in the code

#### ***Reaction (7) : Oxidation of iodide by radiation***



where  $h\nu$  represents the photon energy coming from  $\gamma$  radiation. The rate of oxidation from iodide to elemental iodine is not only dependent on radiation dose rate and liquid phase pH but also on catalytic effects due to suspended particles (Ag, In, Cd, etc.) and dissolved metal ions. Information concerning these catalytic effects is hardly available. The reaction velocity can be modelled by an empirical formula :

$$V_c (7) = - k_7 [I^-]_l [H^+]^{0.25} D_0 + k_{-7} [I_2]_l$$

where  $D_0$  is the radiation dose rate, the term  $[H^+]^{0.25}$  is used to obtain the experimentally derived pH-dependence.

Analysis of analytical experiments performed at CEA showed that this model underestimates the effect of reaction (7) and of the forward reaction (-7) on the chemistry of the system. To model correctly these experiments, the pH-dependency of  $V_c (7)$  was increased from  $[H^+]^{0.25}$  to  $[H^+]^{0.5}$ .

## Remarks

A different analysis performed with the code IMPAIR using the ACE-RTF test data yielded the conclusion that the pH-dependency of  $V_c$  (7) need to be decreased from  $[H^+]^{0.25}$  to  $[H^+]^{0.1}$ . Some additional experimental work is required to establish with more accuracy the temperature, pH and dose rate dependency of the kinetics of the radiolytical oxidation of iodide. In the code IODE, the user is left with the possibility to modify the pH-dependency of  $V_c$  (7) which is given by :

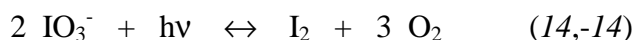
$$V_c (7) = - k_7 [I]_l [H^+]^n D_o + k_{-7} [I_2]_l$$

where  $D_o$  is the radiation dose rate and  $n$  is the power of the radiolysis law, both can be given in input by the user. Note that a change in the pH-dependency of the radiolysis law also implies a change in the value of the correlated kinetic constant  $k_7$  and  $k_{-7}$ .

The dose rate dependency of the radiolysis law needs to be checked as well as the temperature dependency. Experimental, interpretation and validation work concerning these aspects is underway .

### ***Reaction (14) : Decomposition of iodate by radiation***

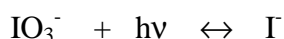
This reaction makes a significant contribution to sump iodine chemistry. It can be written:



where  $hv$  represents the photon energy coming from  $\gamma$  radiation. As for reaction (7), the reaction velocity is given in the code IODE by the empirical formula :

$$V_c (14) = - k_{14} [IO_3^-]_l [H^+]^n D_o + k_{-14} [I_2]_l$$

where  $D_o$  is the radiation dose rate and  $n$  is the power of the radiolysis law, both are given in input by the user. This modelling is based solely on the observation that the rate of formation of  $I_2$  by radiolytic decomposition of  $IO_3^-$  is the same than that of the radiolytic decomposition of  $I^-$ . Thus in the code it is assumed that  $k_{14} = k_7$  and  $k_{-14} = k_{-7}$ . In the code IMPAIR 2.2, this reaction was modelled in an alternative way, considering the global reduction reaction :



### **1.5. Kinetic database of the code IODE**

*For the calculation, the code allows the user to activate only a certain number of chemical reactions. It is important to note that if the system is not irradiated then the user should deactivate all the radiolysis reactions. Activating simultaneously reaction (8) and (15) is redundant. The code gives the user the possibility to change in an easy way the kinetic constants and the activation energies of all chemical reactions.*

Additional notes:

- the kinetic constants at temperature T are calculated using the Arrhenius law :

$$k(T) = k^0 \exp ( E_a (T-T_0) / RT_0T )$$

where  $k^0$  is the kinetic constant at  $T_0 = 298.15$  K,  $E_a$  is the activation energy and R is the ideal gas constant,

- most of the reactions follow Van't Hoff's law.

### **1.6. Data input**

The geometry data include constant data (the total volume of the containment and the exchange area with the sump water) and time dependent data (the water volume and the immersed surface area).

The thermodynamic data only include time dependent data (the composition of the atmosphere, the water and atmosphere temperatures and the total and partial steam pressure in the atmosphere).

The physical data include constant data (the deposition surface areas, the deposition rates and desorption rates on the various types of surfaces both in the gas phase and in the liquid phase, and, if they are required, the mass transfer coefficients for  $I_2$  and  $CH_3I$  both for liquid-gas and gas-liquid mass transfer) and time dependent data (the rate of leakage from the containment, the ratio of calorific convection power to total calorific power, the condensation rates on the sump water and the containment walls, the  $I_2$  and aerosol I sources and the radiation dose rate in the water).

The chemical data include constant data (the silver specific area, the molar mass of the radical R, the initial concentrations of the chemical species in the gas phase and in the water phase and the value of the exponent n of the term  $[H^+]^n$  for the radiolysis law), and time dependent data: the pH of the sump solution when entered by the user. When the sump pH is calculated by the code, constant data must be entered by the user : the initial boric acid, the base (KOH,  $NH_4OH$ , LiOH,  $H_2O$ ) and the strong acid concentrations if any.

The chemical data also include a certain number of option cards. For the calculation, the user has the possibility to activate only the desired chemical reactions. In particular, if the system is not irradiated then all the radiolysis reactions should not be activated. The user has the option to modify the kinetic constants and the activation energies of the chemical reactions.

The input data include a timetable defining the imposed output times.

### **1.7. Calculation**

The coefficients for gas diffusion, viscosity, density and thermal conductivity together with the specific heat of the atmosphere, which are required to calculate the water-atmosphere iodine transfer flux, are derived by the code from the chemical composition of the atmosphere.

As the initial state is given, a system of differential equations can be solved at each instant required. To do this, a digital integrator of the predictor corrector type is used, already implemented in various ESCADRE codes.

### **1.8. Results**

The code results are grouped under four main headings. At each requested output time, we obtain :

- the material transfer flows :
  - the transfer flow of iodine I at the boundary phase area ( $\Phi_1^T$ ), the condensation flow of iodine I ( $\Phi_2^T$ ), the leak flow of iodine I ( $\Phi_3^T$ ), the source flow of iodine I<sub>2</sub> in the gas phase ( $\Phi_4$ ), the source flow of iodine I<sup>-</sup> in the liquid phase ( $\Phi_5$ ), the deposition flow of iodine I<sub>2</sub> in the gas phase ( $\Phi_6^T$ ) and the deposition flow of iodine I<sub>2</sub> in the liquid phase ( $\Phi_7^T$ )
- the chemical constituent concentrations in the gas phase and in the water phase, obtained directly by digital integration
- the iodine masses in the gas phase, in the liquid phase and on deposition surfaces.
- the I<sub>2</sub> and CH<sub>3</sub>I interfacial mass transfer coefficients

- - the sump pH
- the overall iodine partition coefficient P :

$$P = \frac{\text{atomic iodine concentration in the liquid phase}}{\text{atomic iodine concentration in the gas phase}}$$

Finally, results are safeguarded in a file held for subsequent graphic processing. These files can be treated with the graphic post-processors TIC and DRAKKAR .

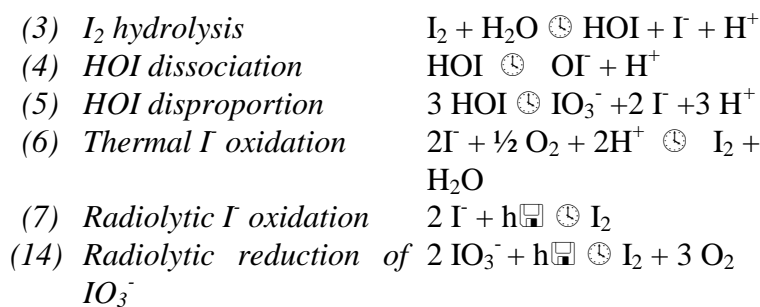
## 2. CALCULATIONS PERFORMED

### 2.1. Main assumptions

The main features of the calculations performed with the code IODE 4.0 are presented below.

#### Reactions considered

It has been assumed that there is only one initial iodine species, I, in the sump. The evolution of iodine has been modelled by considering the following reactions in the sump:



No homogeneous reactions in the gas phase have been included in the modelling. The code has the capability of modelling organic production and homogeneous reactions in the gas phase, but there is evidence that the modelling is oversimplified. In this test there are no painted surfaces nor coupons. Some contamination by organics of the tracer solution has been reported, but it is small (0.01%), and the corresponding organic concentration in the sump is not known. A simple approach has been preferred in this case and no organic species have been considered, and therefore all reactions of organic species have been disabled.

For all the reactions included in the calculations, the rate constants have been set to their default values, except for reaction (7). As mentioned in section 1.4, the formulation of the velocity in the code is expressed as:

$$V_c (7) = - k_7 [I]_l [H^+]^n D_o + k_{-7} [I_2]_l$$

where  $D_o$  is the radiation dose rate, and  $n$  is the power of the radiolysis law. In this study, the influence of the modelling of this reaction has been tested, and two values of  $n$  have been used:  $n= 0.5$ , which is the recommended value, and  $n=0.25$ . The corresponding value of the rate constant  $k_7$  is  $1.7 \cdot 10^{-3} \text{ M}^{-0.5} \text{ Gy}^{-1}$  for  $n=0.5$ , and  $2.5 \cdot 10^{-4} \text{ M}^{-0.25} \text{ Gy}^{-1}$  for  $n=0.25$ .

### Mass transfers

Mass transfer rate coefficients can be calculated by the code or entered by the user. For this test a value of  $10^{-5} \text{ m/s}$  has been selected for  $K_C$ , the molecular iodine mass transfer rate at the sump-atmosphere interface. This value is within the usual range ( $10^{-4} - 10^{-5} \text{ m/s}$ ) reported in RTF and PHEBUS modelling calculations.

Wall condensation of steam has been set to zero, and condensation at the liquid-gas interface has been neglected. The other mechanism modelled by the code for transfer of iodine is wall deposition, both in the gas and the liquid phase. As mentioned in section 1.3, adsorption on steel is only effective when there is no steam condensation on the surface. Considering that in this case the steam fraction is low (0.003 bars, as corresponds to the vapour pressure of water at 25 °C), a relatively high value of the deposition rate in the gas phase has been selected:  $10^{-4} \text{ m/s}$ , with a desorption rate of  $10^{-6} \text{ s}^{-1}$ .

As will be explained in the result section, there is a strong sensitivity towards the inclusion of the deposition process in the sump. To have a assessment of the influence of this mechanism in the overall distribution of iodine, calculations have been performed with and without deposition of molecular iodine on the sump SS surface. When considering deposition on the sump surfaces, a rate constant of  $1.4 \cdot 10^{-6} \text{ m/s}$  has been selected, with a desorption rate of  $10^{-7} \text{ s}^{-1}$ . The proposed deposition rate for the sump is two orders of magnitude lower than for the gas phase, thus reflecting that absorption in the sump is generally less effective than in the gas phase.

## 2.2. Input data

The input data for the calculations are shown in table 1. The data are common to all the calculations performed both for stage 1 and 2.

Gas Volume	0.34 m <sup>3</sup>
Gas Temperature	25 K
Liquid volume	0.025 m <sup>3</sup>
Liquid temperature	25 K
SS Gas phase surface	3.04 m <sup>2</sup>
SS Liquid phase surface	0.8 m <sup>2</sup>
Total Pressure	1 bar
Steam Pressure	0.03 bars
Oxygen Molar Fraction	0.2
Nitrogen Molar Fraction	0.8
I <sub>2</sub> Mass transfer rate for liquid phase	10 <sup>-5</sup> m/s
I <sub>2</sub> Mass transfer rate for gas phase	10 <sup>-3</sup> m/s
Wall Condensation Rate	0.0
Gas Phase Deposition Rate	10 <sup>-4</sup> m/s
Gas Phase Desorption Rate	10 <sup>-6</sup> s <sup>-1</sup>
Initial I mass	2.8575 10 <sup>-5</sup> kg.
Dose rate in sump	0.38 Gy/s
pH	Experimental values

Table 1. **Input data for the calculations.**

### Stage 1

Four calculations have been performed for this stage, taking the input data shown in table 1. The calculation ends at t = 363 h, 0.4 h before the vessel is discharged.

	K <sub>d</sub> (m/s) sump	n <sub>ox</sub>
Case 1	0.0	0.5
Case 2	1.4 10 <sup>-6</sup>	0.5
Case 3	0.0	0.25
Case 4	1.4 10 <sup>-6</sup>	0.25

Table 2. **Cases studied for stage 1**

$K_d$  is the rate constant for molecular iodine deposition on the stainless steel surface of the sump. Case 1 and Case 3 consider that there is no deposition on the SS surfaces of the sump. Cases 2 and 4 have been calculated to check the effect of the deposition mechanism, by setting a value of  $1.4 \cdot 10^{-6}$  m/s for the deposition rate constant, and a desorption rate of  $10^{-7} \text{ s}^{-1}$ .

$n_{\text{ox}}$  is the exponent of the iodide oxidation reaction (7). The corresponding value of the rate constant has been changed as explained before (section 2.1). Cases 3 and 4 try to assess the importance of the radiolytic oxidation modelling in the generation of molecular iodine.

## **Stage 2**

Four calculations have been performed for this stage, using the same set of variables as for stage 1, except for the pH values, which have been taken from the reported experimental measurements. The duration of the calculation is shorter than for stage 1, and has been stopped at  $t = 285$  h, corresponding to the dumping of the charge and washing of the vessel. Table 3 presents the variables used for the sensitivity calculations. The same study as for stage 1 has been performed, with the objective of checking the influence of deposition in the sump and of the value of the exponent of the radiolytic oxidation under different pH conditions.

	$K_d$ (m/s) sump	$n_{\text{ox}}$
Case 5	0.0	0.5
Case 6	$1.4 \cdot 10^{-6}$	0.5
Case 7	0.0	0.25
Case 8	$1.4 \cdot 10^{-6}$	0.25

**Table 3. Cases studied for stage 1**

As for stage 1,  $K_d$  is the rate constant for molecular iodine deposition on the stainless steel surface of the sump. Case 5 and Case 7 consider that there is no deposition on the SS surfaces of the sump. Cases 6 and 8 use a value of  $1.4 \cdot 10^{-6}$  m/s for the sorption rate, and a desorption rate of  $10^{-7} \text{ s}^{-1}$ .

$n_{\text{ox}}$  is the exponent of the iodide oxidation reaction (7). The corresponding value of the rate constant has been changed as explained before.

### **2.3. Results of the calculations**

Table 4 presents the calculated iodine distribution (in kg) at the end of the calculation for the 8 cases simulated. To ease the interpretation of the results, table 5 shows the same information in % relative to the total I inventory. It is assumed that there is no leak of iodine during the test, and possible losses of iodine due to sampling are not accounted for.

	Sump Liquid	Gas Phase	Gas deposits	Sump deposits
Stage 1				
Case 1	$2.666 \cdot 10^{-5}$	$1.810 \cdot 10^{-10}$	$1.916 \cdot 10^{-6}$	---
Case 2	$2.619 \cdot 10^{-5}$	$1.279 \cdot 10^{-10}$	$1.438 \cdot 10^{-6}$	$9.506 \cdot 10^{-7}$
Case 3	$1.591 \cdot 10^{-5}$	$9.130 \cdot 10^{-10}$	$1.267 \cdot 10^{-5}$	---
Case 4	$1.271 \cdot 10^{-5}$	$5.535 \cdot 10^{-10}$	$9.504 \cdot 10^{-6}$	$6.361 \cdot 10^{-6}$
Stage 2				
Case 5	$2.454 \cdot 10^{-5}$	$1.847 \cdot 10^{-10}$	$4.031 \cdot 10^{-6}$	---
Case 6	$2.326 \cdot 10^{-5}$	$1.527 \cdot 10^{-10}$	$2.914 \cdot 10^{-6}$	$2.399 \cdot 10^{-6}$
Case 7	$1.250 \cdot 10^{-5}$	$3.468 \cdot 10^{-10}$	$1.608 \cdot 10^{-5}$	---
Case 8	$9.434 \cdot 10^{-6}$	$2.215 \cdot 10^{-10}$	$1.031 \cdot 10^{-5}$	$8.834 \cdot 10^{-6}$

Table 4. **Iodine distribution at the end of the calculation. Mass of iodine in kg.**

	Sump Liquid	Gas Phase	Gas deposits	Sump deposits
Stage 1				
Case 1	93.29	0.0006	6.70	---
Case 2	91.65	0.0004	5.03	3.33
Case 3	55.67	0.0032	44.33	---
Case 4	44.48	0.0019	33.26	22.26
Stage 2				
Case 5	85.88	0.0006	14.11	---
Case 6	81.40	0.0005	10.20	8.40
Case 7	43.74	0.0012	56.27	---
Case 8	33.01	0.0008	36.08	30.91

Table 5. **Iodine distribution at the end of the calculation. Mass of iodine in % relative to initial inventory of I.**

The iodine species present in the liquid phase are I<sup>-</sup>, HOI, IO<sub>3</sub><sup>-</sup> and I<sub>2</sub>. The only iodine species considered in the gas phase is I<sub>2</sub>. Sump liquid and gas phase entries in tables 4 and 5 are calculated by adding the mass of iodine (I) of all the species composing each phase, excluding the deposits. Sump deposit is zero for cases 1, 3, 5 and 7 where no deposition on the sump surfaces has been included in the modelling.

## **Stage 1**

The only iodine species present in the gas phase is molecular iodine. As no reactions in the gas phase have been considered, the concentration of  $I_2$  in the atmosphere of the vessel is the result of two competing mechanisms: the transfer from the sump, and the removal from the atmosphere by deposition on the wall surfaces.

The transfer is determined by the evolution of the concentration of  $I_2$  in the sump, which depends on the equilibrium among all the iodine species present. The main factor influencing this equilibrium is the pH, as the temperature and radiation dose rate are kept constant. As the test progresses and the pH decreases, there is an increase in the  $I_2$  concentration in the sump. The rate constant for transfer to the atmosphere being relatively high, the curve of molecular iodine concentration in the gas phase follows the same trend of that in the sump, reflecting the changes in the pH. For instance, the decrease of the pH value from 10.1 to 7.7 at  $t = 23.39$  h results in a peak in the concentration of  $I_2$  both in the gas and liquid phases. All the variations in both concentrations can be explained by pH changes. Except for small oscillations, the pH decreases during the duration of the test until  $t = 362.71$  h, and so  $I_2$  production increases. Part of the iodine transferred to the gas phase is deposited onto the wall, and the load of iodine on the wall increases all throughout the test.

From  $t = 362.71$  h to  $t = 363.26$  h there is an increase in the experimental pH from 7.4 to 9.5. The end of the calculation occurs at  $t = 363$  h, which lies in between both data points, and the code interpolates linearly to obtain a pH value of 8.5 for  $t_{\text{end}}$ . As the iodine distribution depends strongly on the pH, the last point of the calculation shows a sharp increase of iodine concentration in the sump and the corresponding decrease of  $I_2$  in the gas phase. This causes an increase of nearly two orders of magnitude in the partition coefficient. Note that the final iodine concentration in the gas and liquid phases, and therefore the value of the partition coefficient, is very dependant on the time selected to stop the calculation, the deposits being unaffected.

## **Sensitivity Studies**

In the cases considered, the main factor influencing iodine evolution is the radiolytic oxidation model. Two values of  $n$ , the exponent of the iodide oxidation reaction, have been chosen, as shown in table 2. As can be seen from the results, the decrease in  $n$  from 0.5 to 0.25 results in an increase of  $I_2$  concentration in the gas and liquid phases of approximately one order of magnitude. As expected, the load of iodine on the walls of the atmosphere is increased by approximately a factor 6, this factor being constant along the duration of the test (not shown in the figures). As a result of the enhancement of the iodide oxidation in the sump,  $I^-$  concentration in the liquid phase at the end of the calculation decreases from  $8 \cdot 10^{-6}$  M (cases 1 and 2) to  $4 \cdot 10^{-6}$  M (cases 3 and 4).

A second factor affecting the final iodine distribution is the value of the  $I_2$  sump deposition rate,  $K_d$ . The inclusion of a deposition process in the sump produces a load of iodine on the wall of 3.3% of the total iodine inventory for  $n=0.5$ . When the value  $n=0.25$  is used, the higher production of  $I_2$  in the sump causes an increase of the load on the sump walls, that reaches a value of 22.3 % at the end of the calculation.

## **Stage 2**

As for stage 1, the equilibrium in the sump is determined by the pH. For the first part of this test, when the pH decreases from 10.2 to 5.4, the behaviour is qualitatively the same as for stage 1: there is an increase in the  $I_2$  concentration both in the gas and liquid phases, with a strong sensitivity towards the value of the exponent of the radiolytic oxidation law.

However, for  $t > 192$  h, the pH changes from 5.4 to 10.2 and there is a sharp decrease of the  $I_2$  concentration in the gas phase with the corresponding increase in the concentration of the ionic iodine species in the liquid phase. The load of iodine in the surfaces decreases slightly until the end of the calculation.

In general, the calculation presents a similar sensitivity towards the value of  $n$  and the sump deposition as for stage 1. No studies have been performed to check the sensitivity towards the value of the desorption rate constants, which could have an effect in the second part of the test ( $t > 192$  h), when some desorption from the walls takes place.

Due to the low values of the pH in Stage 2 for the first 192 h, the average  $I_2$  concentration both in the liquid and the gas phases is higher for Stage 2 than for Stage 1, thus producing a higher deposition both in the liquid and gas phases. This effect can be seen comparing case 1 and case 5, for instance. The effect of the increase of the pH at  $t = 192$  h, that decreases  $I_2$  concentrations, causes a small resuspension of the deposits and alters the value of the partition coefficient in approximately two orders of magnitude when compared with the value obtained before the pH change. A similar pH jump from 7.5 to 10.0 causes the increase in the partition coefficient of stage 1, so that the final partition coefficients are comparable for both stages.

## **2.5. Conclusions**

The modelling used for this study considers the equilibrium among  $I^-$ , HOI,  $IO_3^-$  and  $I_2$  in the liquid phase, followed by the transfer of  $I_2$  to the atmosphere of the vessel and deposition on the walls. A sensitivity study has been performed on the effect of the modelling of the radiolytic oxidation law and on the inclusion of a deposition process on the sump walls.

Iodine evolution is controlled by the pH of the solution. It presents a different behaviour in both stages. With the exception of the last point of the calculation, the pH of stage 1 increases all throughout the test, producing an increase in I<sub>2</sub> production in the liquid and the gas phase. On the contrary, in stage 2 there is a decrease of pH at t = 192 h. At this point the concentrations of I<sub>2</sub> decrease, and desorption from surfaces occurs until the end of the calculation. The average I<sub>2</sub> concentration both in the liquid and the gas phases is higher for stage 2 than for stage 1.

The main factor found influencing the calculation is the modelling of the radiolytic oxidation of iodide. Some influence is also attributed to the inclusion of a deposition mechanism for molecular iodine in the sump. However, only an assessment of the importance of these factors has been made, and detailed sensitivity calculations should be undertaken to check the effect of a broader range of values of the deposition constants and the parameters of the kinetic expression of the radiolytic oxidation expression.

The values partition coefficient at the end of the calculation are similar for both stages, reflecting the high pH value at that time. Nevertheless, the load of iodine on the surfaces is higher for stage 2 due to the fact that the average I<sub>2</sub> concentrations are higher for that stage.

## **2.6. Acknowledgements**

The author wishes to thank C. Poletiko for fruitful discussions and Consejo de Seguridad Nuclear for financial support.

**SIMULATION OF THE ISP41 IODINE TEST PROBLEM WITH  
THE MELCOR IODINE MODEL**

M.F. Young and R.O. Gauntt  
Sandia National Laboratories



## 1 INTRODUCTION

The ISP41 International Standard Test Problem was simulated using the MELCOR fully integrated, engineering-level, nuclear power plant analysis code [2].

The simulation was done using standard MELCOR features and the new MELCOR iodine pool chemistry model. ISP41 is an iodine pool experiment conducted in the AECL Radioiodine Test Facility (RTF) as part of a program to develop data on the behaviour of iodine in reactor containment pools[3].

## 2 THE MELCOR IODINE MODEL

The MELCOR iodine pool model was developed to simulate behaviour of iodine in reactor containment pools. The model operates within the MELCOR integrated reactor plant accident analysis code[1]. The MELCOR code, developed at Sandia National Laboratories for the Nuclear Regulatory Commission, models virtually all aspects of a severe accident in a nuclear reactor power plant including:

- accident initiation and reactor core uncovering;
- fuel heatup, damage, cladding oxidation and hydrogen generation;
- fission product release and transport from the reactor coolant system to the containment building,
- fission product vapour and aerosol transport in the containment system, and
- releases to the environment.

The recently developed aqueous iodine chemistry model operates within the MELCOR Radionuclide Package and includes treatments for:

- formation of water radiolysis species,
- atmospheric radiolysis products (nitric acid formation from air and hydrochloric acid formation from plastics),
- pool pH calculation including effects of buffers
- iodine chemical reactions in the aqueous phases,
- formation of organic iodine
- pool-to-atmosphere mass transfer,
- wall deposition and revolatilisation.
- 

Other modules in MELCOR provide boundary and source conditions to the iodine chemistry models including:

- water pool mass and enthalpy sources from pipe leaks and vapour condensation
- ionising radiation sources from fission product transport in the containment
- iodine source from CsI and I vapour and aerosol transported from reactor system into containment.
- Sources for other operative species: CO, CO<sub>2</sub>, Ag, buffers, etc.

The iodine chemistry model operates in co-ordination with the other MELCOR models to predict the evolution of iodine species in the containment system with the aim of predicting iodine transport within the containment and release to the environment.

## 2.1 Aqueous iodine chemistry

The aqueous iodine chemistry model is a semi-mechanistic model based in large part on the INSPECT equation set[4] and on numerous extensions by Powers[5], including additional reactions and modified rate coefficients. The model includes the effects of radiolysis, uptake of iodine by silver, metal ions (represented by iron), and acid-base buffers. Equations are included for organic iodine, represented as methyl iodine.

The chemical equations in the set are of the general form



with forward reaction rate  $k_f$  and reverse rate  $k_r$ . These are used to set up chemical reaction kinetic equations for each chemical species in the set. Using the above equation as an example, the reaction rate equation for species  $C$  would include terms from this equation, and where appropriate, a source from radiolysis:

$$\frac{d[C]}{dt} = k_f[A][B] - k_r[C][D] + \dot{S}$$

where the brackets [ ] indicate concentration of the species, and the  $\dot{S}$  is the source of  $C$  from radiolysis. The set of chemical reaction kinetics equations form a coupled set of nonlinear ordinary differential equations, which are solved using a standard stiff differential equation solver[6] to get the pool speciation. Initial conditions are set up by assuming some species, termed driver species, are given and constant over a calculational timestep. Some are set by assuming equilibrium with the atmosphere; these are aqueous  $O_2$ ,  $H_2$ , and  $CH_4$ . The  $OH^-$  and  $H^+$  are set by determining the pool pH. The initial iodine concentration is specified at the beginning of the timestep, as is the iron ion concentration. Other species in the pool, such as silver, nitric and hydrochloric acids, and phosphate and borate buffers, do not actually participate in the calculation of speciation other than to set the initial pH and iodine level. Pool pH is determined either from an acid-base balance or is read in directly via user input.

## 2.2 Pool-atmosphere mass transfer

Mass transfer of iodine species between the pool and the atmosphere is accomplished using a two-film model. It is assumed that the iodine concentration in the pool is in equilibrium with that in the atmosphere at the pool surface as determined using a partition

coefficient. The transport to the bulk atmosphere is then given by a mass transport equation relating the atmospheric surface concentration and the bulk atmosphere concentration:

$$\frac{d[I_{2atm}]}{dt} = k_{pool} \frac{A_{pool}}{V_{atm}} \left( \frac{[I_{2aq}]}{PC} - [I_{2atm}] \right)$$

where  $PC$  is a partition coefficient.

### 2.3 Atmospheric radiolysis

The atmospheric radiolysis model considers homogeneous radiolytic decomposition of iodine species, and formation of nitric and hydrochloric acids. The chlorine to form hydrochloric acid is released from radiolysis of chlorine-containing plastics in the control volume; the mass of these plastics and a wall dose can be specified via user input to MELCOR. At present, only molecular iodine and methyl iodine species are tracked in the atmosphere, so other iodine species (atomic iodine, iodate) are combined into the molecular iodine class for transport purposes. Nitric and hydrochloric acids formed in the atmosphere by radiation can be deposited in the pool or in the water films on wet walls via a non-reversible mass transport equation. Acids deposited in wall films are transported to the pool using the MELCOR film transport model.

### 2.4 Iodine wall deposition

Atmospheric iodine or methyl iodine can be deposited on or released from dry walls via a reversible mass transport equation. If the walls subsequently become wetted, the deposited iodine is assumed to be released into the wall film, which can carry the iodine into the pool using the MELCOR film transport model. The wall transport equation is a physical adsorption-desorption model of the form

$$\frac{d[I_{2wall}]}{dt} = k_{ad} [I_{2atm}] - k_{de} [I_{2wall}].$$

In the above equation,  $k_{ad}$  is the adsorption coefficient (m/s),  $k_{de}$  is the desorption coefficient ( $s^{-1}$ ), and the wall concentration is in ( $\text{mole}/\text{m}^2$ ).

## 3 SIMULATION OF ISP41

### 3.1 Data provided

The ISP41 initial and boundary conditions were provided to the exercise participants and are shown in Table 2. These consist of the RTF vessel dimensions, wall material, temperature and pressure, radiation dose level, and initial caesium iodide concentration. Also provided (not shown) were the pool pH and dissolved oxygen levels versus time for Stages 1 and 2 of the experiment.

Table 2. **ISP41 Initial and boundary conditions**

Vessel	316 Stainless Steel
Dose Rate	~ 1.36 kGy/hr
Temperature	25° C (±3° C)
Initial I <sub>2</sub> Concentration	9 x 10 <sup>-6</sup> mol/L CsI (±10%)
Aqueous Volume	25 L (±10%)
Gas Volume	315 L (±1%)
Aqueous Surface Area	5200 cm <sup>2</sup>
Interfacial Surface Area	3700 cm <sup>2</sup>
Gas Surface Area	22000 cm <sup>2</sup>

### 3.2 MELCOR problem set-up

The RTF experiment vessel was set up in MELCOR as a single control volume (CV) 0.688 m in diameter by 0.918 m high with stainless steel walls, top and bottom. The cylinder walls and top were given constant temperature boundary conditions of 300 K, whereas the bottom (under the pool) was given a constant temperature boundary condition of 298.15 K. This arrangement is to keep a water film from forming on the vessel walls. The experiment pool and atmosphere sampling loops were not simulated.

Initial conditions were set up in MELCOR by injecting caesium iodide as a radionuclide source. The dose was set by user input for the iodine pool model, and the provided pH history was read in from an external data file (EDF). The provided pool oxygenation history was not used; the MELCOR pool model assumes that the pool oxygen concentration is in equilibrium with the atmosphere via a Henry's law relationship; however, this assumption gives an oxygen concentration very close to the measured oxygen concentration in the experiment.

The wall adsorption and desorption coefficients were set at values ( $9 \times 10^{-4}$  m/s,  $9 \times 10^{-7}$  s<sup>-1</sup>) derived from a published results on RTF tests[7]. These result in fairly high deposition rates, but the results seem consistent with the reported high pool iodine depletion rates in RTF tests. It was found necessary to increase the pool-atmosphere mass transfer coefficient by a factor of 3 (to 0.01 m/s) to accommodate the high wall deposition rate.

## 4 RESULTS OF ISP41 SIMULATION

### 4.1 Stage 1 Simulation

The pH history shown in [ ] was used as input in the simulation of Stage 1. The initial condition was set by sourcing in  $5.88 \times 10^{-5}$  kg of cesium iodide, resulting in an initial I

concentration of  $9 \times 10^{-6}$  mol/L. The concentration of  $I^-$  in the pool (essentially the same as the total iodine concentration), the molecular iodine concentration in the atmosphere, and the amount of iodine deposited on the walls are shown in Figures 2-4 versus time. As seen in [ ], at the initial pH level of 10, essentially all of the iodine remains in the aqueous phase. When the pH is lowered to 9, a small amount of iodine begins to build in the atmosphere, resulting in a low level of wall deposition (Figure 4) and some resulting depletion of total pool iodine (Figure 3). As the pH of the pool is adjusted downward, the atmospheric iodine concentration continues to increase and the wall deposition rate and pool depletion rates both increase correspondingly. At the end of the first phase of the test, just after 350 hours, the pool pH is adjusted back up to  $\sim 10$ . At this time, the MELCOR model predicts a drop of iodine concentration in the atmosphere as iodine is reabsorbed into the water. The wall deposition of iodine then begins to decrease. At the end of the test, the iodine mass was distributed between the pool, atmosphere and walls in the fractions 0.394,  $2.5 \times 10^{-6}$ , and 0.604, respectively. In this simulation, only molecular iodine is released to the atmosphere, although partition coefficients are included in the model for  $I^0$  and HOI. Some of the principal pool species ( $I_2$ , HOI,  $IO_3^-$ ,  $I^0$ ) are shown in Figure 9.

## 4.2 Stage 2 simulation

Stage 2 was simulated essentially the same way as Stage 1, except than the pH history in Figure 5 was used. Figures 6-8 and 10 show the corresponding results. At the end of the test, the iodine mass was distributed between the pool, atmosphere and walls as 0.256,  $3.1 \times 10^{-6}$ , and 0.743, respectively.

## 4.3 Discussion

Generally, by the end of the test, most of the iodine was predicted to be deposited on the walls of the vessel. Iodine desorption from the walls was predicted at then end of the test when the pH was increased to  $\sim 10$ . It is possible that some amount of the iodine deposited on the walls might be permanently bound, however the MELCOR model currently treats wall adsorption as reversible. Some variation of parameters was done to determine model sensitivities, and it was found that the most sensitive parameter was the dose rate, the pH being given. Following this was the aqueous oxygen concentration. It was found that the aqueous iodine level was insensitive to the metal ion concentration at the given ISP-41 oxygen concentration, although it is sensitive at lower oxygen levels.

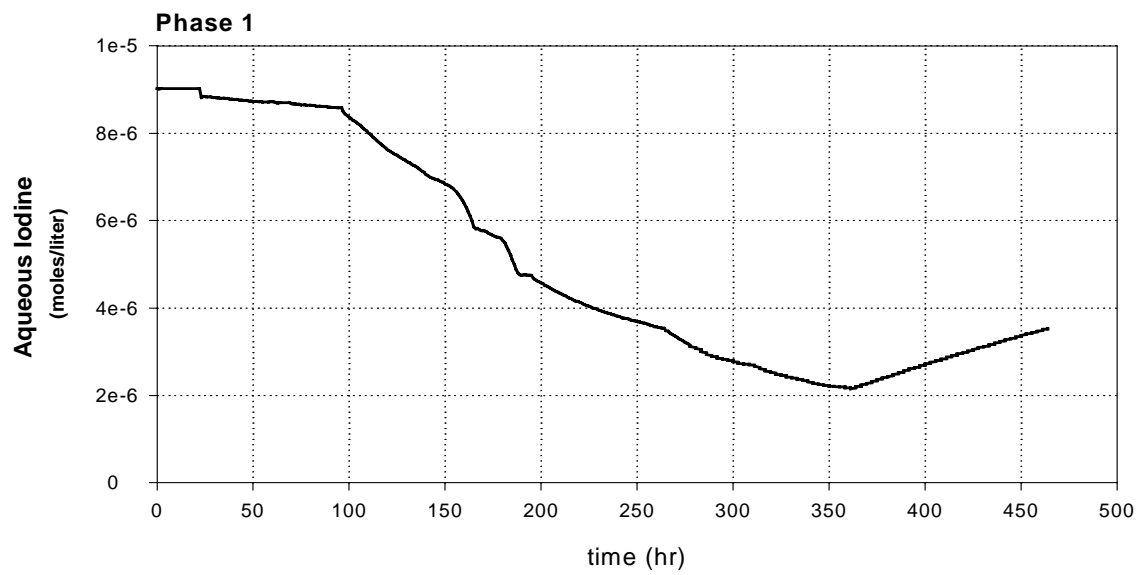


Figure 1. Phase 1 aqueous iodine predicted by MELCOR.

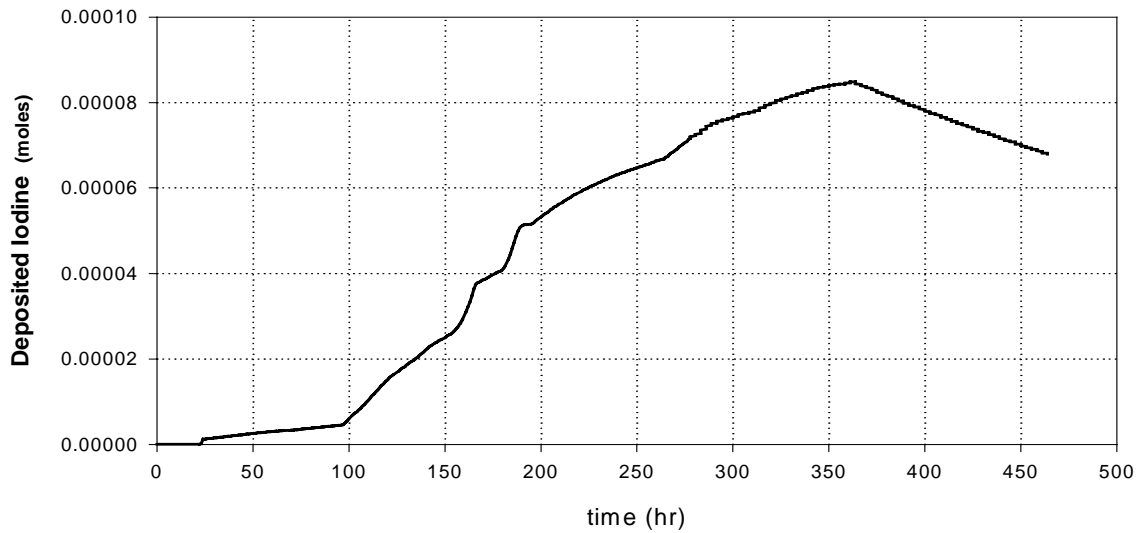


Figure 2. Phase 1 deposited iodine predicted by MELCOR.

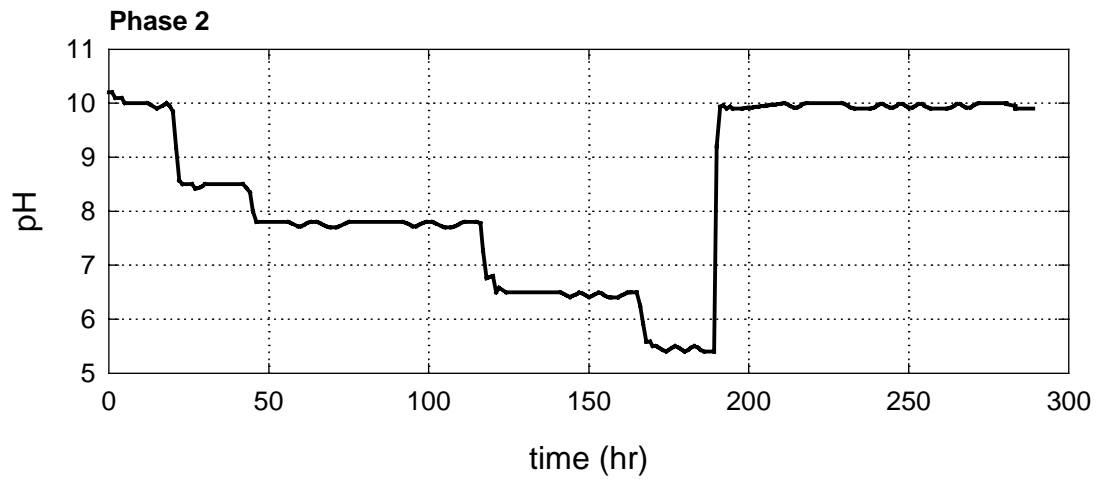


Figure 3. Phase 2 pH history.

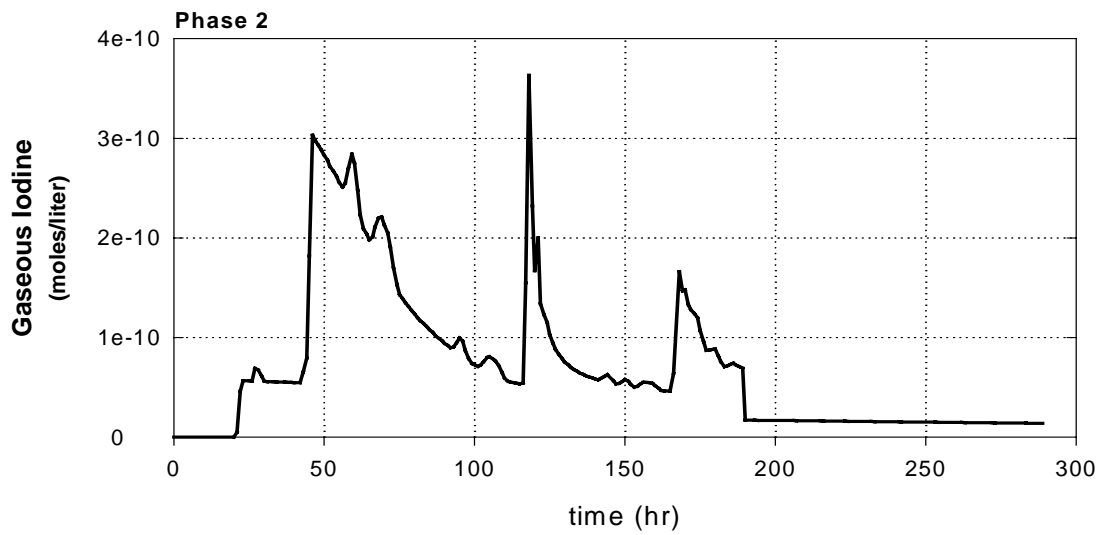


Figure 4. Phase 2 gaseous iodine predicted by MELCOR.

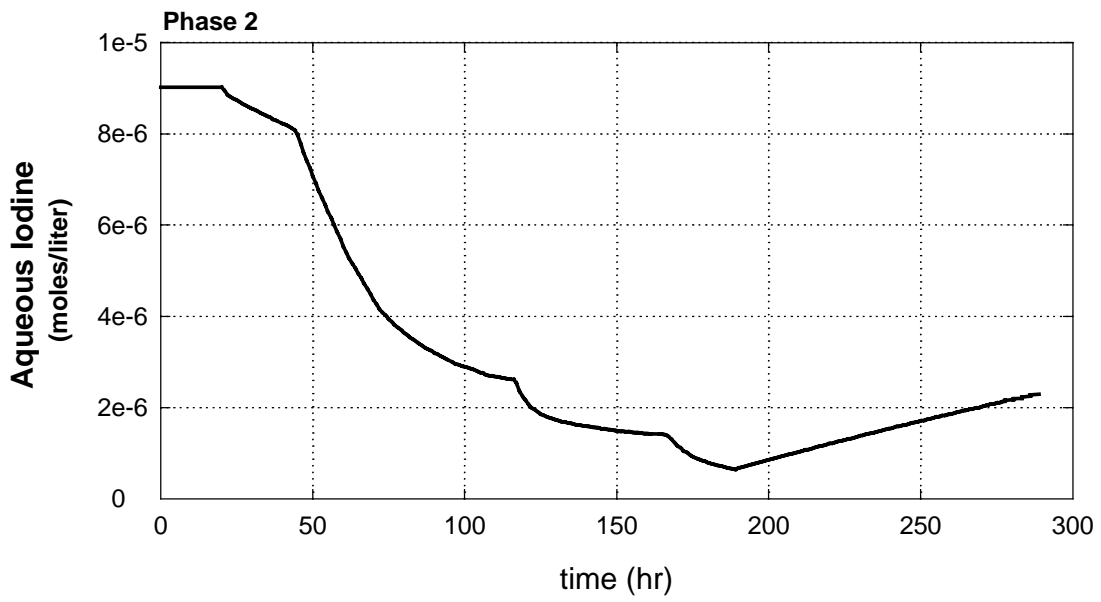


Figure 5. Phase 2 aqueous iodine predicted by MELCOR.

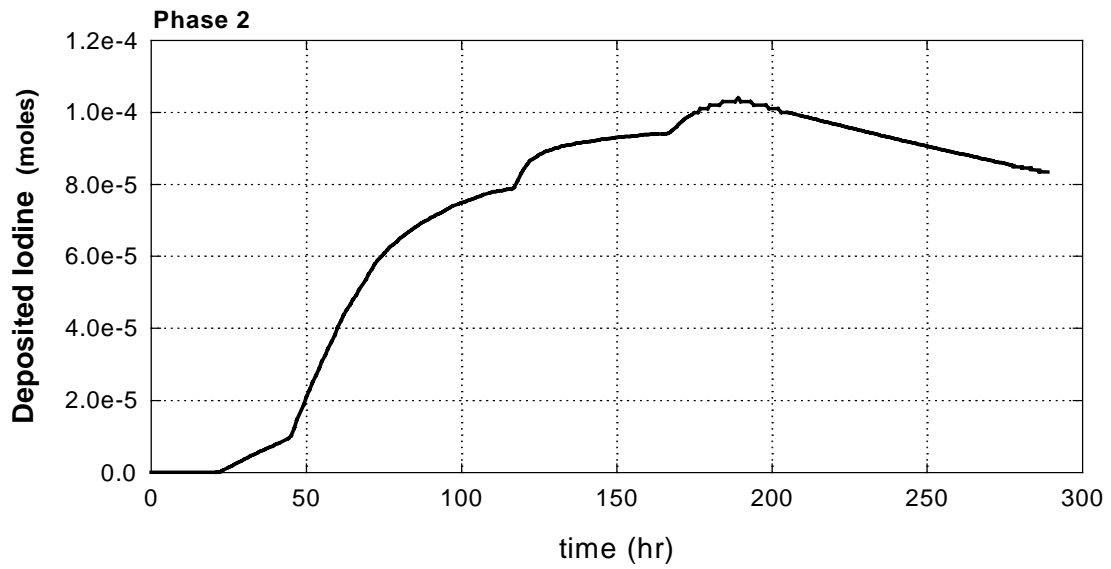


Figure 6. Phase 2 deposited iodine predicted by MELCOR.

## **APPENDIX B**

# **INPUT DATA AND RESULTS FROM THE FIRST SET OF CALCULATIONS**



Table 1  
**Mass transfer and adsorption-desorption rate constants used as input into each model for 1<sup>st</sup> set of calculations<sup>a</sup>**

	$k_t$ (dm·s <sup>-1</sup> )	$v_d$ (dm·s <sup>-1</sup> ) (gas phase unless otherwise indicated)	$k_{des}$ (s <sup>-1</sup> ) (gas phase unless otherwise indicated)
CIEMAT	$1 \times 10^{-4}$ (I <sub>2</sub> )	$1 \times 10^{-3}$	$10^{-6}$
CIEMAT	$1 \times 10^{-4}$ (I <sub>2</sub> )	$1 \times 10^{-3}$ $1.4 \times 10^{-6}$ (sump)	$10^{-6}$ $10^{-7}$ (sump)
IPSN	$1 \times 10^{-4}$	$10^{-3}$	0
NRIR	$5 \times 10^{-4}$ (I <sub>2</sub> )	$9 \times 10^{-3}$	$9 \times 10^{-7}$
Siemens	$6 \times 10^{-5}$ (I <sub>2</sub> ) $1 \times 10^{-4}$ (CH <sub>3</sub> I)	$2.9 \times 10^{-10}$	0
GRS	$6 \times 10^{-5}$ $1 \times 10^{-4}$ (CH <sub>3</sub> I)	$2.9 \times 10^{-10}$	0
PSI	$5 \times 10^{-5}$ $1 \times 10^{-4}$ (CH <sub>3</sub> I)	$2.9 \times 10^{-10}$	0
JAERI	$5 \times 10^{-5}$	$2.5 \times 10^{-2}$	0
Sandia	$1.2 \times 10^{-3}$ (I <sub>2</sub> )	$9 \times 10^{-3}$	$9 \times 10^{-7}$
AECL	$5 \times 10^{-4}$ (I <sub>2</sub> )	$9 \times 10^{-3}$	$9 \times 10^{-7}$

<sup>a</sup> For the second set of calculations all participants used  $9 \times 10^{-3}$  dm·s<sup>-1</sup> and  $9 \times 10^{-7}$  s<sup>-1</sup> for adsorption and desorption rate constants and  $5 \times 10^{-4}$  dm·s<sup>-1</sup> for the rate constant for interfacial mass transfer. The exception was GRS who used  $6 \times 10^{-5}$  dm·s<sup>-1</sup> for the interfacial mass transfer coefficient.

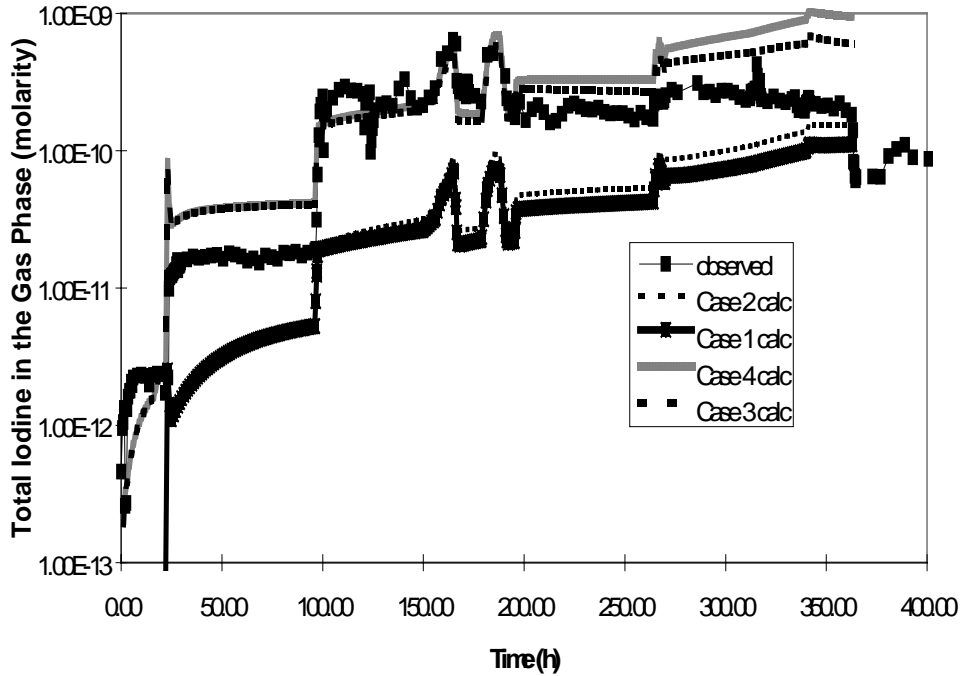
Table 2  
**Radiolysis rate constants used in IODE and IMPAIR: 1<sup>st</sup> calculation**

	$k_{13}$ (mol·dm <sup>-3</sup> ) <sup>a</sup>	$k_{-13}$ (s <sup>-1</sup> )	$n_1$	$k_{13} \cdot D \cdot [H^+]^n$ at pH 5 (s <sup>-1</sup> )	$k_{17} (s^{-1})^{-0.3}$	$n_{17}$
IMPAIR PSI	$3 \times 10^{-5}$ kGy <sup>-1</sup>	$2 \times 10^{-7}$	0.35	$1.48 \times 10^{-10}$	$5 \times 10^{-5}$	1.3
IMPAIR Siemens	$2.3 \times 10^{-4}$ kGy <sup>-1</sup>	$2 \times 10^{-7}$	0.4	$8.9 \times 10^{-10}$	$5 \times 10^{-5}$	1.3
IMPAIR GRS	$2.3 \times 10^{-4}$ kGy <sup>-1</sup>	$2 \times 10^{-7}$	0.4	$8.9 \times 10^{-10}$	$5 \times 10^{-5}$	1.3
IMPAIR JAERI	$7 \times 10^{-4}$ kGy <sup>-1</sup>	$2 \times 10^{-7}$	0.25	$1.5 \times 10^{-8}$	$5 \times 10^{-5}$	1.3
IODE CIEMAT <sup>a,b</sup>	$1.7 \times 10^{-3}$ Gy <sup>-1</sup>	$2 \times 10^{-5}$	0.5	$2.1 \times 10^{-6}$	n.a.	n.a.
IODE CIEMAT <sup>a,b</sup>	$2.5 \times 10^{-4}$ Gy <sup>-1</sup>	$2 \times 10^{-5}$	0.25	$5.5 \times 10^{-6}$	n.a.	n.a.
IODE NRIR <sup>a,b</sup>	$0.1$ Gy <sup>-1</sup>	0	0.5	$3.2 \times 10^{-2}$	0.01	1.3
IODE IPSN <sup>b</sup>	$1.7 \times 10^{-3}$ Gy <sup>-1</sup>	$2 \times 10^{-5}$	0.5	$2.1 \times 10^{-6}$	n.a.	n.a.

<sup>a</sup> The rate constants  $k_{14}$  and  $k_{-14}$  in IODE, used to represent  $2\text{IO}_3 = \text{I}_2 + \text{O}_2$  are set to be the same as  $k_{13}$  and  $k_{-13}$

<sup>b</sup> The user performed four calculations in total, two with each rate constant and different adsorption desorption rates.

a)



b)

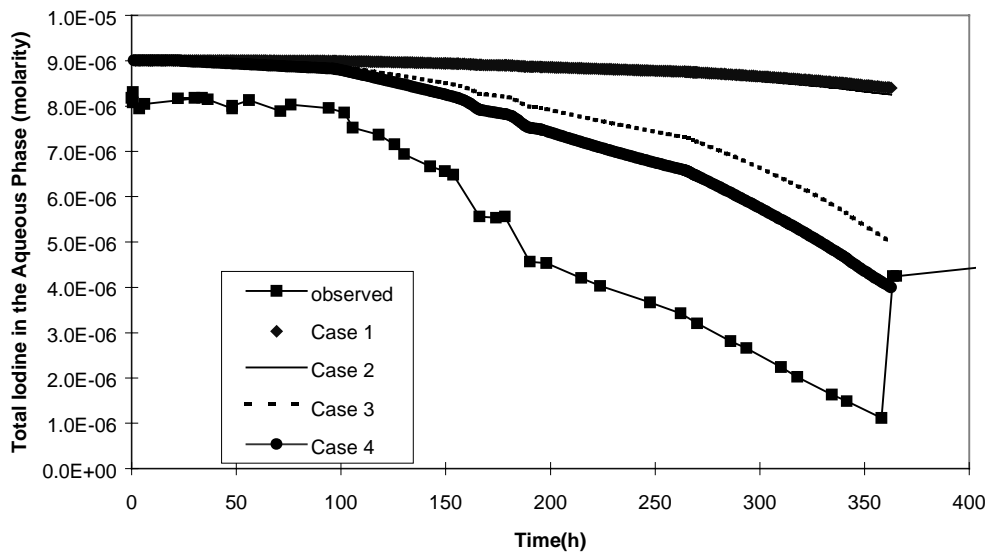
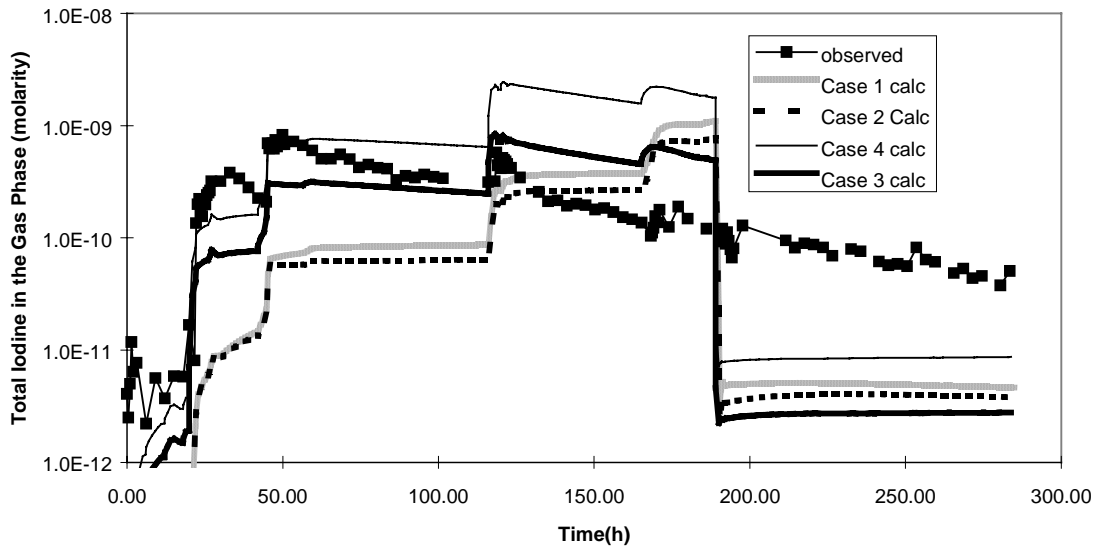


Figure 1. CIEMAT: Observed vs. calculated results for Stage 1. a) Total concentration of iodine in the gas phase b) Total concentration of iodine in the aqueous phase

Case 1:  $k_{13} = 1.7 \times 10^{-3} \text{ Gy}^{-1}$ ,  $k_{-13} = 2 \times 10^{-5} \text{ s}^{-1}$ ,  $n=0.5$  no aqueous phase adsorption  
 Case 2:  $k_{13} = 1.7 \times 10^{-3} \text{ Gy}^{-1}$ ,  $k_{-13} = 2 \times 10^{-5} \text{ s}^{-1}$ ,  $n=0.5$  aqueous phase adsorption  
 Case 3:  $k_{13} = 2.5 \times 10^{-4} \text{ Gy}^{-1}$ ,  $k_{-13} = 2 \times 10^{-5} \text{ s}^{-1}$ ,  $n=0.25$  no aqueous phase adsorption  
 Case 4:  $k_{13} = 2.5 \times 10^{-4} \text{ Gy}^{-1}$ ,  $k_{-13} = 2 \times 10^{-5} \text{ s}^{-1}$ ,  $n=0.25$  aqueous phase adsorption

a)



b)

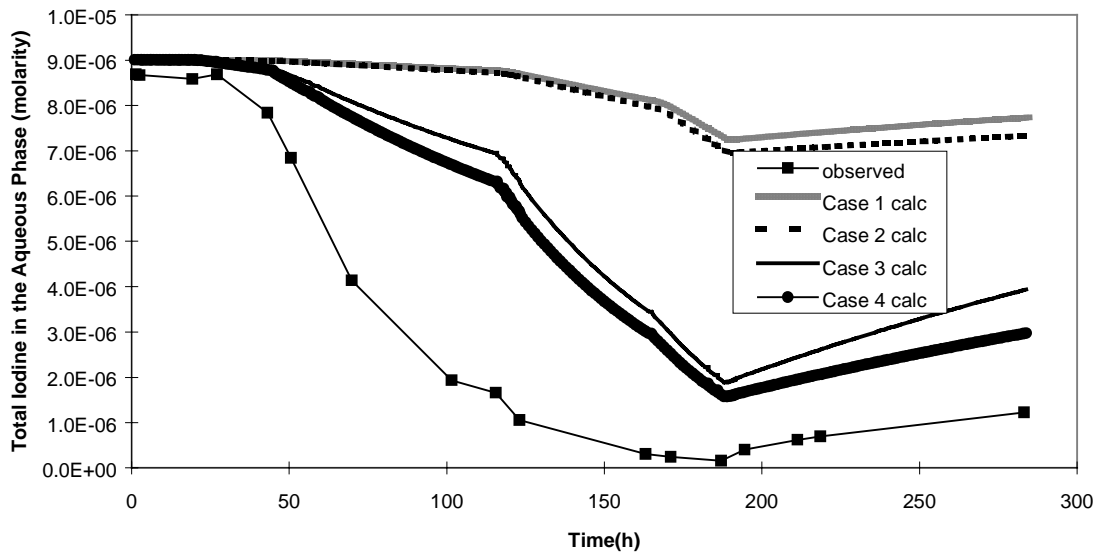
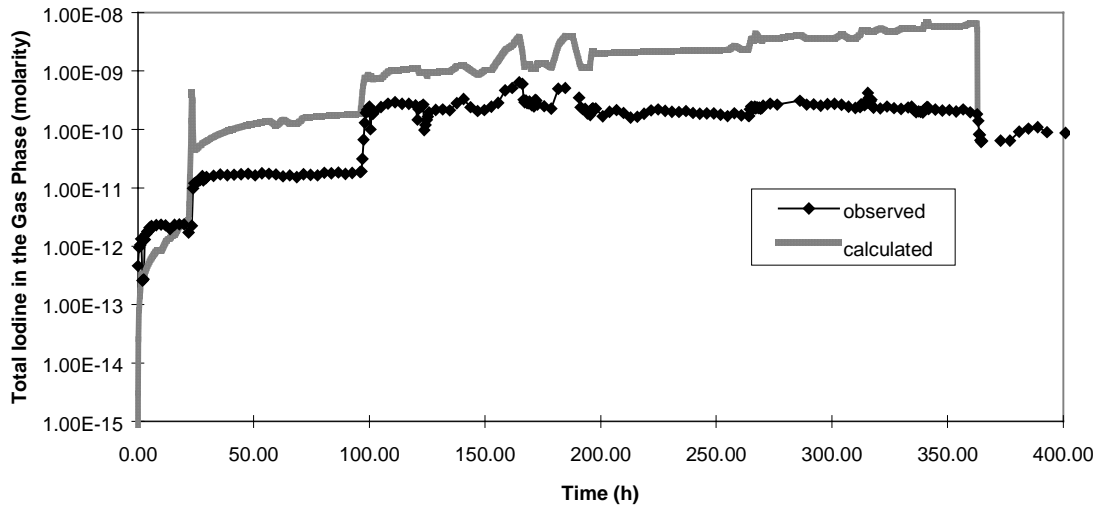


Figure 2. **CIEMAT: Observed vs. calculated results for Stage 2. a) Total concentration of iodine in the Gas phase b) Total concentration of iodine in the aqueous phase**

Case 1:  $k_{13} = 1.7 \times 10^{-3} \text{ Gy}^{-1}$ ,  $k_{-13} = 2 \times 10^{-5} \text{ s}^{-1}$ ,  $n=0.5$  no aqueous phase adsorption  
 Case 2:  $k_{13} = 1.7 \times 10^{-3} \text{ Gy}^{-1}$ ,  $k_{-13} = 2 \times 10^{-5} \text{ s}^{-1}$ ,  $n=0.5$  aqueous phase adsorption  
 Case 3:  $k_{13} = 2.5 \times 10^{-4} \text{ Gy}^{-1}$ ,  $k_{-13} = 2 \times 10^{-5} \text{ s}^{-1}$ ,  $n=0.25$  no aqueous phase adsorption  
 Case 4:  $k_{13} = 2.5 \times 10^{-4} \text{ Gy}^{-1}$ ,  $k_{-13} = 2 \times 10^{-5} \text{ s}^{-1}$ ,  $n=0.25$  aqueous phase adsorption

a)



b)

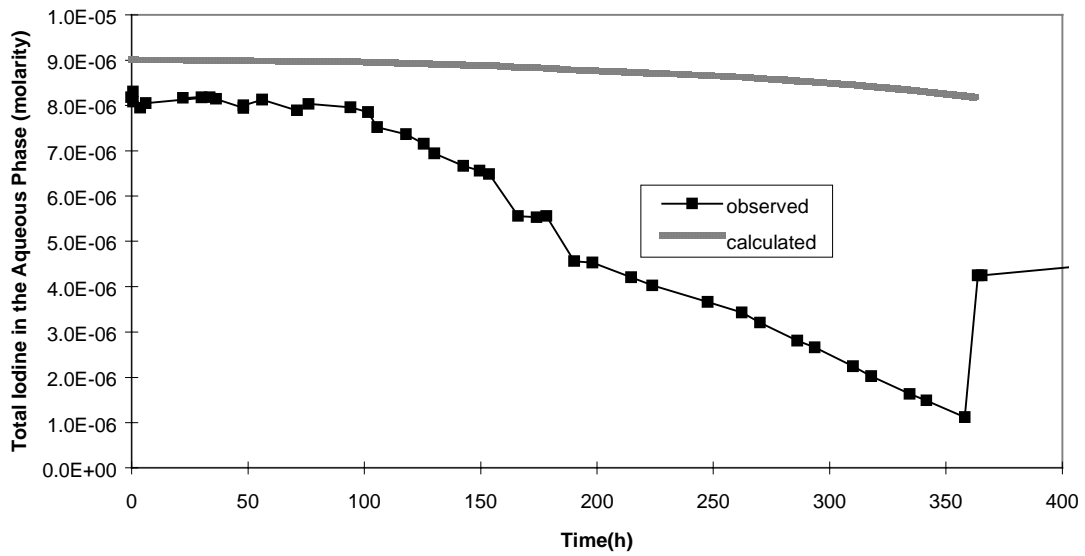
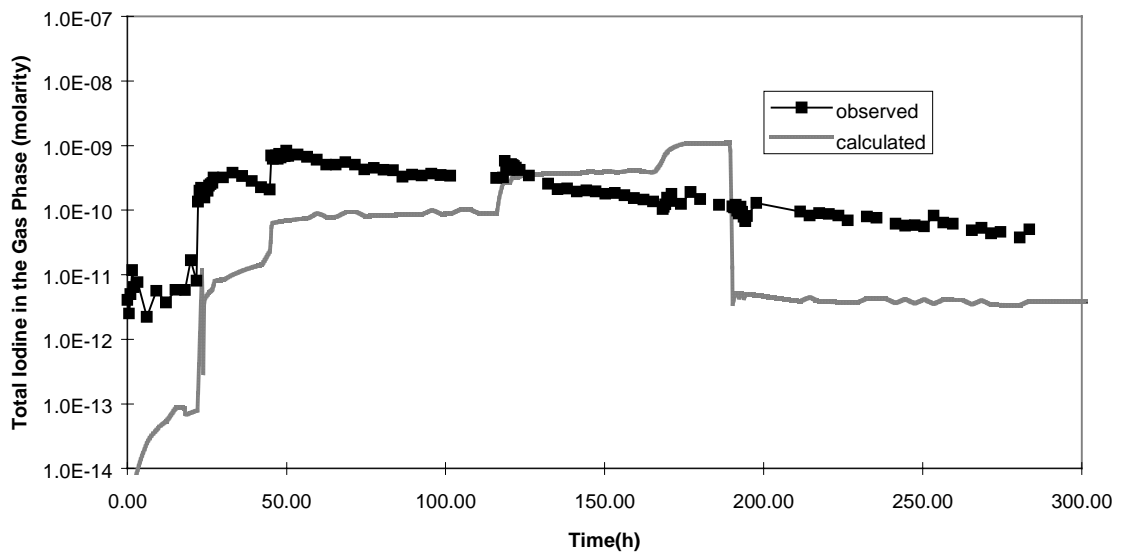


Figure 3. **IPSN: Observed vs. calculated results for Stage 1. a) Total concentration of iodine in the gas phase. b) Total concentration of iodine in the aqueous phase**

a)



b)

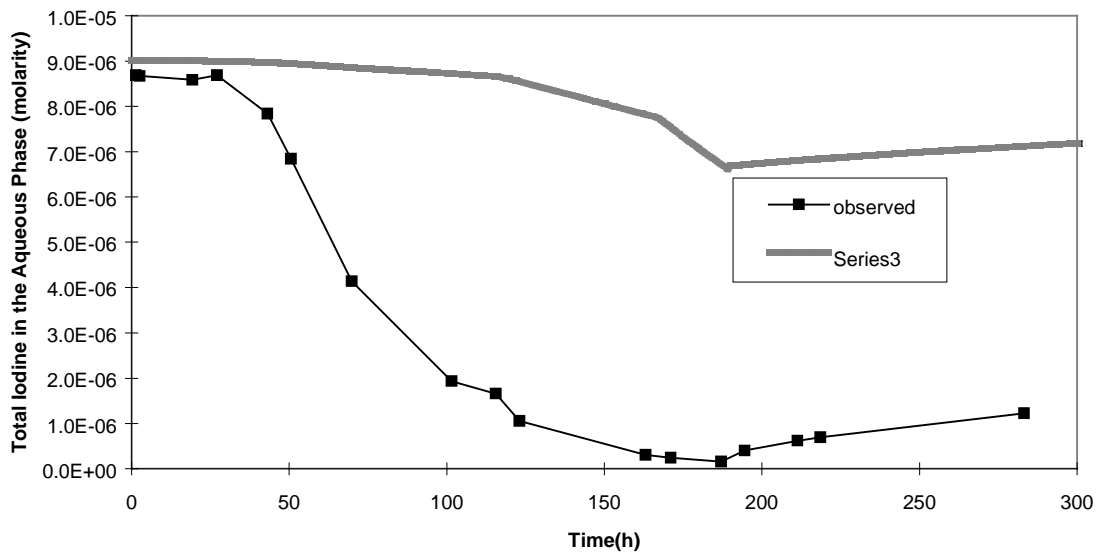
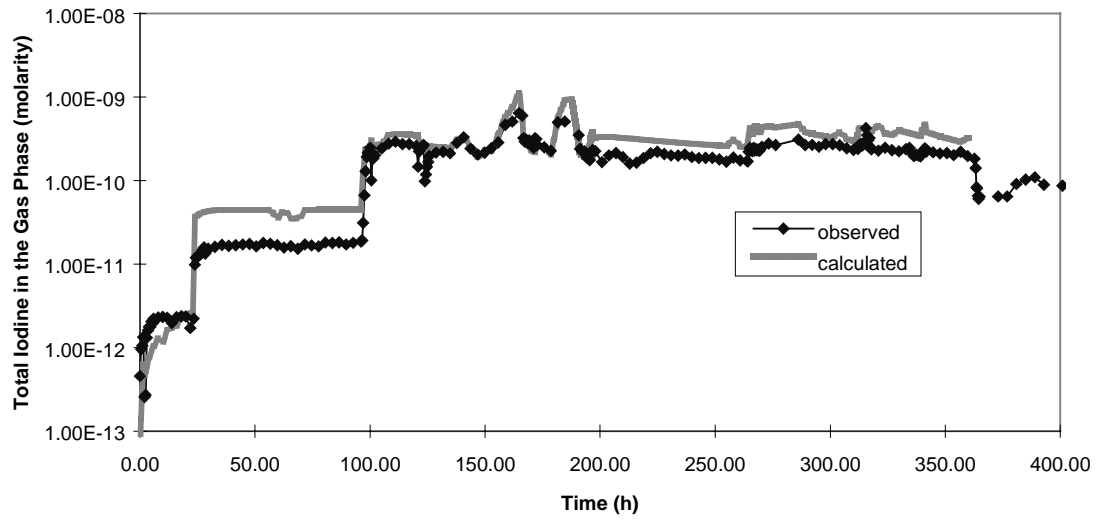


Figure 4. IPSN: Observed vs. calculated results for Stage 2. a) Total concentration of iodine in the gas phase. b) Total concentration of iodine in the aqueous phase

a)



b)

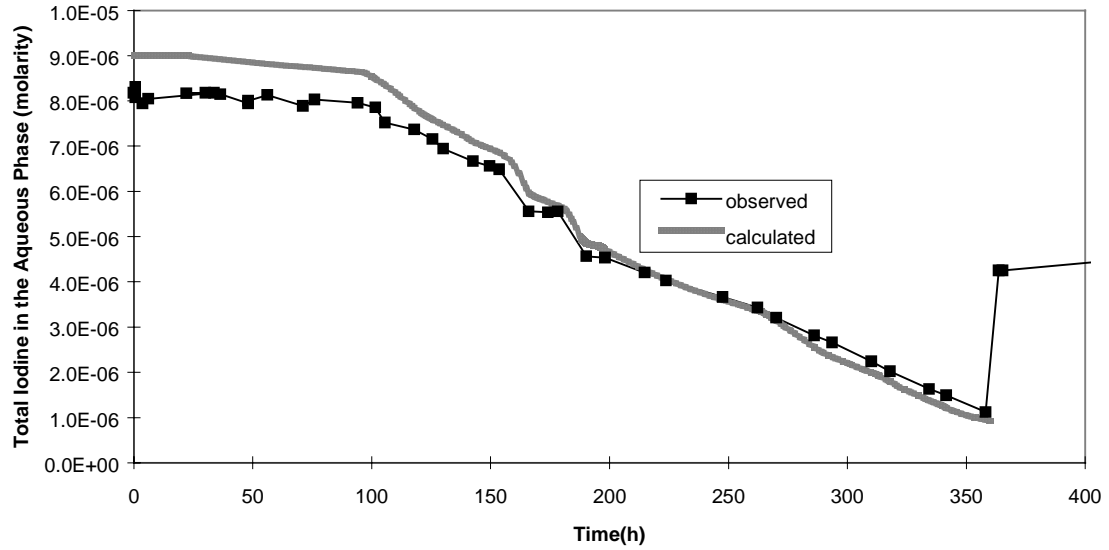
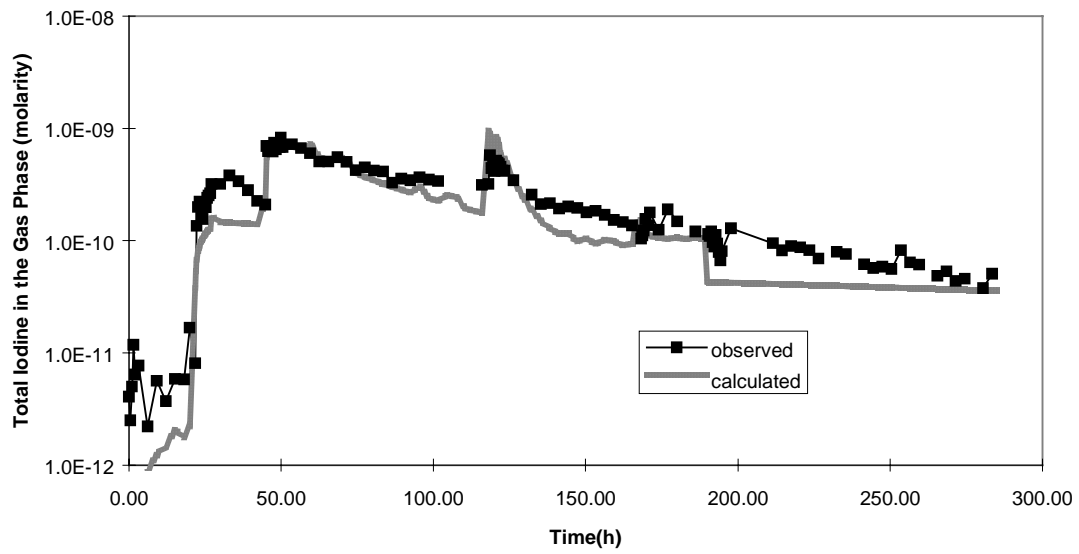


Figure 5. NRIR: Observed vs. calculated results for Stage 1. a) Total concentration of iodine in the gas phase b) Total concentration of iodine in the aqueous phase

a)



b)

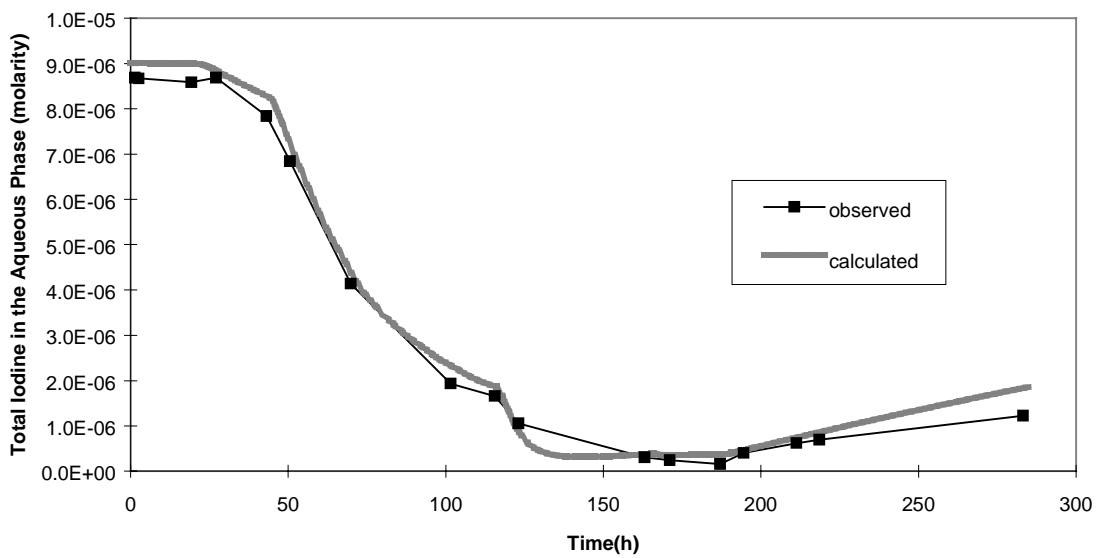
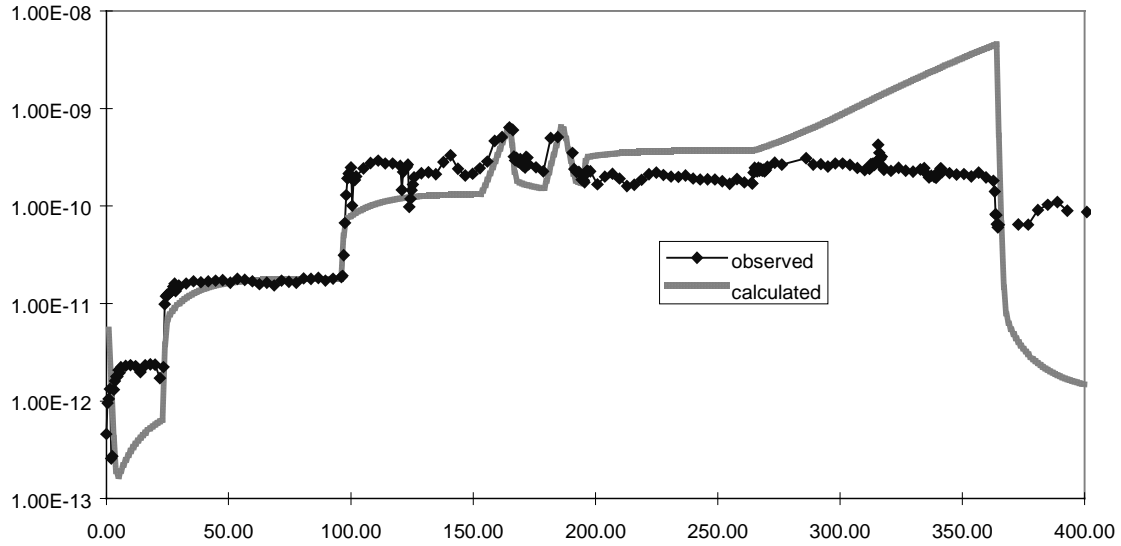


Figure 6. **NRIR: Observed vs. calculated results for Stage 2. a) Total concentration of iodine in the gas phase. b) Total concentration of iodine in the aqueous phase**

a)



b)

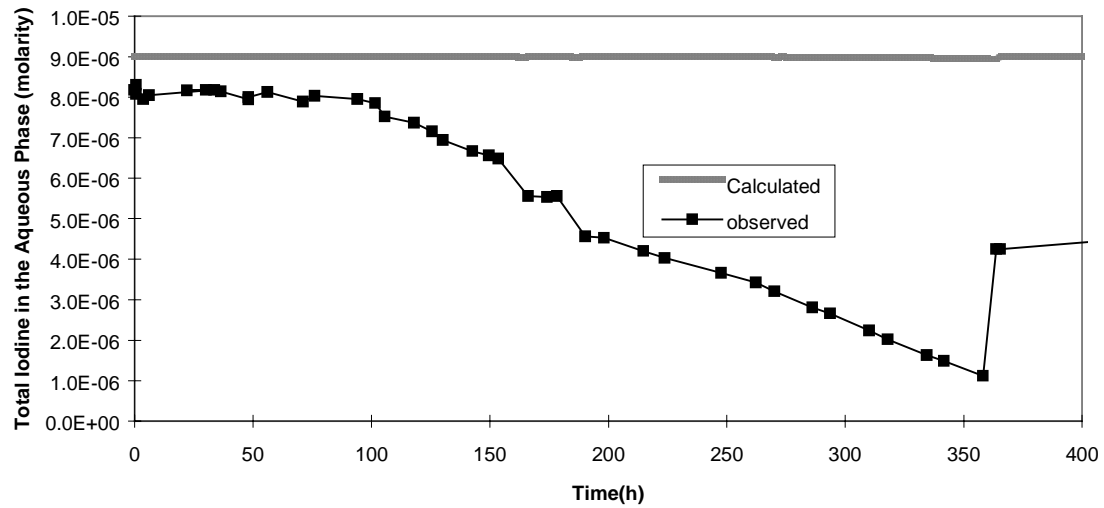
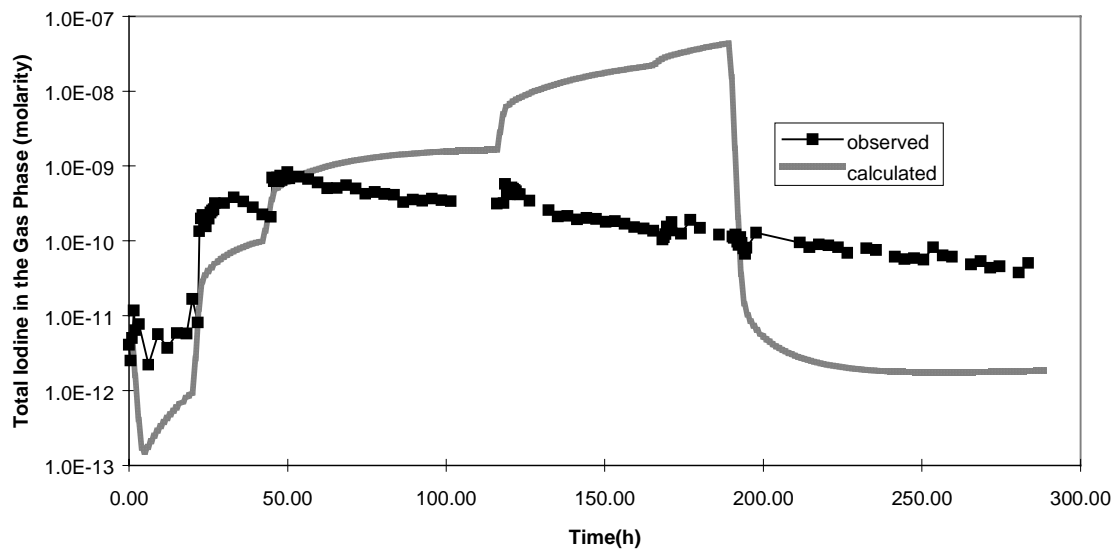


Figure 7. **SIEMENS: Observed vs. calculated results for Stage 1. a) Total concentration of iodine in the gas phase. b) Total concentration of iodine in the aqueous phase**

a)



b)

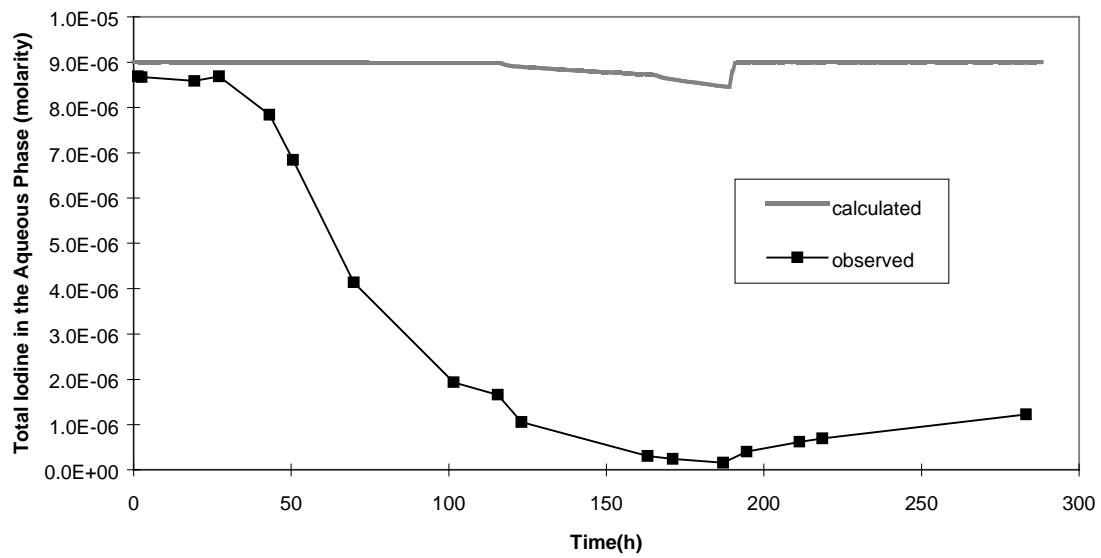
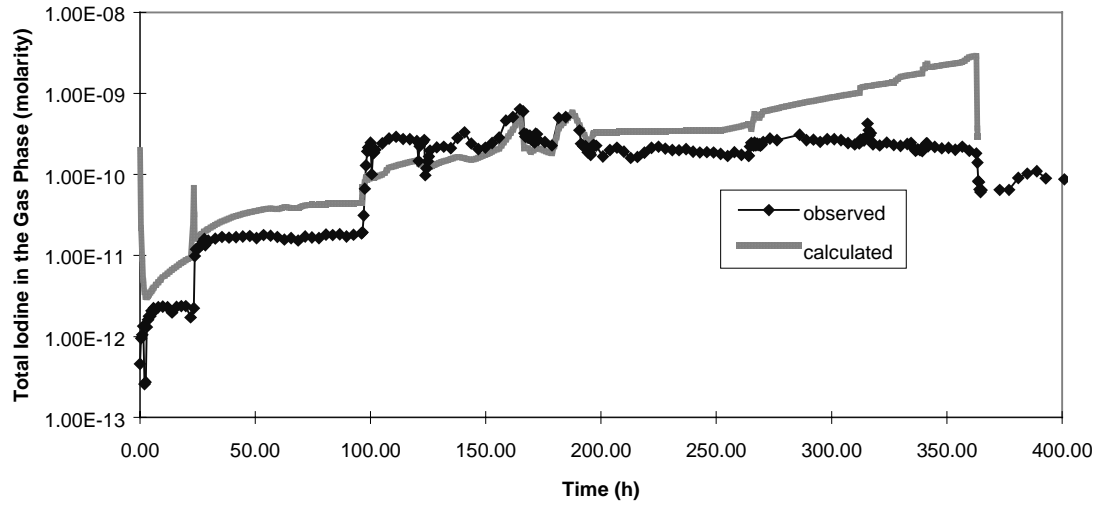


Figure 8. SIEMENS: Observed vs. calculated results for Stage 2. a) Total concentration of iodine in the gas phase. b) Total concentration of iodine in the aqueous phase

a)



b)

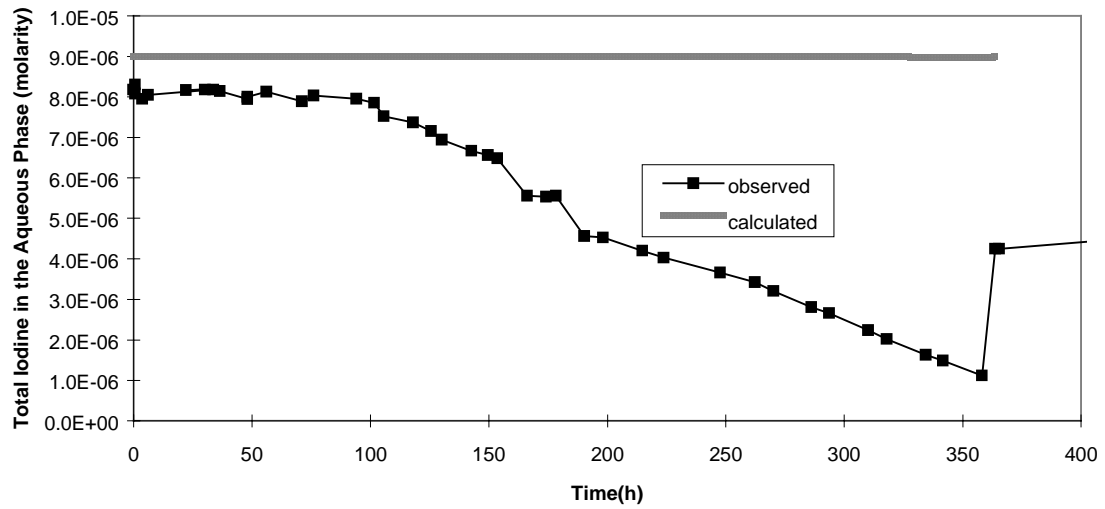
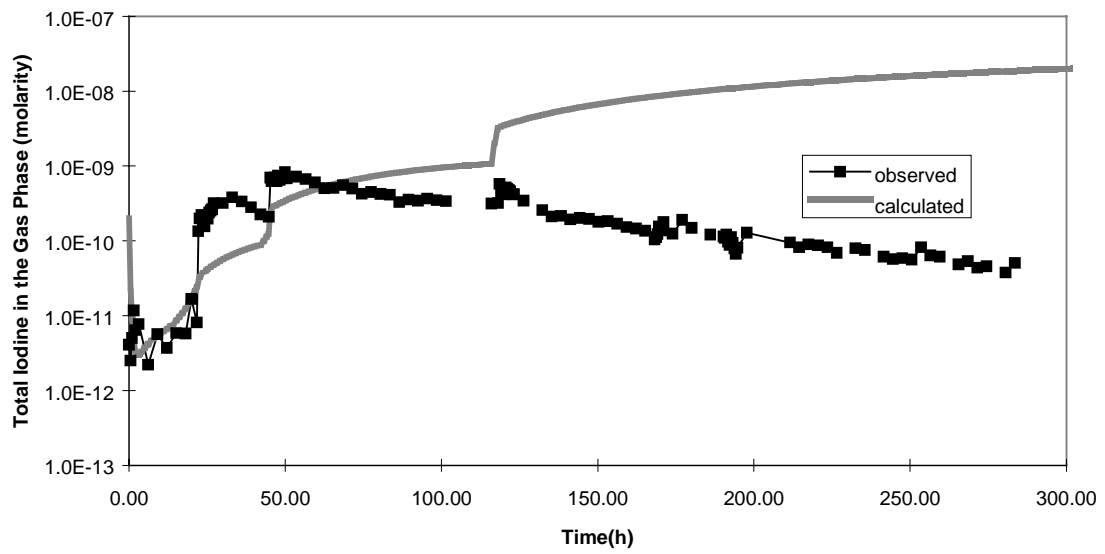


Figure 9. **PSI: Observed vs. calculated results for Stage 1. a) Total concentration of iodine in the gas phase. b) Total concentration of iodine in the aqueous phase**

a)



b)

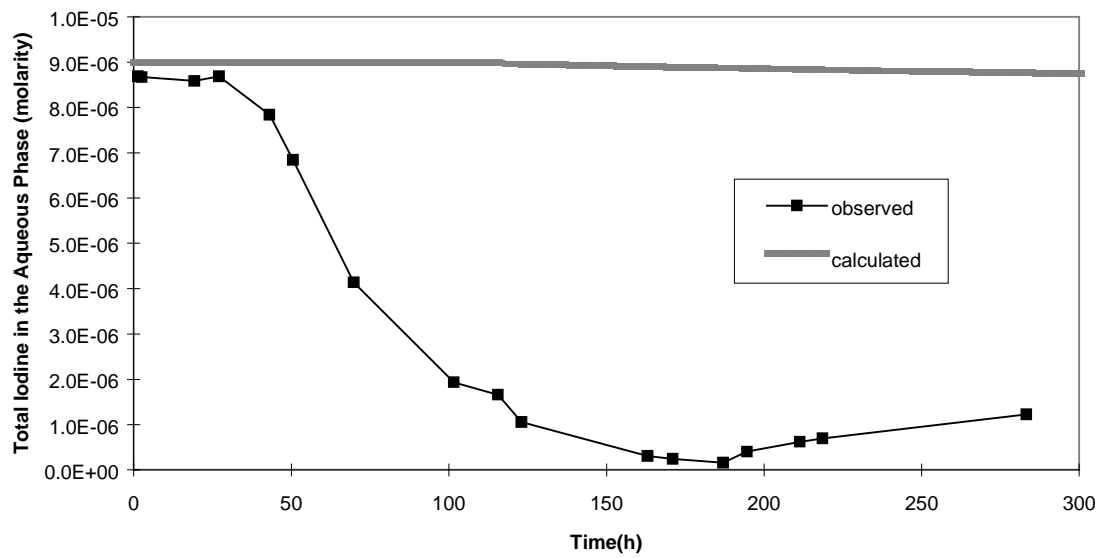
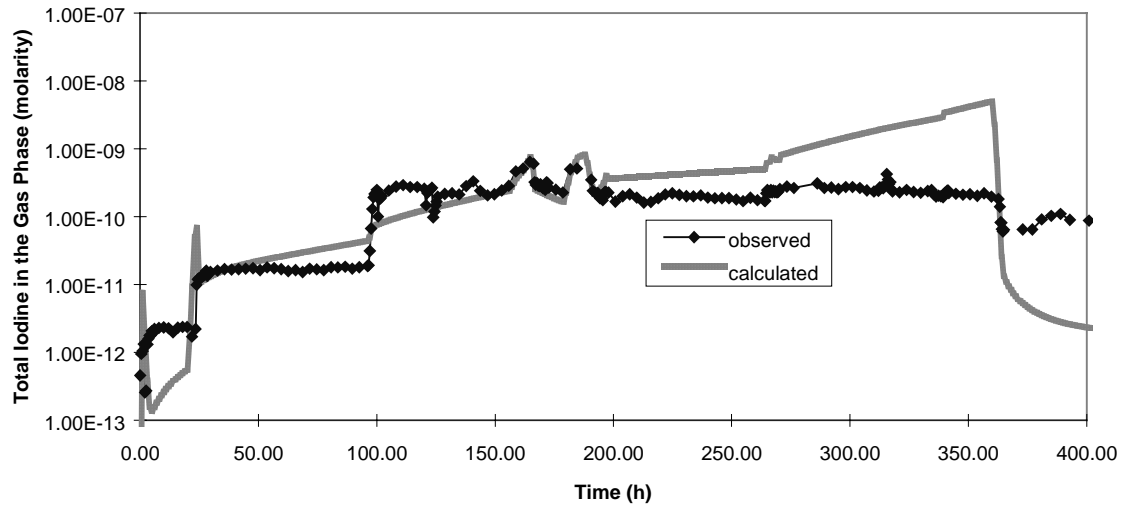


Figure 10. **PSI: Observed vs. calculated results for Stage 2. a) Total concentration of iodine in the gas phase. b) Total concentration of iodine in the aqueous phase**

a)



b)

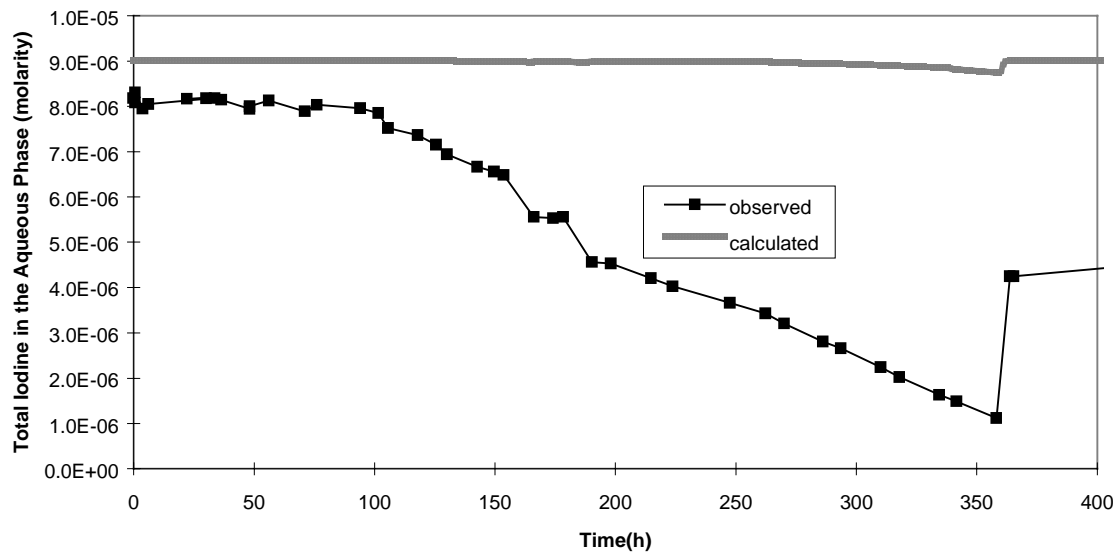
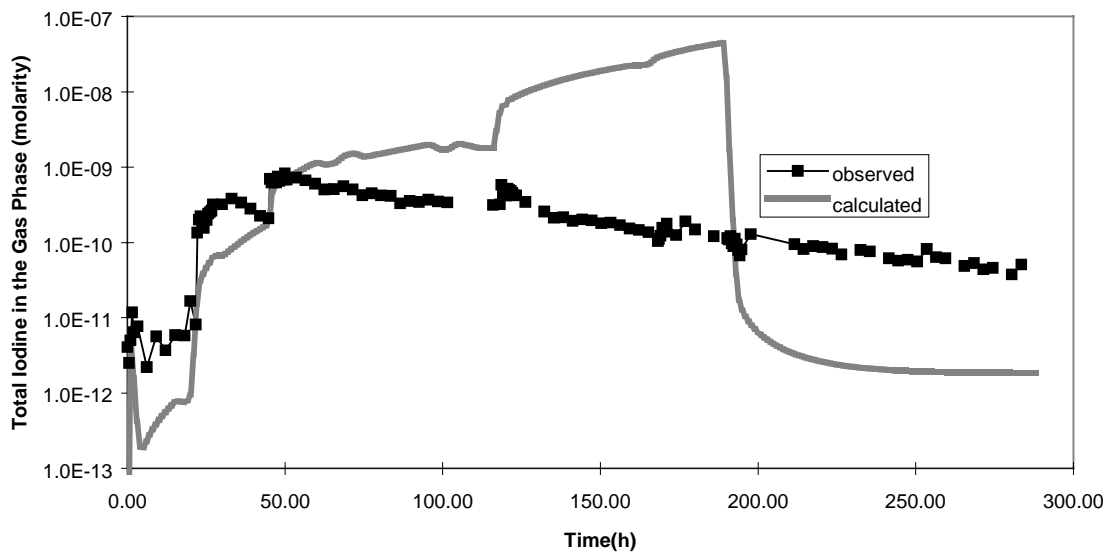


Figure 11. GRS: Observed vs. calculated results for Stage 1. a) Total concentration of iodine in the gas phase. b) Total concentration of iodine in the aqueous phase

a)



b)

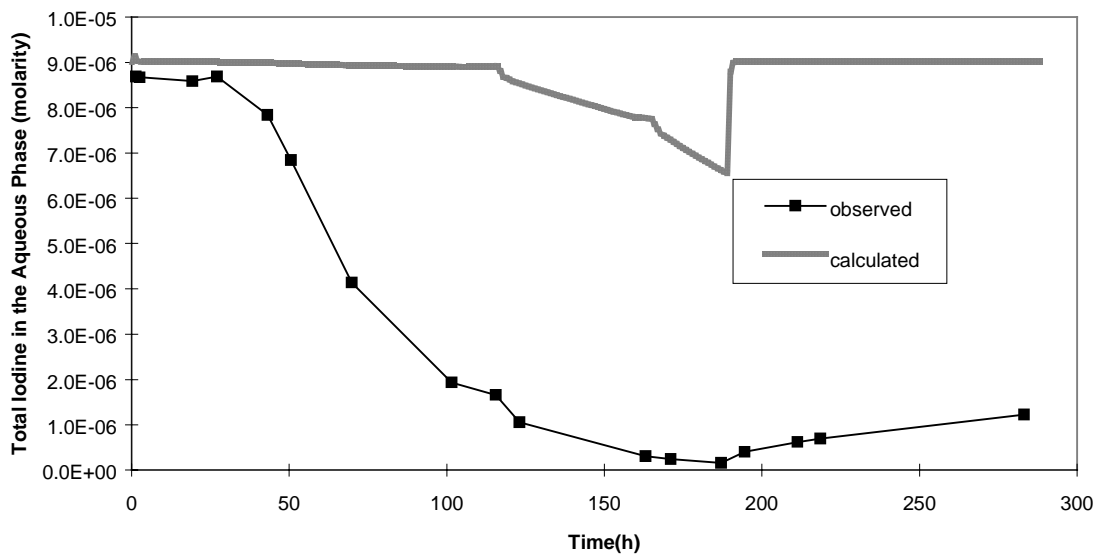
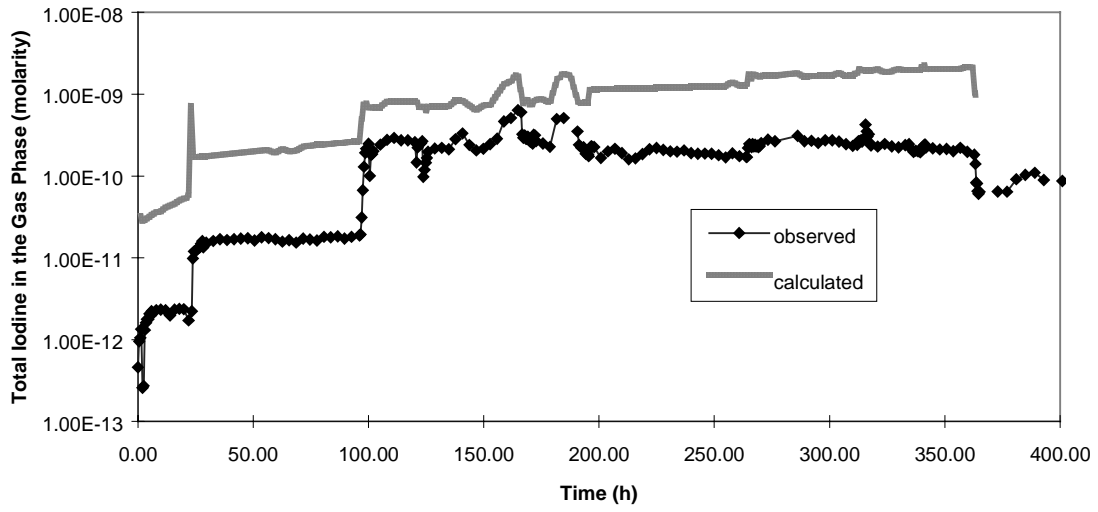


Figure 12. **GRS: Observed vs. calculated results for Stage 2. a) Total concentration of iodine in the gas phase. b) Total concentration of iodine in the aqueous phase**

a)



b)

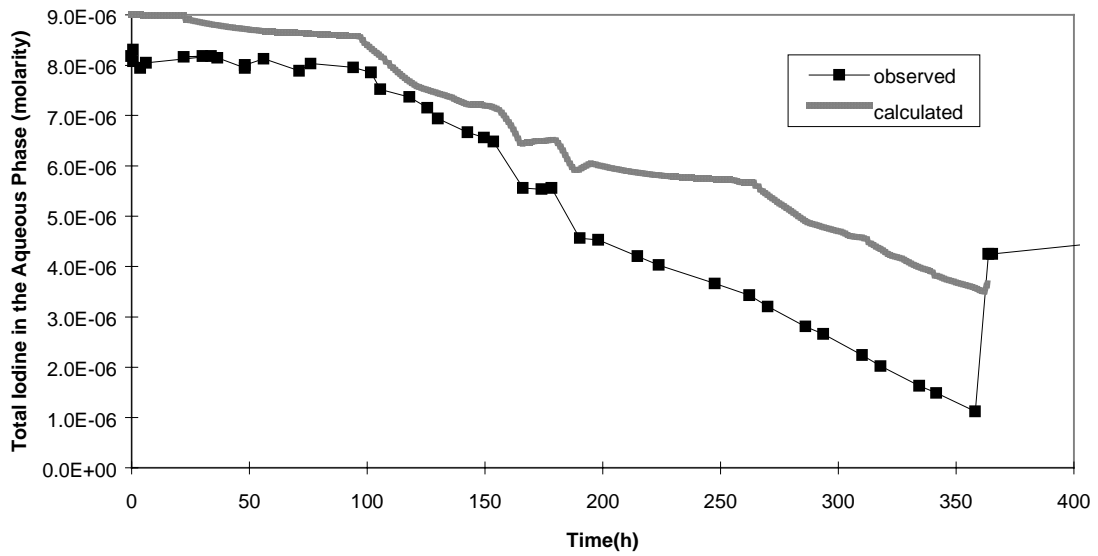
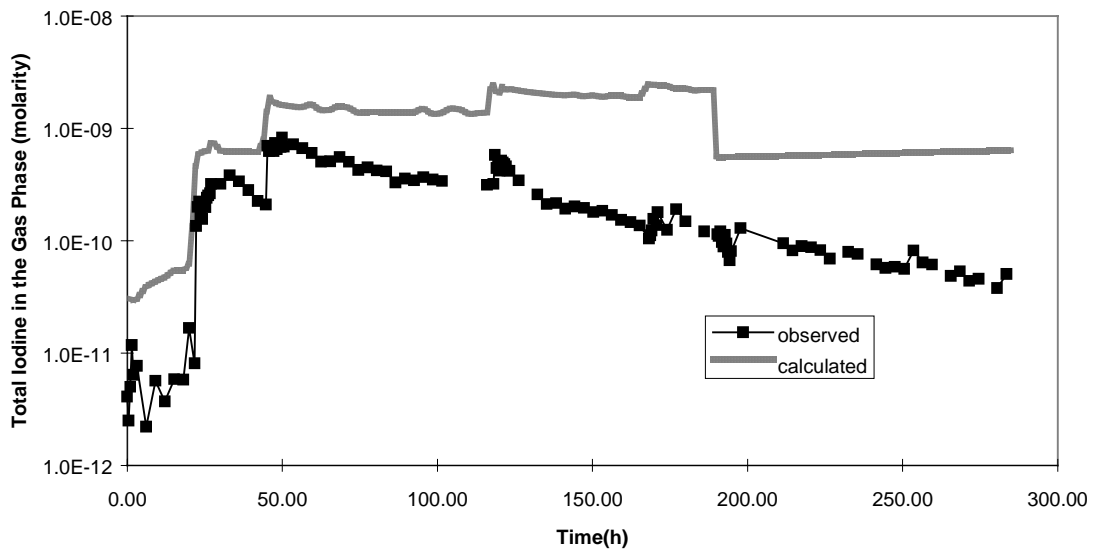


Figure 13. **JAERI: Observed vs. calculated results for Stage 1. a) Total concentration of iodine in the gas phase. b) Total concentration of iodine in the aqueous phase**

a)



b)

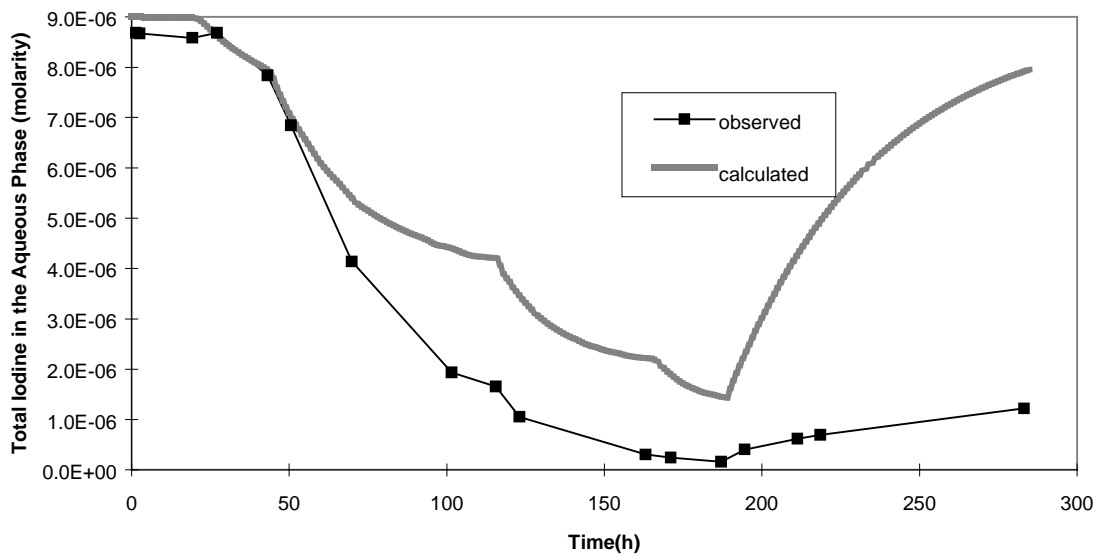
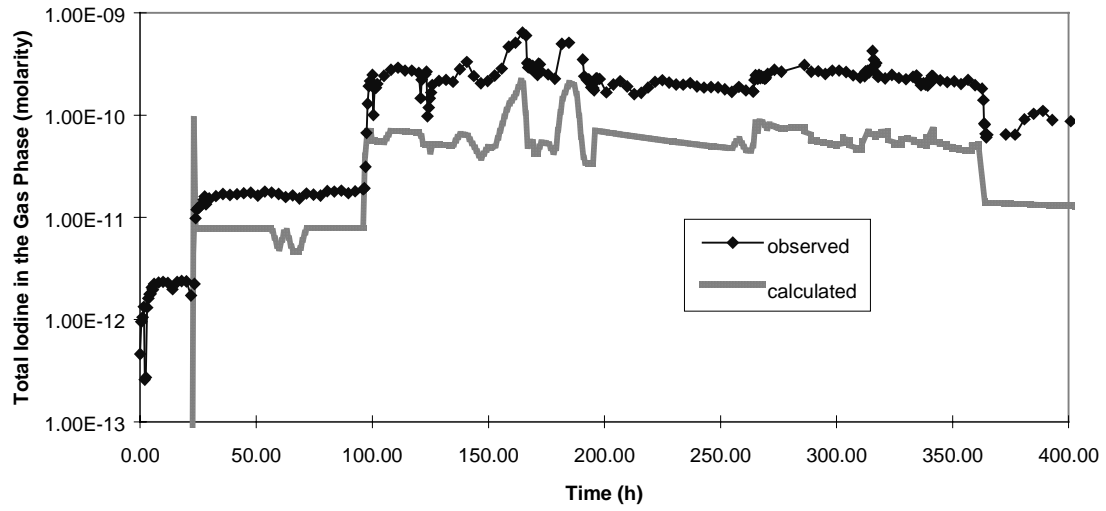


Figure 14. **JAERI: Observed vs. calculated results for Stage 2. a) Total concentration of iodine in the gas phase. b) Total concentration of iodine in the aqueous phase**

a)



b)

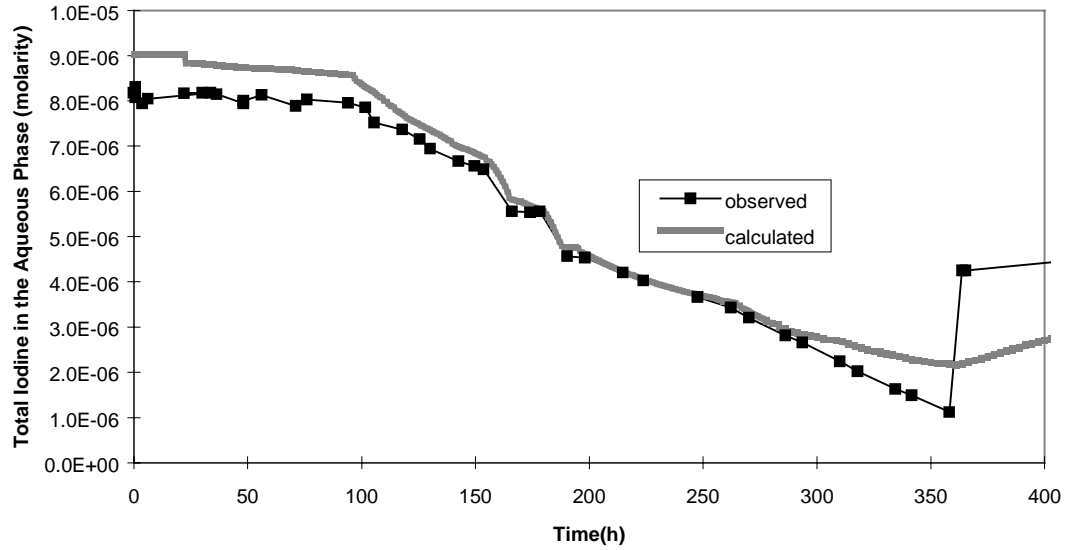
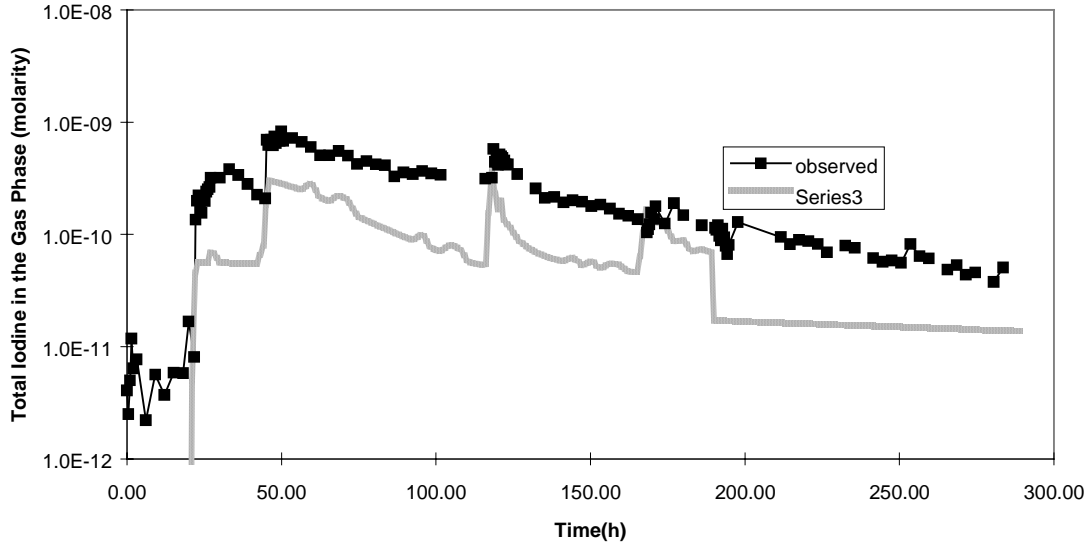


Figure 15. SANDIA: Observed vs. calculated results for Stage 1. a) Total concentration of iodine in the gas phase. b) Total concentration of iodine in the aqueous phase

a)



b)

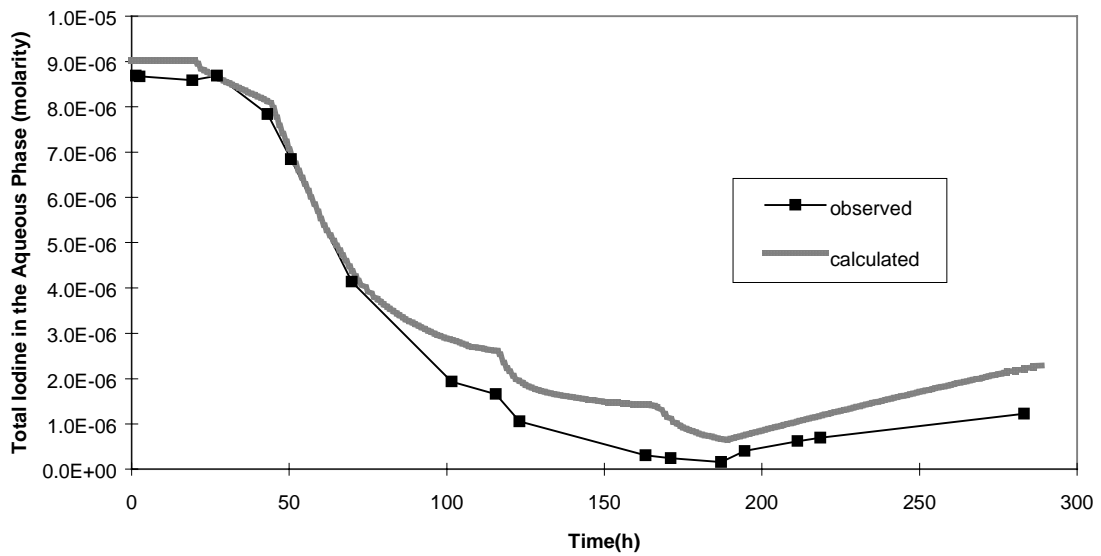
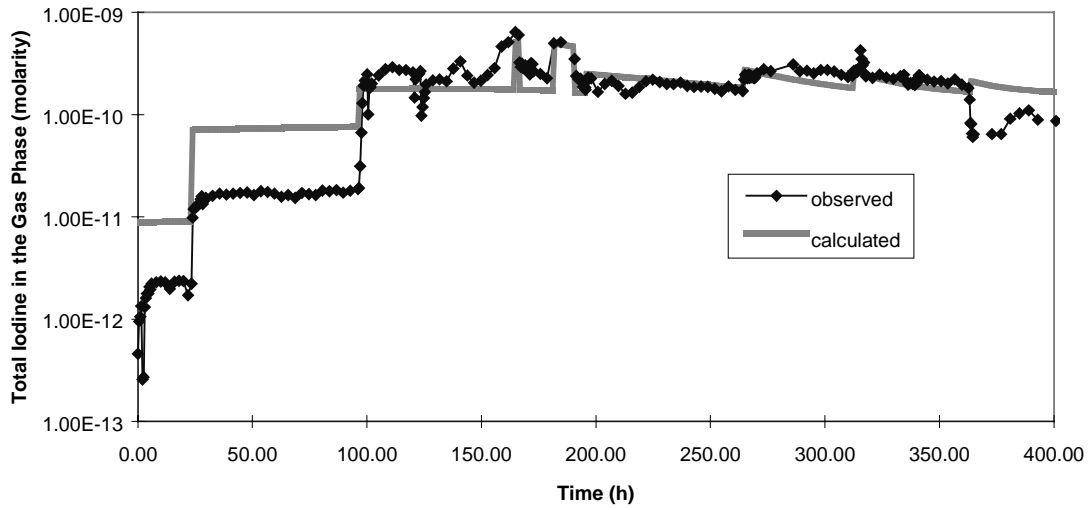


Figure 16. SANDIA: Observed vs. calculated results for Stage 1. a) Total concentration of iodine in the gas phase. b) Total concentration of iodine in the aqueous phase

a)



b)

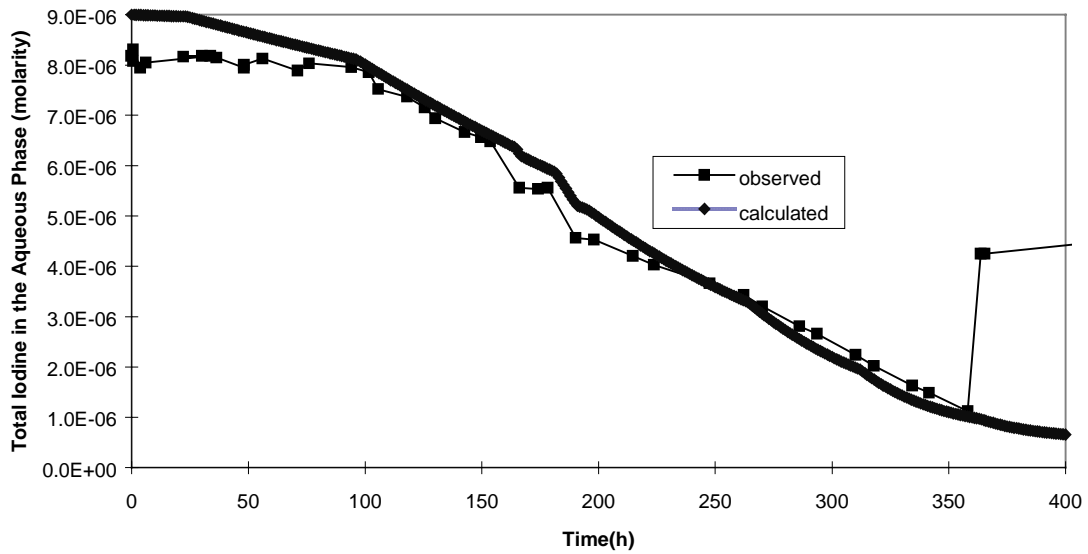
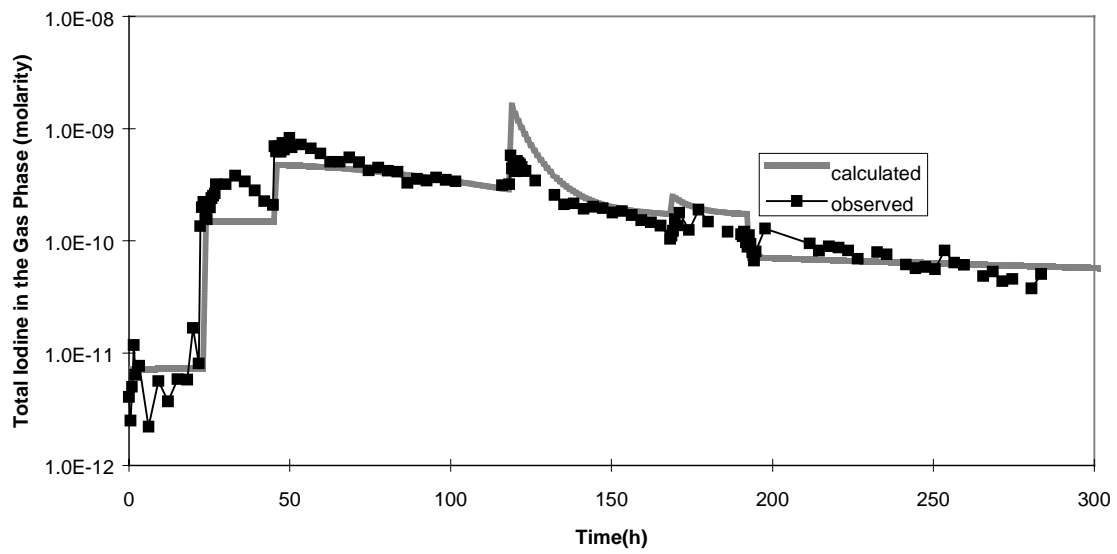


Figure 17. **AECL: Observed vs. calculated results for Stage 1. a) Total concentration of iodine in the gas phase. b) Total concentration of iodine in the aqueous phase**

a)



b)

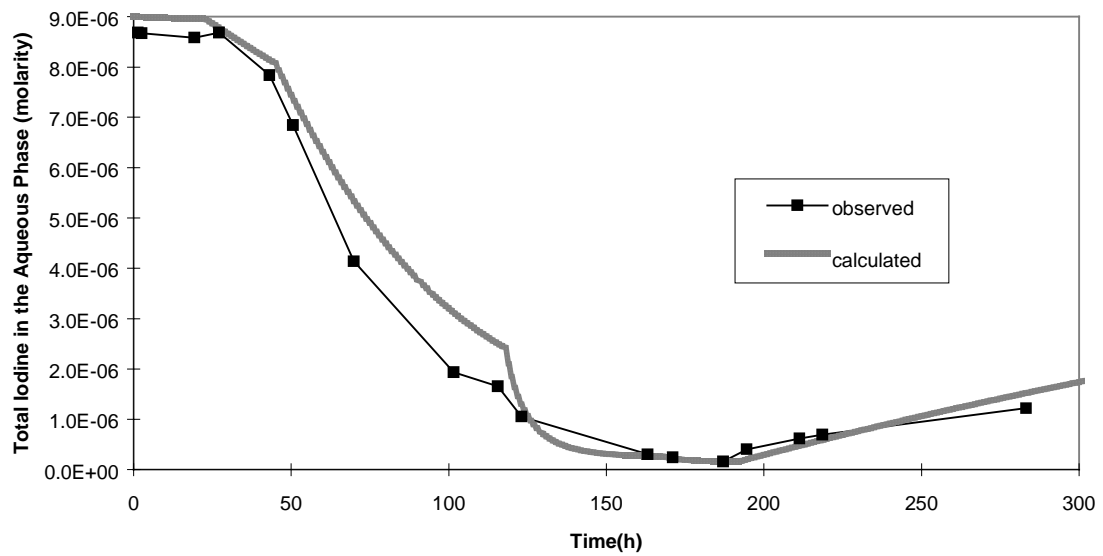


Figure 18. **AECL: Observed vs. calculated results for Stage 1. a) Total concentration of iodine in the gas phase. b) Total concentration of iodine in the aqueous phase**

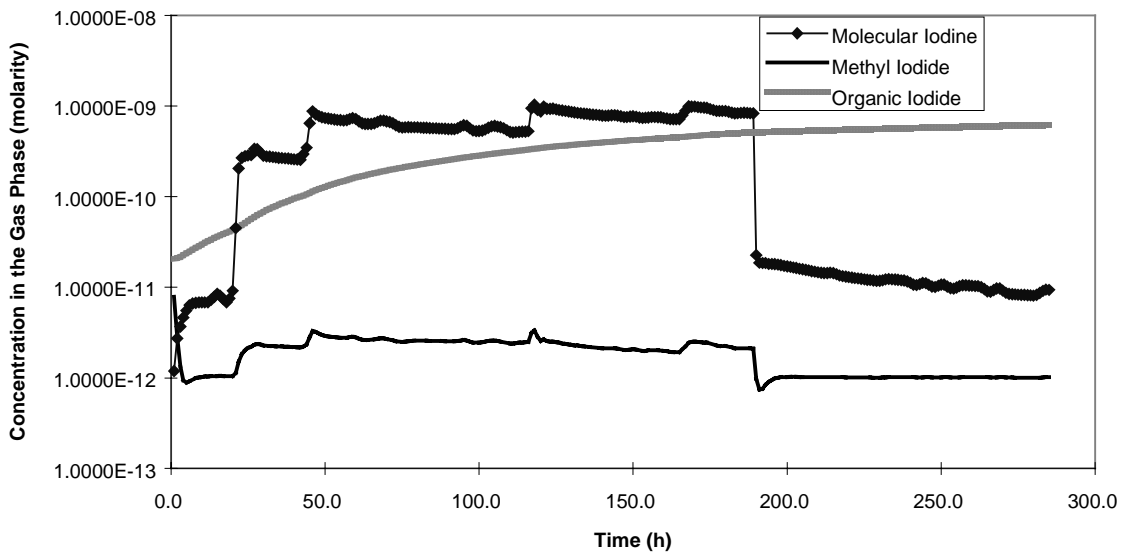


Figure 19. **JAERI: Speciation of iodine in the gas phase for Stage 2**

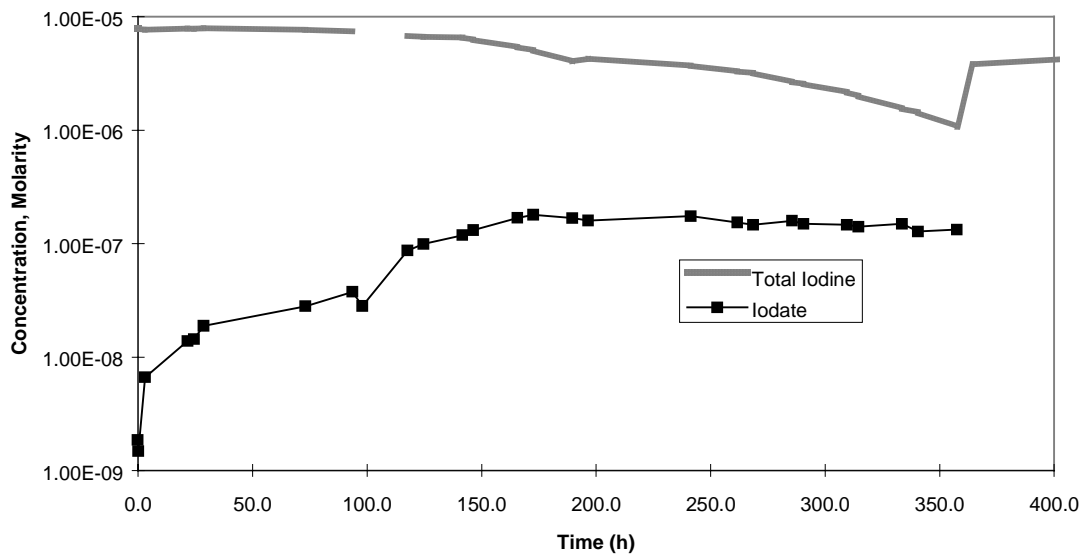


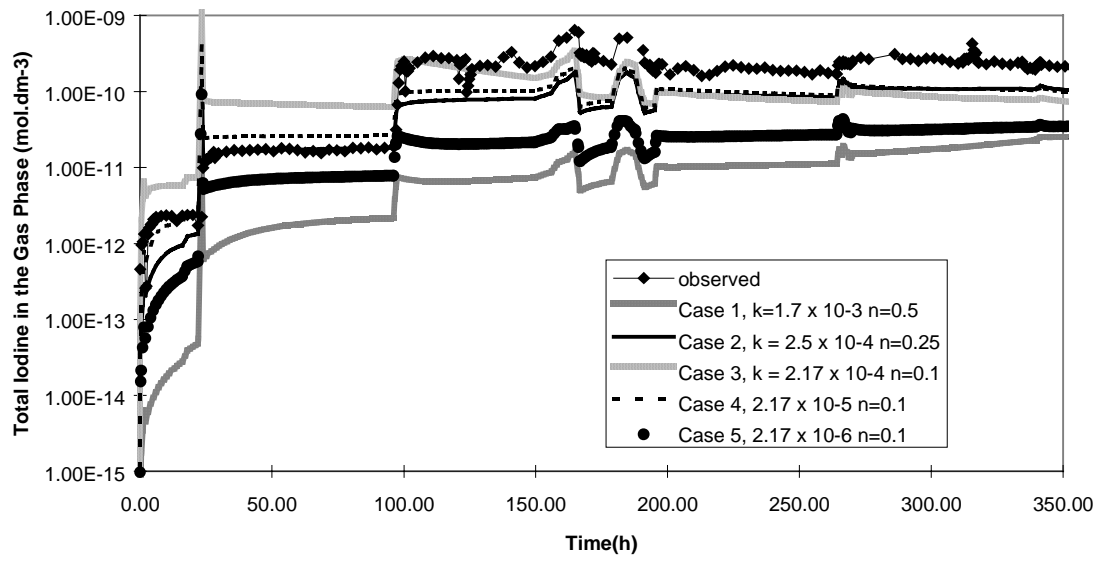
Figure 20. **Concentration of iodate in the aqueous phase as a function of time for Stage 1**

## **APPENDIX C**

# **RESULTS FROM THE SECOND CALCULATION**



a)



b)

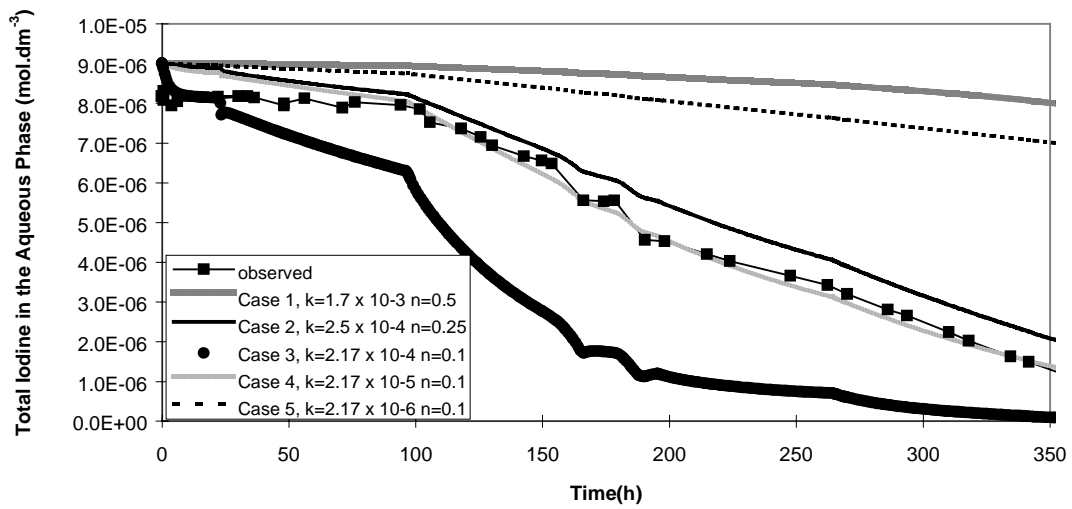
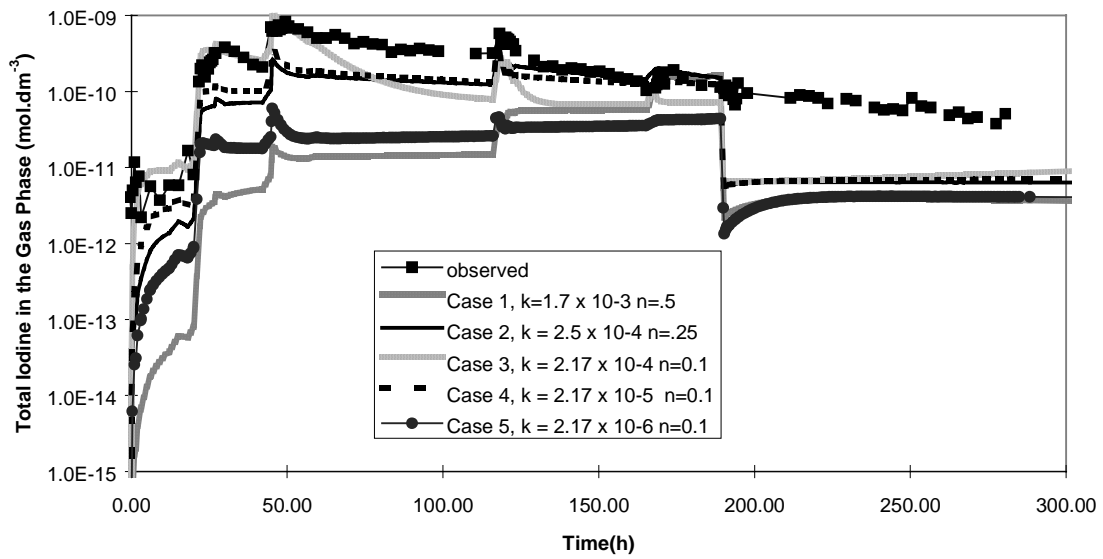


Figure 1. CIEMAT: Observed vs. calculated results for Stage 1. a) Total concentration of iodine in the gas phase. b) Total concentration of iodine in the aqueous phase

a)



b)

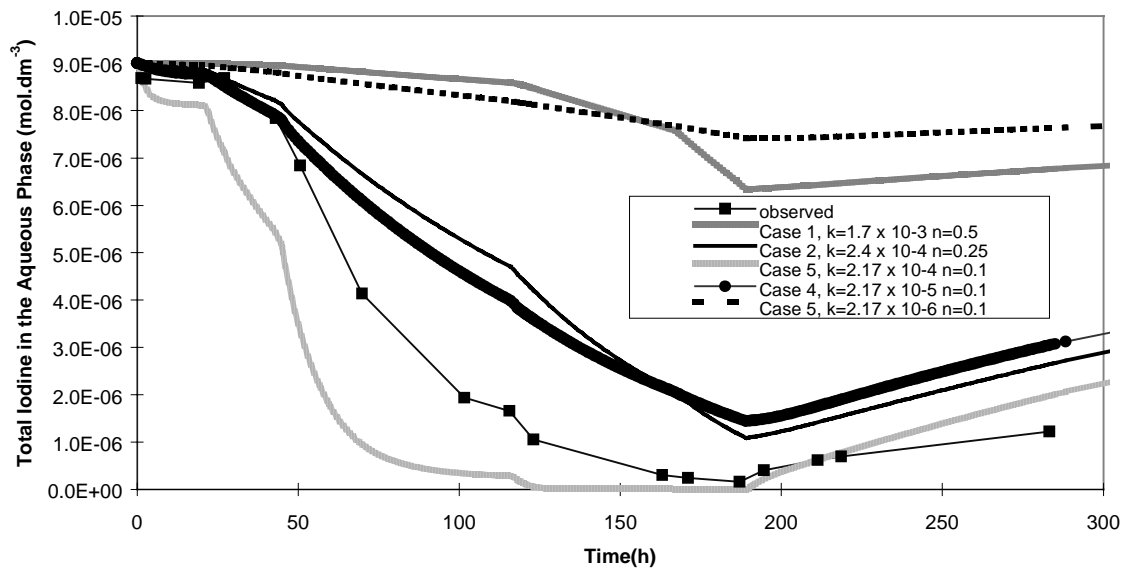
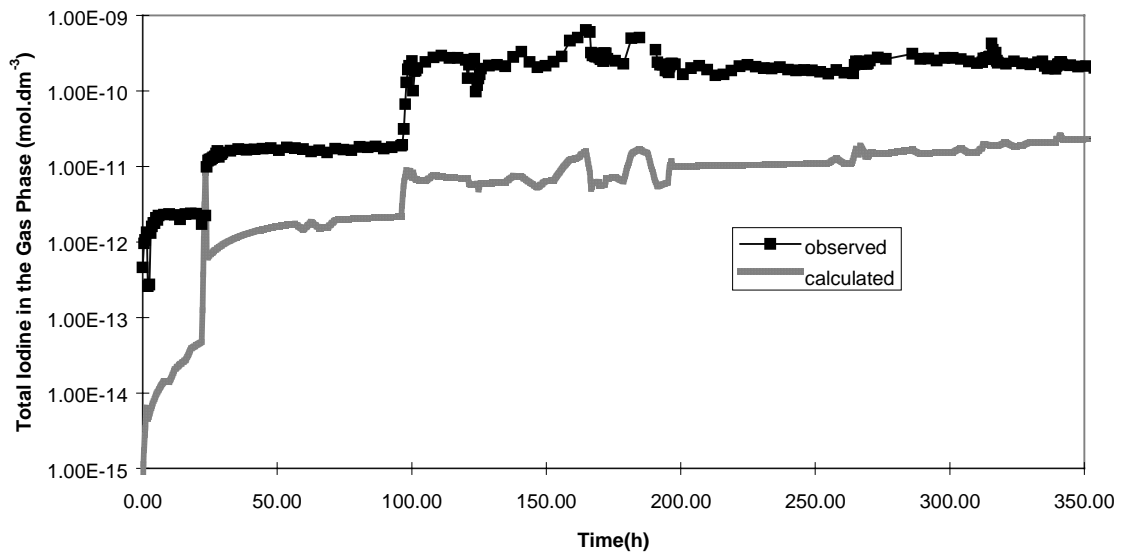


Figure 2. CIEMAT: Observed vs. calculated results for Stage 2. a) Total concentration of iodine in the gas phase. b) Total concentration of iodine in the aqueous phase

a)



b)

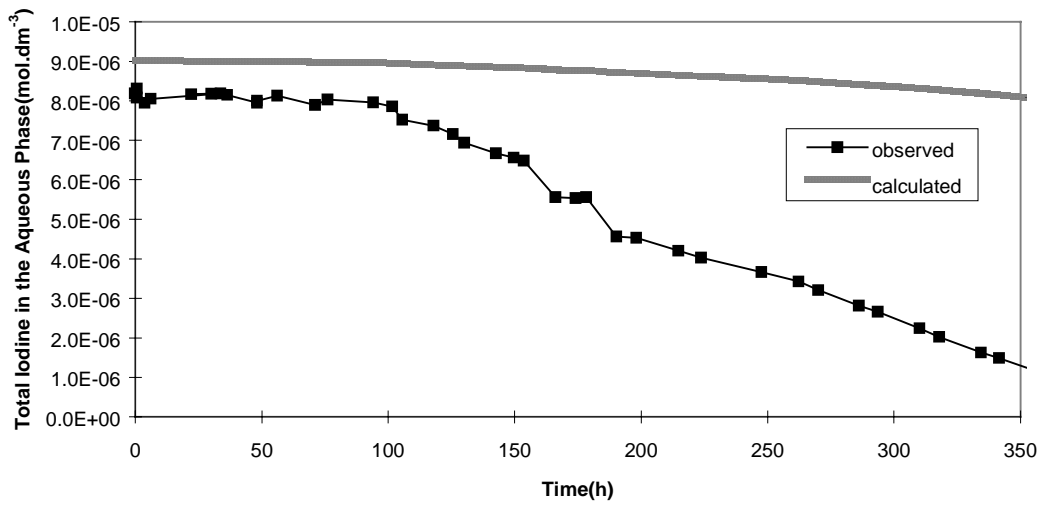
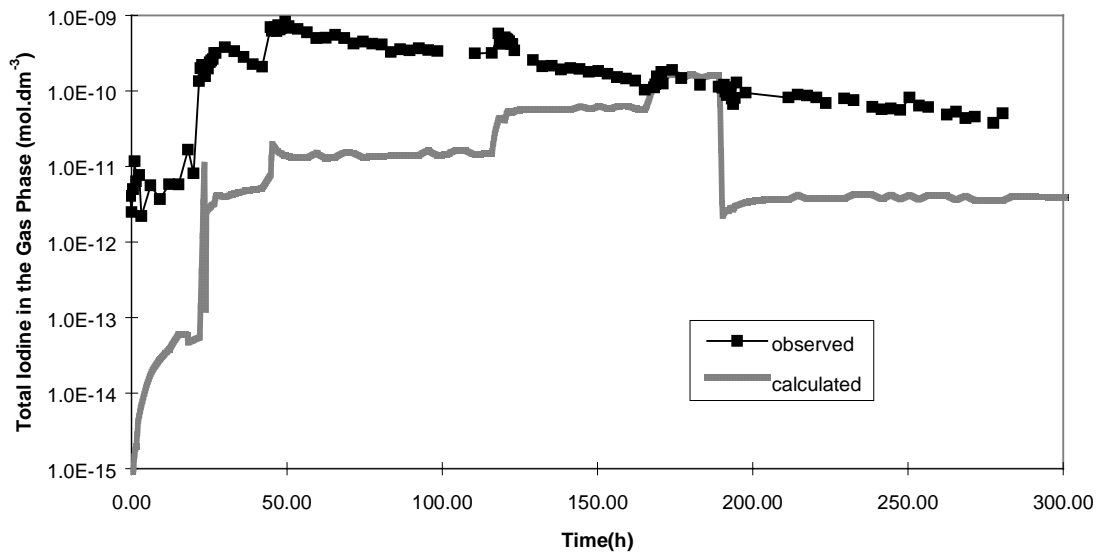


Figure 3. **IPSN: Observed vs. calculated results for Stage 1. a) Total concentration of iodine in the gas phase. b) Total concentration of iodine in the aqueous phase**

a)



b)

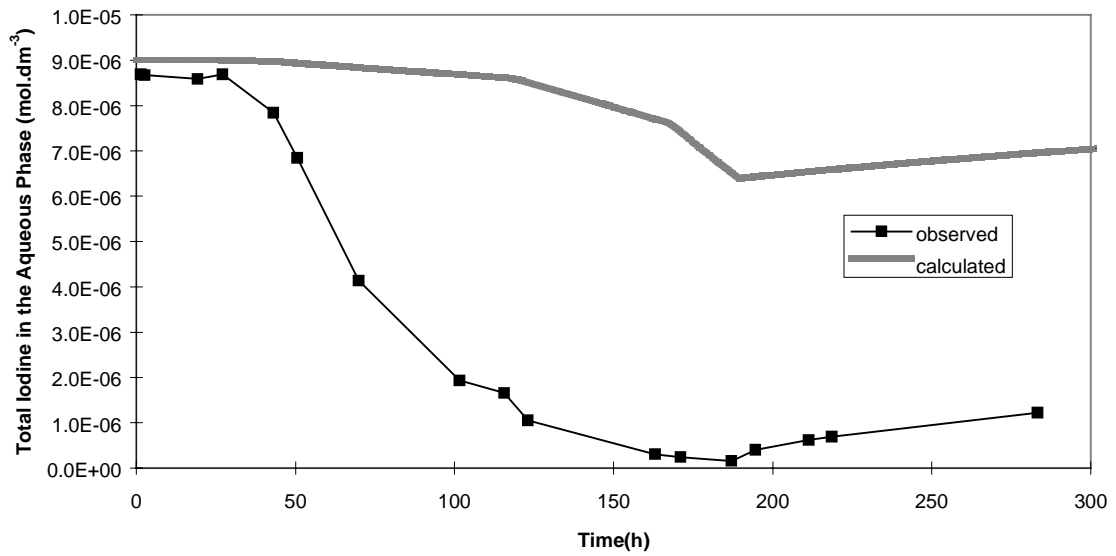
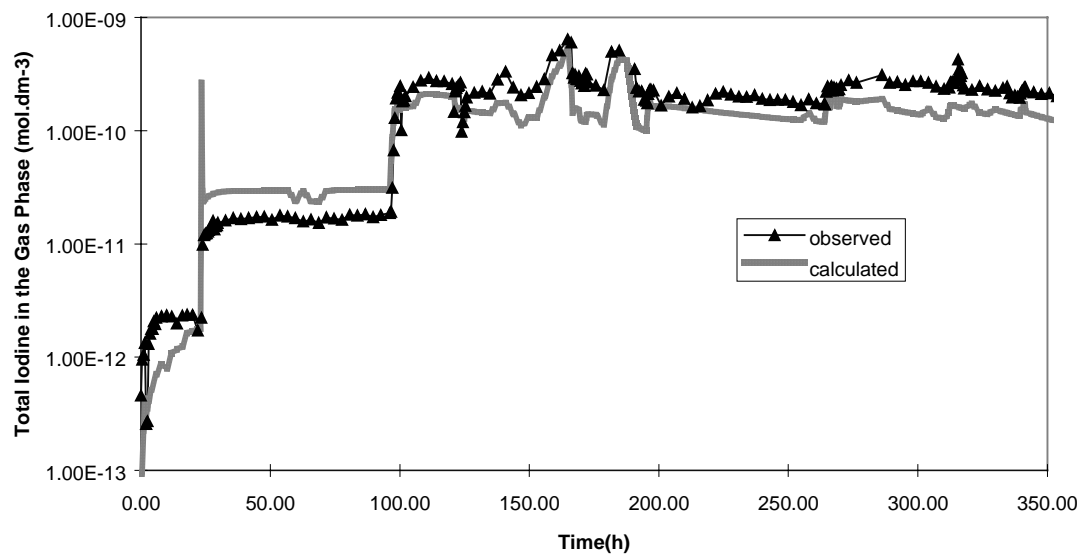


Figure 4. **IPSN: Observed vs. calculated results for Stage 2. a) Total concentration of iodine in the gas phase. b) Total concentration of iodine in the aqueous phase**

a)



b)

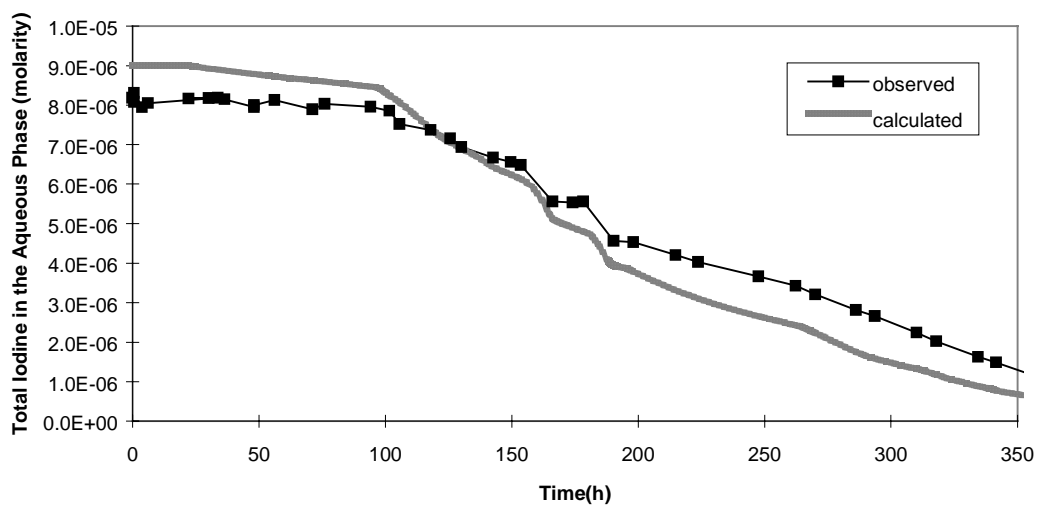
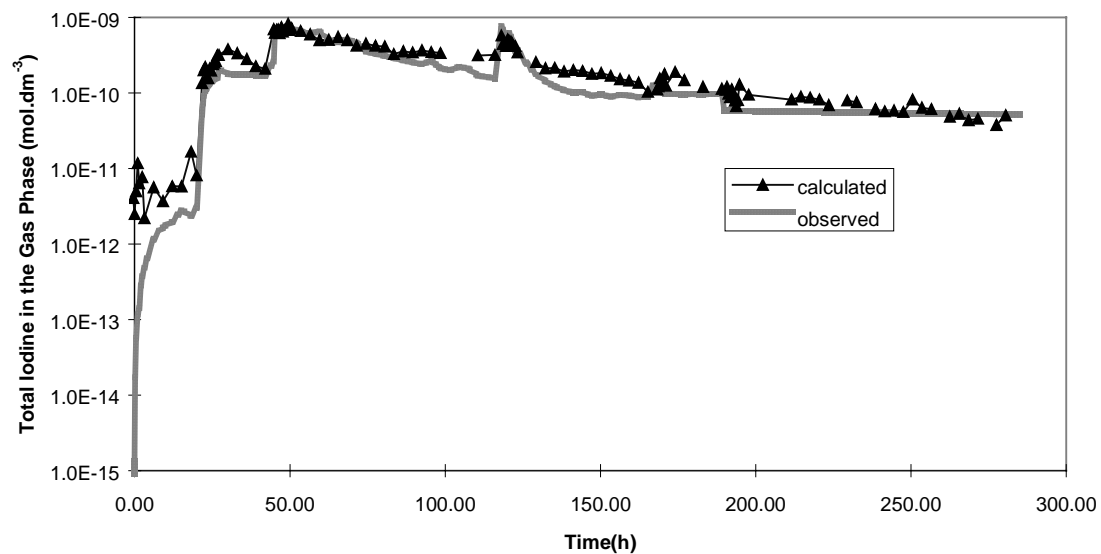


Figure 5. **NRIR: Observed vs. calculated results for Stage 1. a) Total concentration of iodine in the gas phase. b) Total concentration of iodine in the aqueous phase**

a)



b)

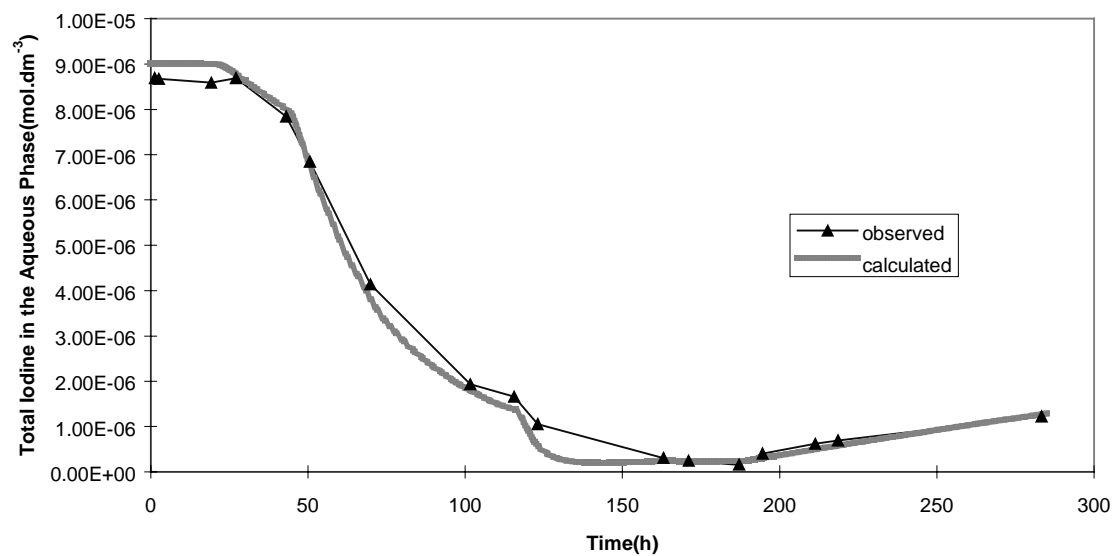
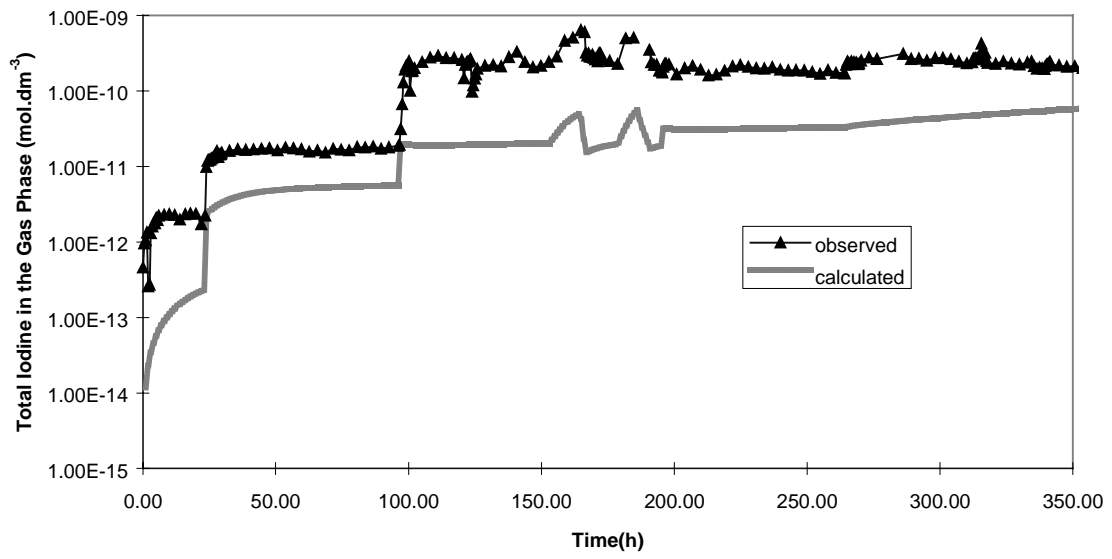


Figure 6. NRIR: Observed vs. calculated results for Stage 2. a) Total concentration of iodine in the gas phase. b) Total concentration of iodine in the aqueous phase

a)



b)

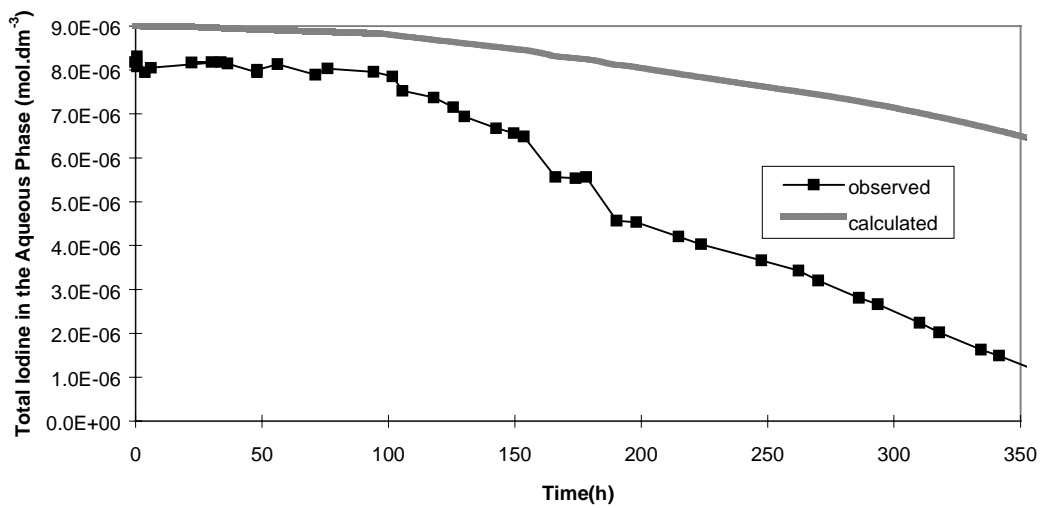
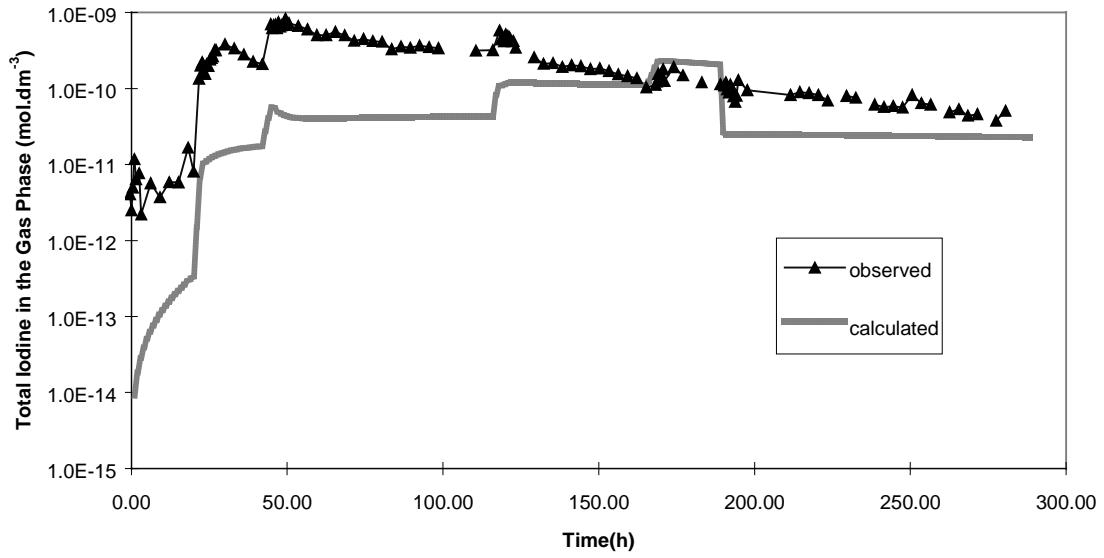


Figure 7. **SIEMENS: Observed vs. calculated results for Stage 1. a) Total concentration of iodine in the gas phase. b) Total concentration of iodine in the aqueous phase**

a)



b)

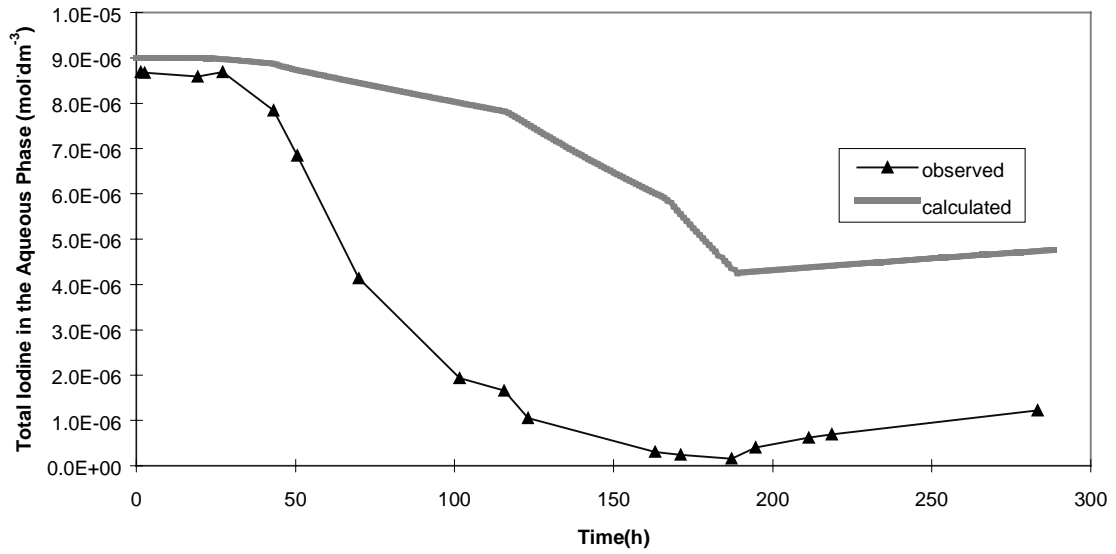
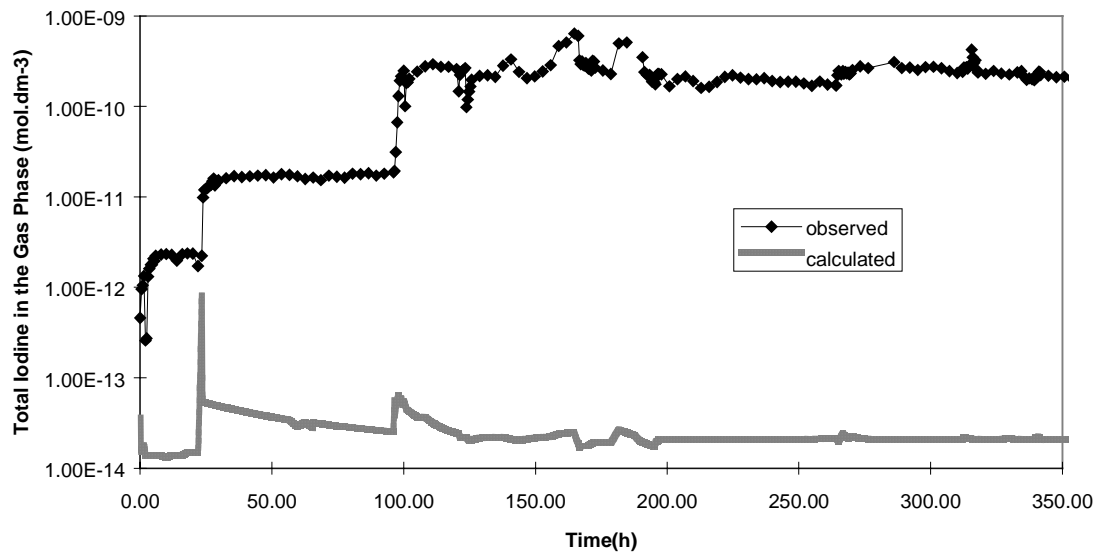


Figure 8. **SIEMENS: Observed vs. calculated results for Stage 2. a) Total concentration of iodine in the gas phase. b) Total concentration of iodine in the aqueous phase**

a)



b)

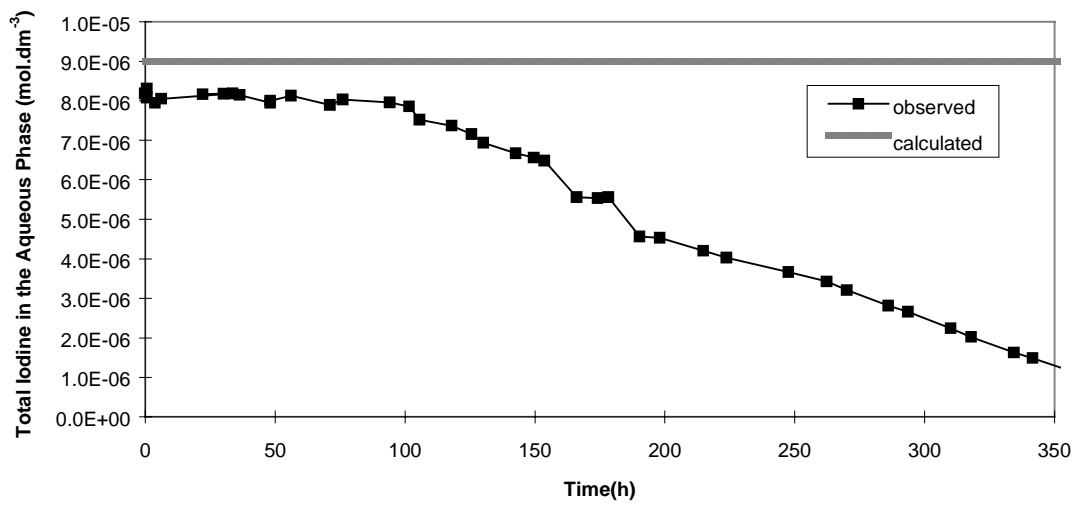
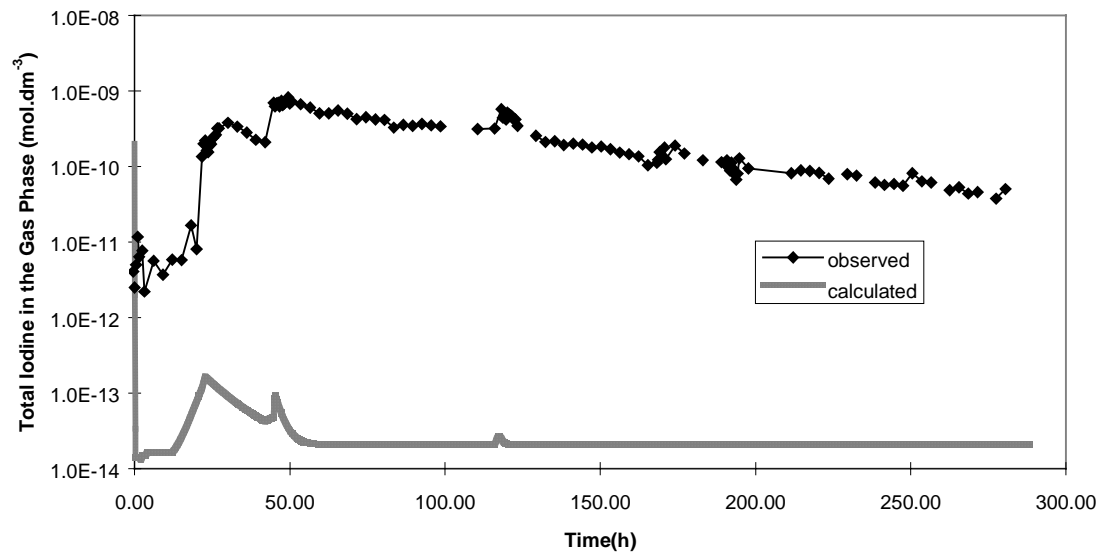


Figure 9. **PSI: Observed vs. calculated results for Stage 1. a) Total concentration of iodine in the gas phase. b) Total concentration of iodine in the aqueous phase**

a)



b)

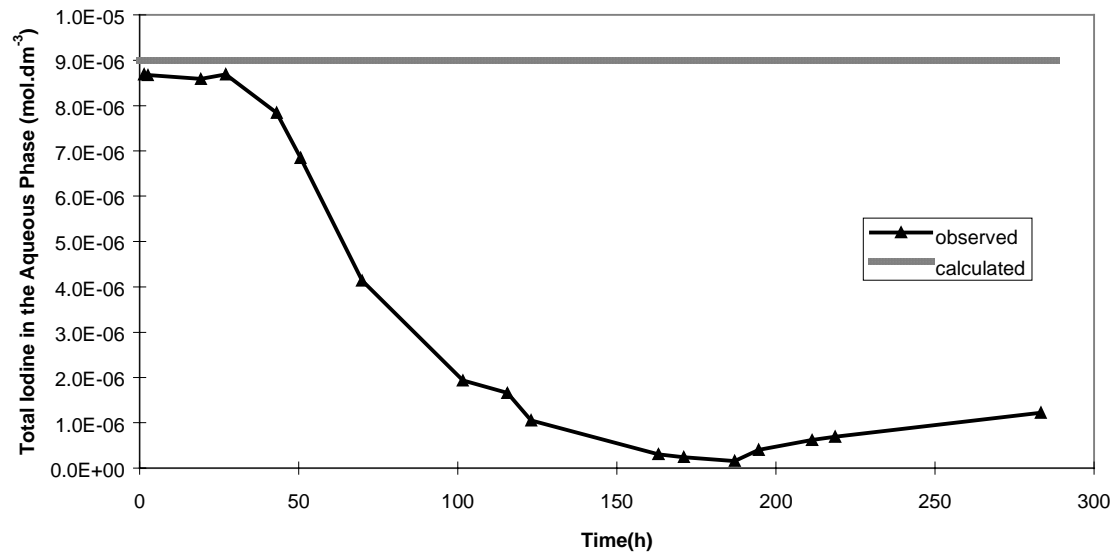
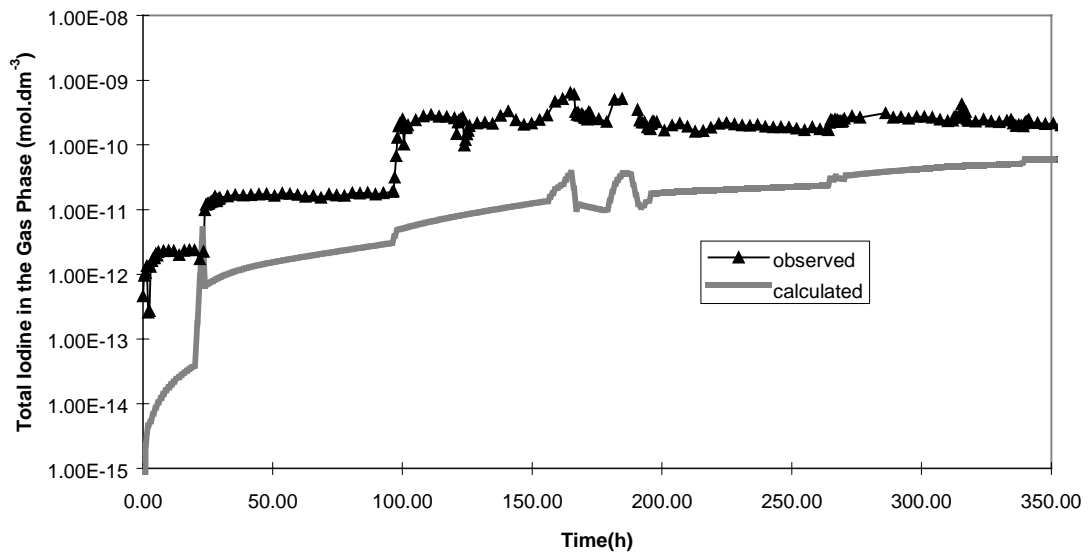


Figure 10. **PSI: Observed vs. calculated results for Stage 2. a) Total concentration of iodine in the gas phase. b) Total concentration of iodine in the aqueous phase**

a)



b)

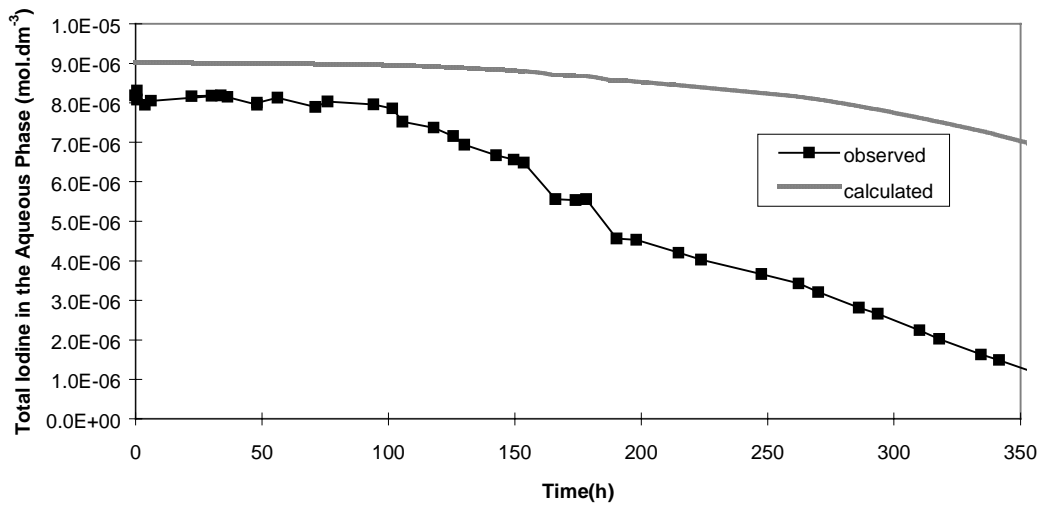
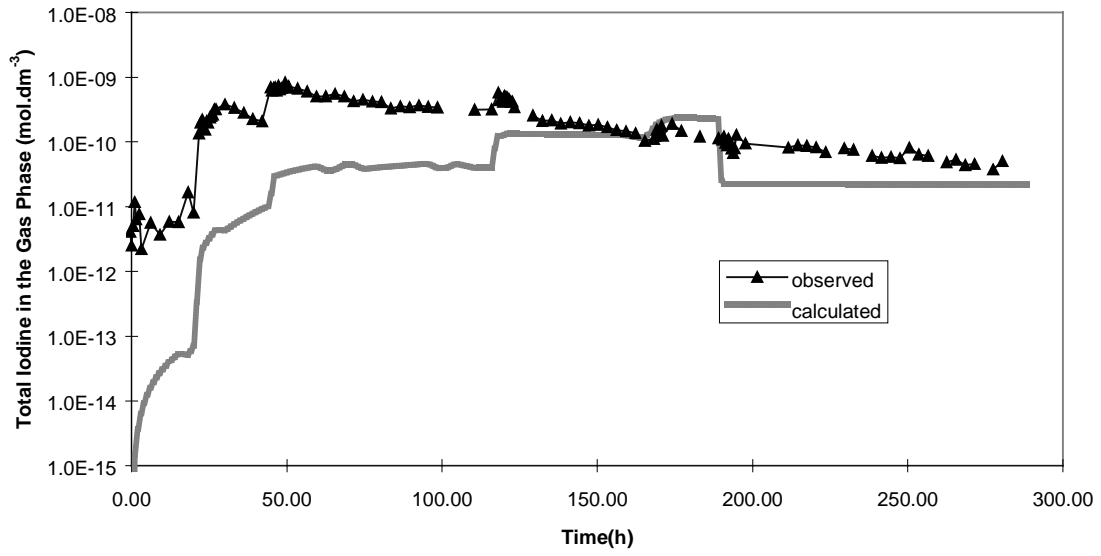


Figure 11. GRS: Observed vs. calculated results for Stage 1. a) Total concentration of iodine in the gas phase. b) Total concentration of iodine in the aqueous phase

a)



b)

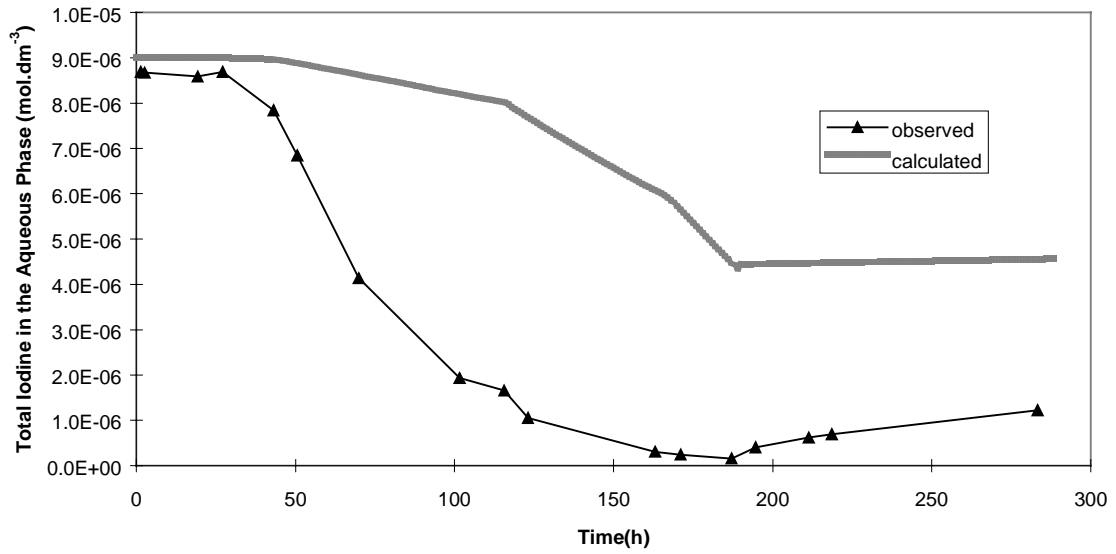
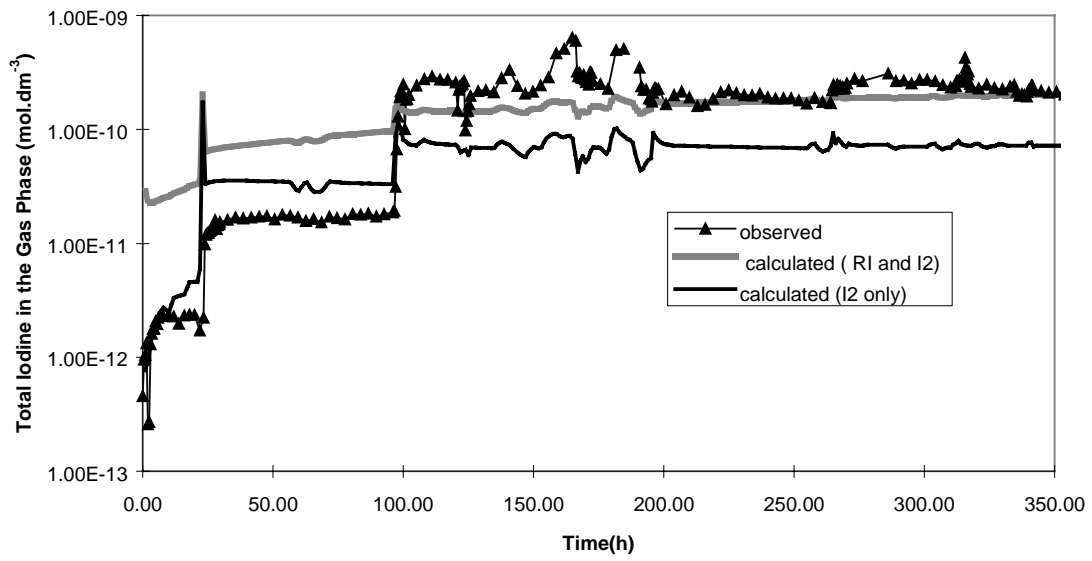


Figure 12. **GRS: Observed vs. calculated results for Stage 2. a) Total concentration of iodine in the gas phase. b) Total concentration of iodine in the aqueous phase**

a)



b)

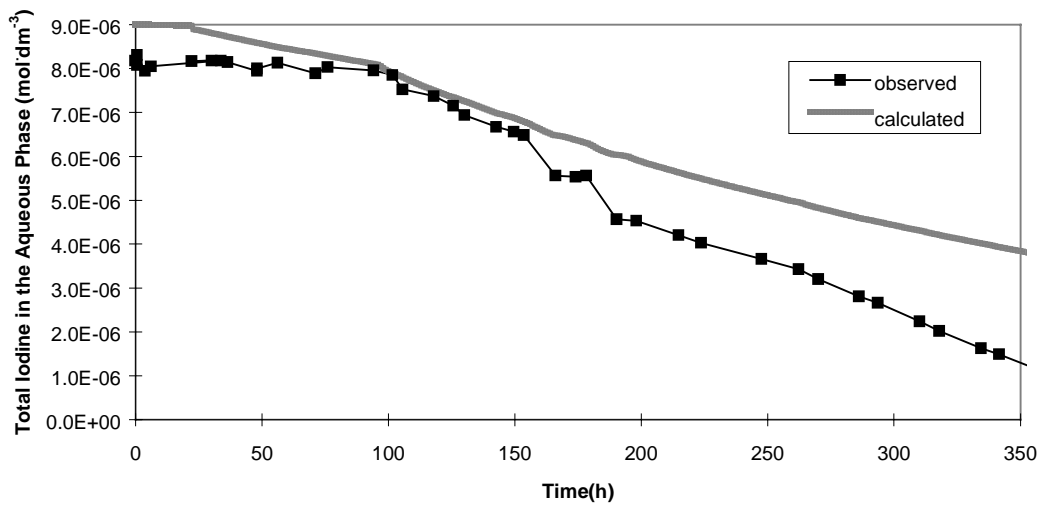
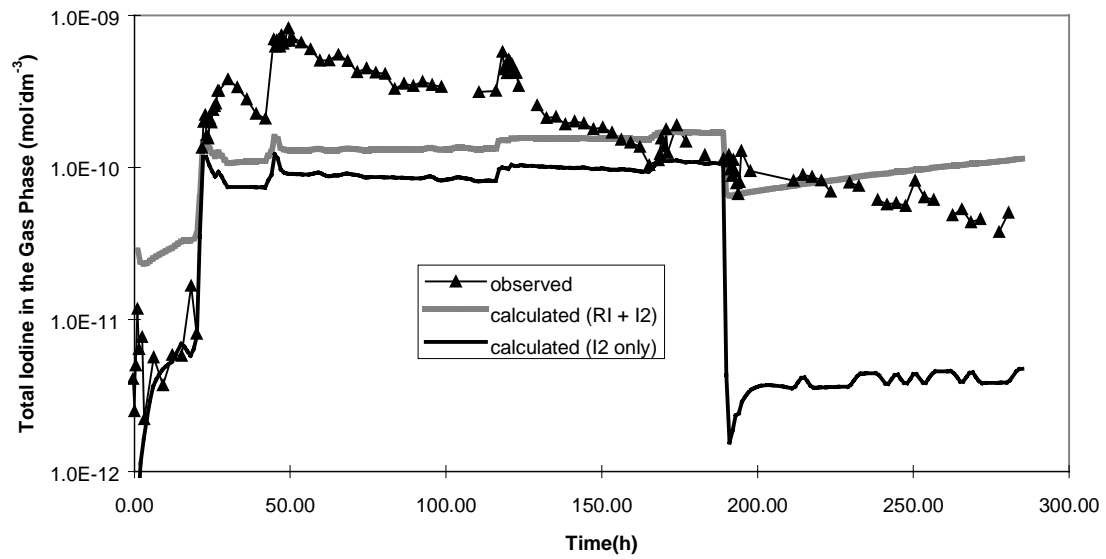


Figure 13. **JAERI: Observed vs. calculated results for Stage 1. a) Total concentration of iodine in the gas phase. b) Total concentration of iodine in the aqueous phase**

a)



b)

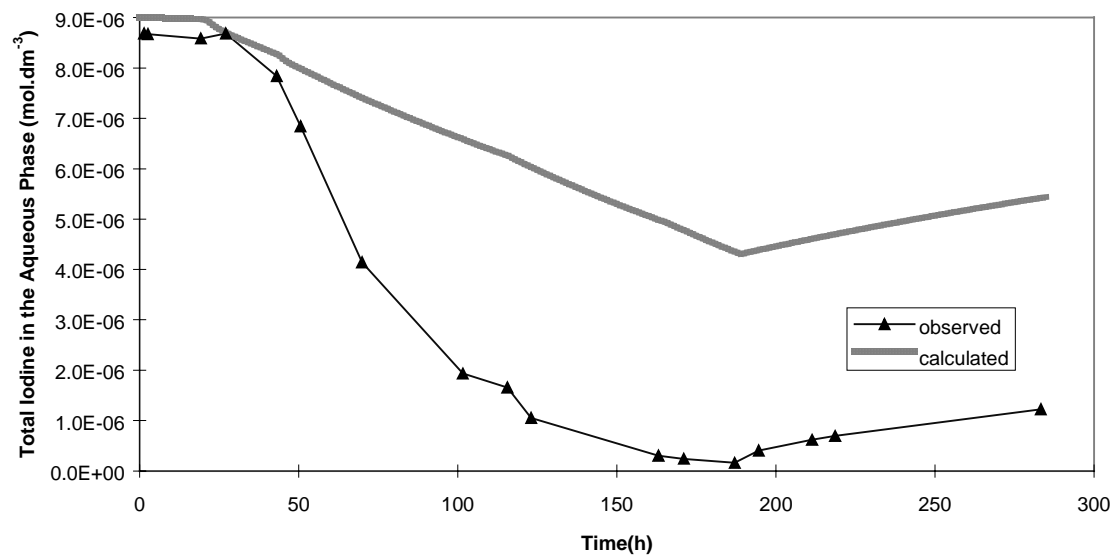
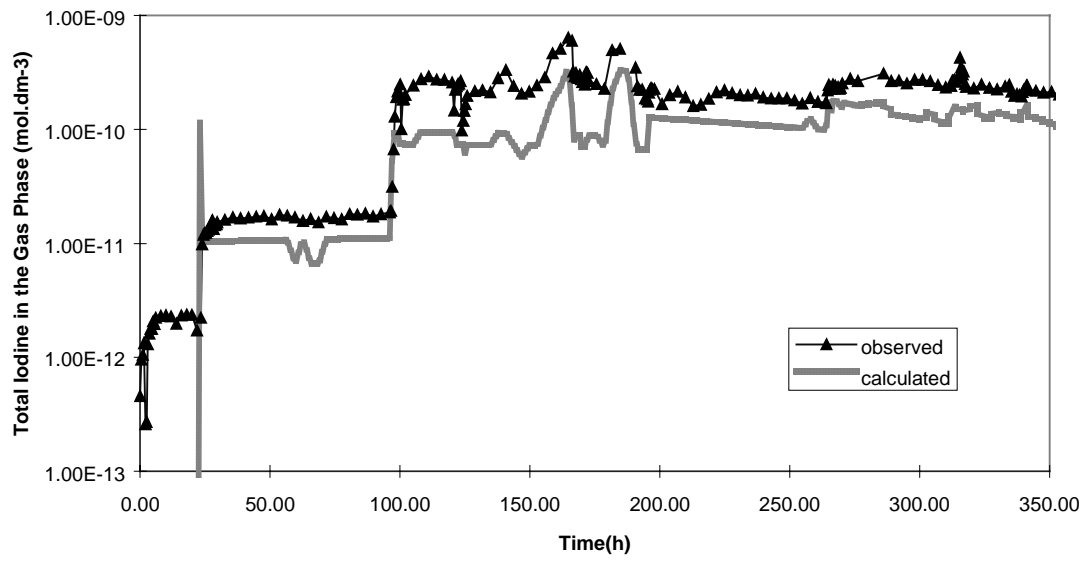


Figure 14. **JAERI: Observed vs. calculated results for Stage 2. a) Total concentration of iodine in the gas phase. b) Total concentration of iodine in the aqueous phase**

a)



b)

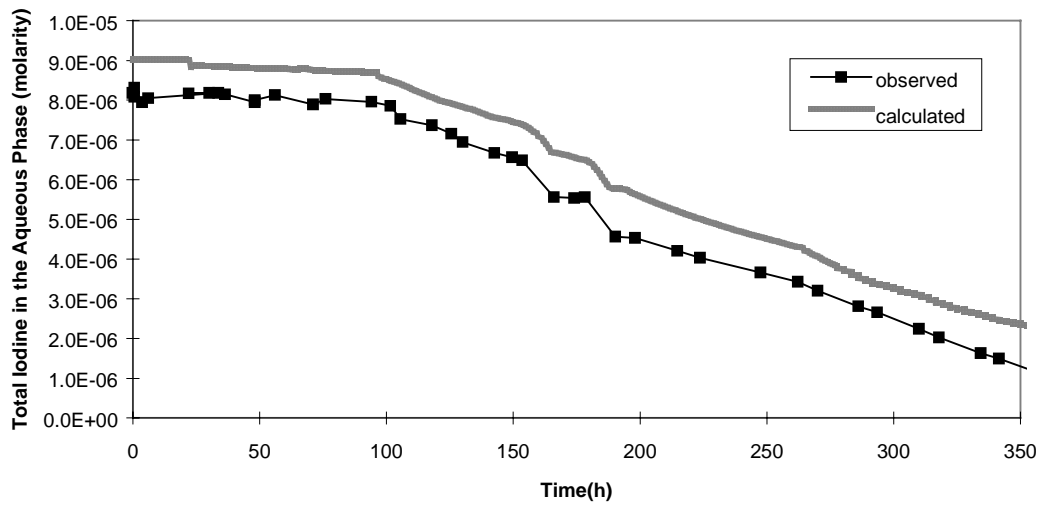
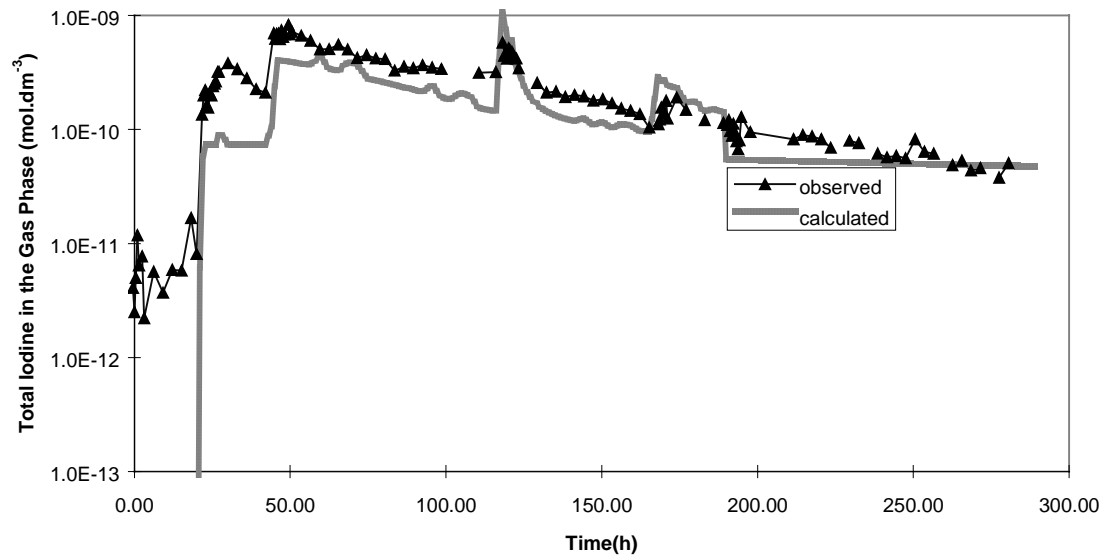


Figure 15. SANDIA: Observed vs. calculated results for Stage 1. a) Total concentration of iodine in the gas phase. b) Total concentration of iodine in the aqueous phase

a)



b)

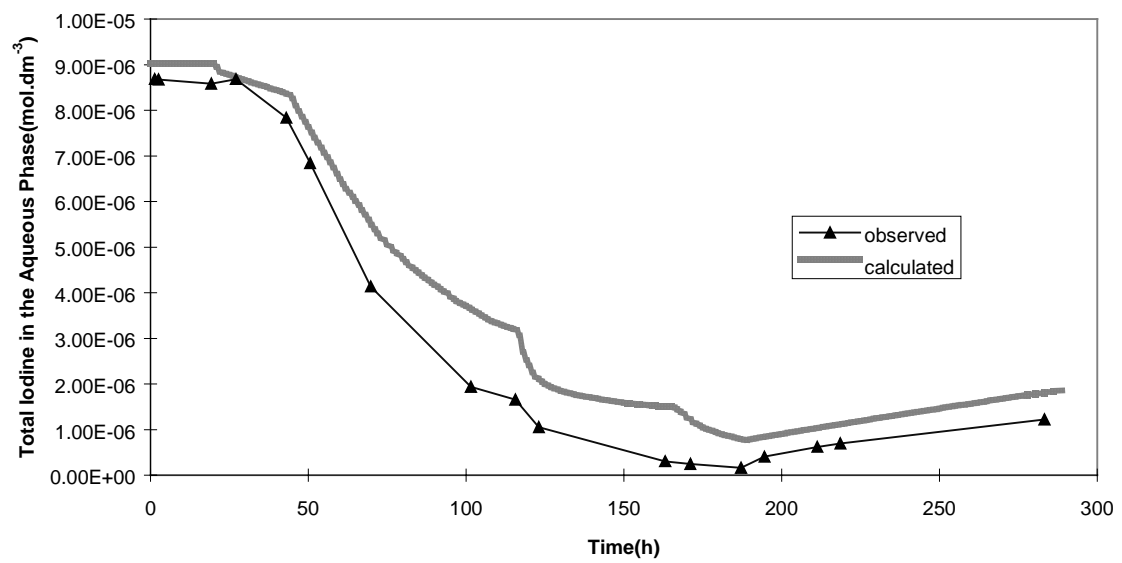
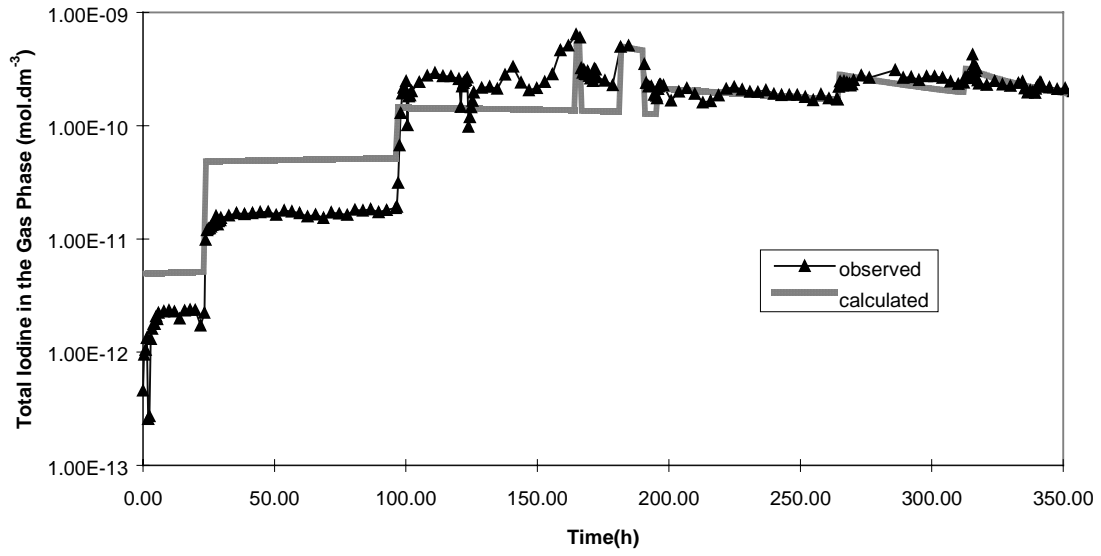


Figure 16. SANDIA: Observed vs. calculated results for Stage 2. a) Total concentration of iodine in the gas phase. b) Total concentration of iodine in the aqueous phase

a)



b)

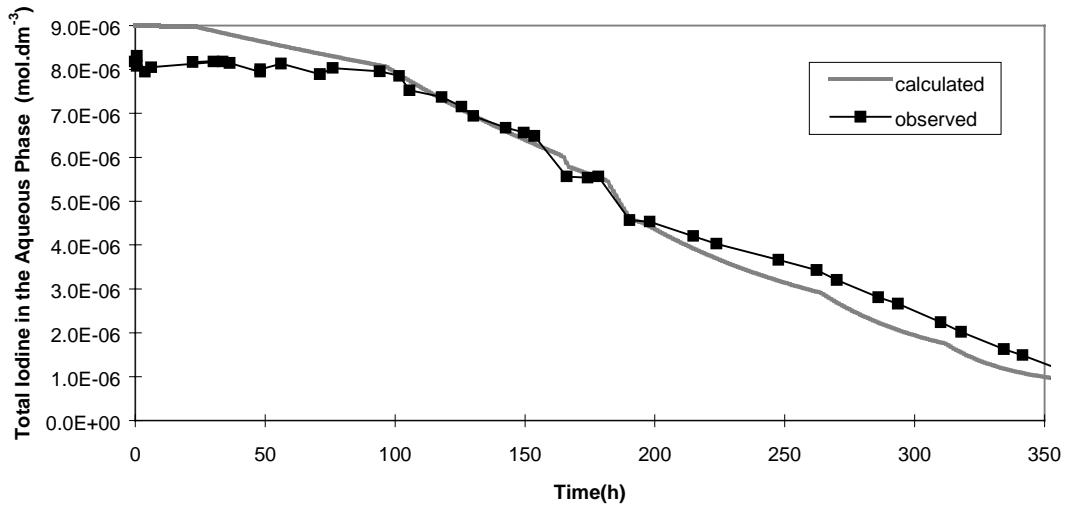
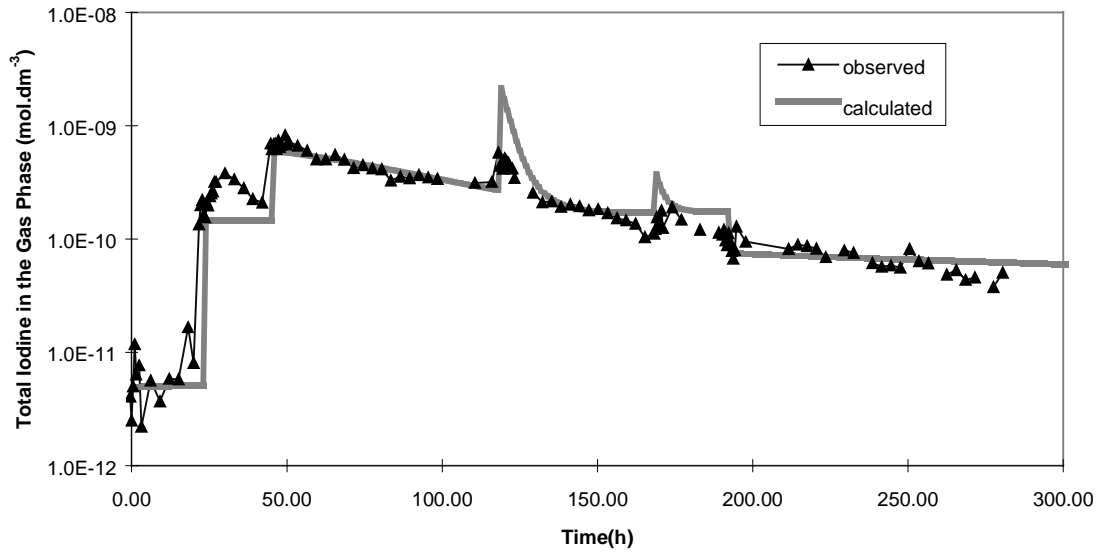


Figure 17. **AECL: Observed vs. calculated results for Stage 1. a) Total concentration of iodine in the gas phase. b) Total concentration of iodine in the aqueous phase**

a)



b)

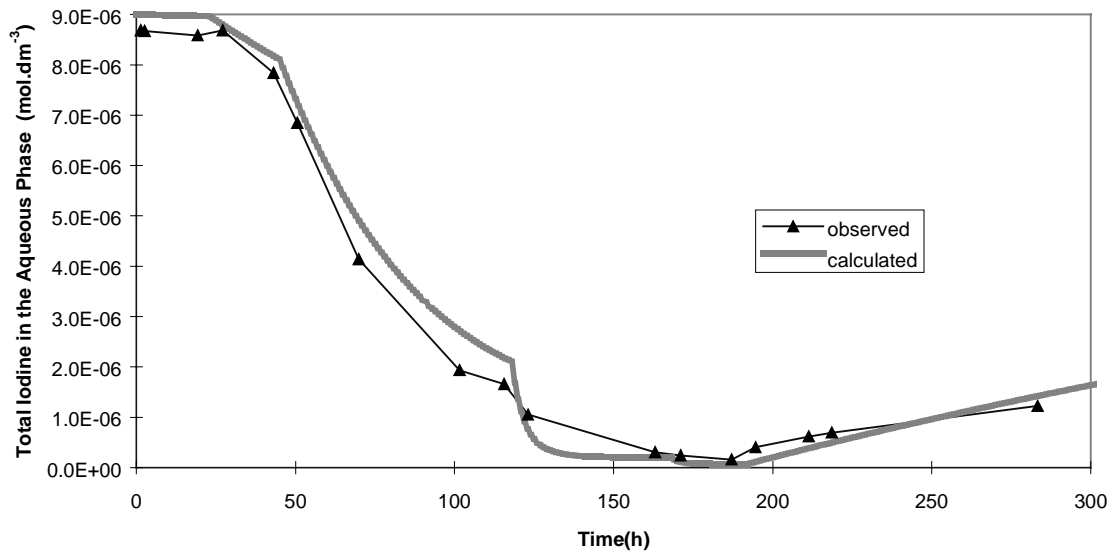


Figure 18. AECL: Observed vs. calculated results for Stage 1. a) Total concentration of iodine in the gas phase. b) Total concentration of iodine in the aqueous phase

## ENDNOTES

1. 2 parameters are provided as input :

- mass transfer coefficient  $k_g$  (from liquid to gas) which was selected from RTF studies criteria and set to  $10^{-5}$  m/s at such a temperature.
- adsorption coefficient on steel which has been set to  $10^{-4}$  m/s at  $25^\circ\text{C}$ . This has been chosen from ACE/RTF 4 experiments where  $0.006$  mmol/cm<sup>2</sup> have been adsorbed after 24 hours for an iodine concentration close to  $5.10^{-12}$  mol/l in the gas phase ( $t^\circ\text{C} = 60^\circ\text{C}$ ):

$$0.6 \cdot 10^{-5} \text{ mol.m}^{-2} / 24 \cdot 3600 = k_{\text{ads}} * 5.10^{-9} \text{ mol.m}^3.$$

where calculation means  $k_{\text{ads}} = 10^{-4}$  m/s

The dominant process in the speciation and distribution of iodine is the pH . Light variation (using true pH and ordered pH) has been observed.

The input parameter which has the most influence on the behaviour of iodine in the gas phase was the adsorption coefficient on stainless steel surfaces.

2. R. O. Gauntt *et al.*, "MELCOR Computer Code Manuals, Version 1.8.4, NUREG/CR-6119, SAND97-2398, Sandia National Laboratories, Albuquerque, NM (1997).
3. W. C. H. Kupferschmidt *et al.*, "A Description of the Radiiodine Test Facility (RTF) and Results of Initial RTF Full-System Tests," in Proc. Second CSNI Workshop on Iodine Chemistry in Reactor Safety, AECL-9923, CSNI-149, pp.292-311 (1989).
4. H. Sims *et al.*, "Iodine Code Comparison," EUR 16507 EN, European Commission, Luxembourg (1995).
5. D. A. Powers, R. K. Cole, T. J. Heames, "A Simplified Model of Iodine Chemistry for MELCOR," to be published, Sandia National Laboratories, Albuquerque, NM.
6. K. H. Haskell, W. H. Vandevender, W. L. Walton, "The SLATEC Common Mathematical Subprogram Library: SNLA Implementation," SAND80-2792, Sandia National Laboratories, Albuquerque, NM (1980).
7. J. C. Wren, G. A. Glowa, J. M. Ball, "Modelling Iodine Behaviour Using LIRIC 3.0," Proc. Fourth CSNI Workshop on the Iodine Chemistry in Reactor Safety, Wurenlingen, Switzerland, pp.507-530 (1996).